DETERMINANTS OF CLONAL EVOLUTION IN *JAK2*^{V617F}-DRIVEN MYELOID MALIGNANCIES

by

Brittany A. Woods

A Dissertation

Presented to the Faculty of the Louis V. Gerstner, Jr. Graduate School of Biomedical Sciences,

Memorial Sloan Kettering Cancer Center

in Partial Fulfillment of the Requirements for the Degree of Doctor of Philosophy

New York, NY

June 6th, 2019

_____ _____

Ross L. Levine, M.D. Date

Dissertation Mentor

DEDICATION

To my parents, Marianne and Daniel Woods –

For teaching me the meaning of unconditional love, and for their unwavering support.

Looks like this little frog finally won.

To my friends –

For respect, love, and laughter.

To Thomas Woods, Ray Bigliani, and Austin Travis –

For inspiring me to dream big and stay curious, then and always.

ABSTRACT

The classical myeloproliferative neoplasms (MPNs) are clonal hematopoietic disorders characterized by the overproduction of mature myeloid cells. There are three main phenotypes of MPN, including: Polycythemia Vera (PV), Essential Thrombocythemia (ET), and Primary Myelofibrosis (PMF). Despite their clinical heterogeneity, all 3 MPNs are characterized by mutational activation of the JAK/STAT signaling pathway. The most frequent of these events is a V617F gain-of-function mutation in *JAK2*. Mutation tracing studies revealed that hematopoietic stem cells are the bona fide cell-of-origin for MPN, which implicates that *JAK2*^{V617F} is present in and likely affects all hematopoietic lineages, regardless of clinical phenotype. The regulators of this phenotypic heterogeneity are, to date, poorly defined.

In this thesis, we generated several novel murine MPN models to investigate additional factors that modulate the expansion of the MPN clone. First, we sought to determine *JAK2*^{V617F}'s impact on the megakaryocyte (Mk) lineage. We generated a murine model of Mk lineage-restricted *Jak2*^{V617F} expression. Characterization of this model revealed that mutant Mks contribute to MPN pathogenesis by promoting increased erythroid differentiation of *Jak2* wild-type hematopoietic stem/progenitor cell populations. I went on to show that this effect is mediated, at least in part, by increased production of Interleukin-6 by *Jak2*-mutant Mks. Furthermore, we demonstrated that mutant Mks contribute to MPN maintenance in vivo using diptheria toxin receptor-mediated cell ablation in two bone marrow transplant models of MPN. These findings highlight a previously under-

appreciated role of *JAK2*^{V617F} in promoting MPN pathogenesis via cytokine-mediated expansion of the wild type hematopoietic compartment.

Next, we investigated how epigenetic deregulation arising from *ASXL1* loss cooperates with *JAK2*^{V617F} to promote clonal expansion. To this end, we generated a compound *Jak2/Asxl1* mutant mouse model that allowed for simultaneous expression of mutant *Jak2* and *Asxl1* loss throughout the hematopoietic compartment and rigorously determined the phenotypic differences that *Asxl1* loss conferred to *Jak2*-driven MPN. These differences included accelerated disease onset, as well as increased bone marrow fibrosis and alterations to the HSPC compartment. Furthermore, *Jak2/Asxl1* double-mutant HSPCs showed continued expansion in vitro and in vivo, These findings describe an important role for *ASXL1* loss in promoting the expansion and evolution of the MPN clone.

ACKNOWLEDGEMENTS

There are so many individuals to thank, that it would probably take the equivalent of a second thesis to give appropriate credit everywhere it is due. Let's start at the beginning…

First and absolutely foremost, I have to thank my extraordinary mentor, Ross Levine. When I decided to pursue my PhD at MSK, everyone in my former lab mentioned Ross's name. From my first interactions with Ross as a first-year, during my rotation, and ever since, he has endlessly supported my growth as a scientist. In addition to teaching me how to formulate meaningful questions and hunt down the answers, you encouraged me to develop my own style and voice. From day one of my rotation, you urged me to follow my instincts and to never shy away from asking the "Big Questions", even if they seemed beyond my abilities. Thank you for teaching me how to not just ask a practical question, but an impactful one. You also gave me the space, and respect above all, that I needed to discover my own style and approach to science. I am eternally in your debt. Furthermore, thank you for assembling the phenomenal cadre of postdoctoral fellows, clinical fellows, graduate students, and research technicians (past and present) who made every day in the lab an adventure.

I am truly blessed to work and train in an environment like the Levine Lab, where I am surrounded by such an incredibly passionate and productive group of individuals. Your collective enthusiasm for science is infectious, and it made even the bitterest of days in the lab bearable. I especially need to thank Drs. Aaron Viny and Elodie Pronier, who joined the lab around the same time as I did in 2013. In addition to serving as exceptional role models, you selflessly offered me assistance (scientific or personal) whenever I was in

need. I also need to thank Dr. Alan Shih, who patiently endured my endless questioning during my rotation and my initial freak-out the first time I tried to scruff a mouse. You have been a tremendous support from day one. I also need to thank Drs. Neha Bhagwat, Lindsay LaFave, and Sophie McKenney, former graduate students, for being such remarkable role models. Thank you all for setting such a high bar, and for inviting me to learn from each of you. It has been an honor and a privilege.

The work in this thesis would have been almost impossible without the help of Sophia Chiu, Keith Cordner, and Matt Keller - Thank you for all of your tremendous efforts developing and managing the mouse models used in this thesis, and for your camaraderie. I also need to acknowledge the enthusiastic summer students who worked with me over the years, Lilly Gu, Isabella Rainieri, and Donovan Sandoval-Heglund, who directly contributed to experimental results presented in this thesis. Thank you for your willingness to learn, and for all that you taught me in the process.

Thank you to our incredible collaborators, Drs. John Crispino and Jeremy Wen at Northwestern University. Your insights and efforts were invaluable to this thesis. I am blessed to have worked alongside such thoughtful and engaging scientists.

Thank you to my advisory committee, Drs. Ping Chi and Scott Lowe, for your insightful and sage advice into the various projects I have tackled over the years. Your critical and frank advice helped to refine my work, and always kept me on track. Thank you to Drs. Monica Guzman and Omar Abdel-Wahab for serving as my examining committee. Extra thanks are certainly due to Dr. Abdel-Wahab for providing several mouse models used to complete this work, and for truly pioneering one of the projects in this thesis.

Thank you to the founding Dean of the GSK Graduate School, Dr. Ken Marians, for establishing such a unique graduate program and training environment. Further thanks to Linda Burnley, Iwona Abramek, Maria Torres, Ivan Gerena, Tom Magaldi, David McDonough, and the rest of the graduate school office (past and present), for being the stalwart backbone of this program. The GSK student body is absolutely blessed to have all of you supporting us. Thank you to Dr. Michael Overholtzer, for your enthusiasm in taking charge of the next generation. They are in excellent hands.

Thank you to the GSK entering class of 2012, for your camaraderie from first year, through qualifying exams, and beyond. You all forced me to be a better student and scientist. I am still in awe of your determination, focus, and dedication. Kelsey Temprine: because I knew you, I have been changed for good. Wudan Yan: I hit the jackpot of first-year roommates. Can't wait to Google/PubMed stalk y'all.

Thank you to my friends, in New York, Massachusetts, and across the globe, for your warmth, support, and inspiration to never settle. Jenna Kazarian: you really are the sister I never had.

And finally, thank you to my parents, Marianne and Daniel Woods, for your unconditional love and support. I would not be the woman I am today without you both. Thank you for always encouraging me to run down my dreams and go wherever they lead.

To all those who will continue to walk in and out of my life - Thank you.

TABLE OF CONTENTS

TABLE OF FIGURES

TABLE OF TABLES

LIST OF ABBREVIATIONS

AML: Acute Myeloid Leukemia
ASXL: Addition of Sex Combs-Like
BFU-E: Burst-Forming Unit - erythroid
BM: Bone Marrow
BMT: Bone Marrow Transplant(ation)
CFU: Colony-Forming Unit
CML: Chromic Myeloid Leukemia
CMML: Chronic Myelomonocytic Leukemia
CXCL: Chemokine Ligand
DT: Diphtheria Toxin
(i)DTR: (Inducible) Diphtheria Toxin Receptor
ET: Essential Thrombocythemia
EZH2: Enhancer of Zeste 2
EPO/EPO-R: Erythropoietin/Erythropoietin Receptor
GFP: Green Fluorescent Protein
GMP: Granulo-monocyte Progenitor
H&E: Hematoxylin and Eosin Staining
HP1: Heterochromatin-associated Protein 1
HSC: Hematopoietic Stem Cell
HSPC(s): Hematopoietic Stem/Progenitor Cell(s)
IL: Interleukin
JAK: Janus-Associated family of Kinases
JAK2: Janus-Associated Kinase 2
LSK: Lineage-negative Sca1-positive Kit-positive
NGS: Next-Generation Sequencing
MAPK: Mitogen-Activated Protein Kinase
MDS: Myelodysplastic Syndrome(s)
MEP: Megakaryocyte-Erythroid Progenitor
MF: Myelofibrosis
Mk: Megakaryocyte
MkP: Megakaryocyte Progenitor
MNC: Mononuclear Cell
MP: Myeloid Progenitor
MPD: Myeloproliferative Disease/Disorder
MPL: Myeloproliferative leukemia virus proto-oncogene/Thrombopoietin Receptor
MPN(s): Myeloproliferative Neoplasm(s)
PB: Peripheral Blood
PBS: Phosphate-Buffered Saline
PCR: Polymerase Chain Reaction
PF4: Platelet Factor 4
PHD: Plant Homology Domain

pIpC: Polyinosinic:polycytidylic acid
PLT: Platelet
PMF: Primary Myelofibrosis
PRC: Polycomb Repressive Complex
Pre-CFUe: Pre-Erythroid Colony Forming Unit
Pre-MegE: Pre-Megakaryocyte/Erythroid Precursor Cell
PV: Polycythemia Vera
RARS-T: Refractory Anemia with Ring Sideroblasts with Thrombocytosis
RFP: Red Fluorescent Protein
RTK: Receptor Tyrosine Kinase
SCF: Stem Cell Factor
SCL: Stem Cell Leukemia
Sp/Spl: Spleen
STAT: Signal Transducer and Activator of Transcription
TAM: Tamoxifen
TPO/Tpo-R: Thrombopoietin/Thrombopoietin Receptor

Chapter 1 - INTRODUCTION

THE SPECTRUM OF MYELOID MALIGNANCIES

Myeloid malignancies are clonal disorders of hematopoiesis that arise from alterations in hematopoietic stem and progenitor cells (HSPCs). Mutations contributing to the pathogenesis of these malignancies perturb key hematopoietic processes, including: aberrant differentiation, proliferation, and/or self-renewal. This diverse class of disorders includes chronic conditions - myelodysplastic syndromes (MDS) and myeloproliferative neoplasms (MPN) - as well as acute presentations, i.e.- acute myeloid leukemia (AML) (Murati et al. 2012). MDS are heterogenous disorders that are characterized by impaired hematopoietic differentiation and peripheral blood cytopenias (deficiencies in peripheral blood cell counts), whereas MPNs represent the converse of this – the overproduction of mature myeloid cell types. AML represents a paradoxical intermediate disease state between MDS/MPN; it is characterized by the accumulation of immature myeloid blasts. Therapeutic options for AML are limited, with bone marrow transplantation being the only curative treatment option at this time (Abdel-Wahab & Levine 2013). While AML can arise de novo, a significant portion of cases (secondary AML) arise from a preceding MDS/MPN. Patients can also present with MDS/MPN overlap disorders, such as Chronic Myelomonocytic Leukemia (CMML). These disorders are characterized by the presence of both dysplastic features and hyper-proliferative symptoms. Collectively, MDS, MPN, and AML comprise a continuum of biologically-related, yet clinically heterogeneous malignancies (**Figure 1.1**).

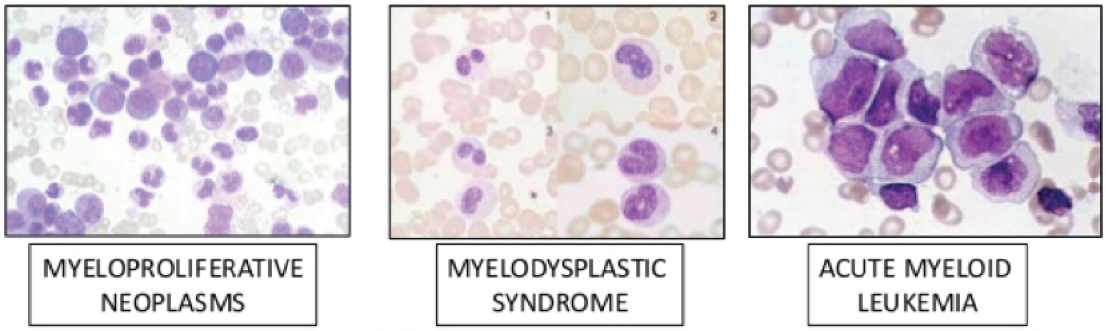

FIGURE 1.1: OVERVIEW OF MYELOID MALIGNANCIES

Image Credit: Dr. Omar Abdel-Wahab, Memorial Sloan Kettering Cancer Center

THE CLASSICAL MYELOPROLIFERATIVE NEOPLASMS

The myeloproliferative neoplasms (MPNs) are characterized by aberrant hyperproliferation of one or multiple mature myeloid lineages. They are generally classified in to two distinct groups: Philadelphia chromosome positive (Ph^+), which includes chromic myeloid leukemia (CML), and the Philadelphia chromosome negative (Ph^-). The latter comprises the "classical" MPNs, which include: Polycythemia Vera (PV), Essential Thrombocythemia (ET), and Primary Myelofibrosis (PMF). These disorders differ phenotypically from CML, which is characterized by the presence of the BCR-ABL fusion protein and neutrophilia. In addition to being genetically distinct (lacking the *BCR-ABL* fusion), the hallmark pathologic features of PV and ET are elevated hematocrit (red blood cell burden) and platelet counts respectively. These features are not entirely mutually exclusive, as PV patients can present with thrombocytosis. However, elevated hematocrit is the defining feature. PMF is a heterogeneous presentation, that is defined by the presence of bone marrow fibrosis and megakaryocytic hyperplasia. MPN cases usually present with splenomegaly (enlarged spleen), extramedullary hematopoiesis, and bone marrow fibrosis, along with constitutional symptoms including weight loss, fever, and fatigue. The overall prevalence of classical MPNs in the United States is estimated to be at least 300,000 (Mehta et al. 2014). MPN patients are at high-risk for a variety of hematologic and vascular complications, including thrombosis, hemorrhage, and infection. Patients are also at a very high-risk for disease transformation to acute myeloid leukemia (AML), and these cases have a particularly poor prognosis (Mesa et al. 2005).

Despite their varied presentation, it was long suspected that these three clinicopathologic entities (PV, ET, and MF) share common biological roots. The noted hematologist William Dameshek, in 1951, first observed that these distinct malignancies shared common features. He remarked that:

"It is possible that these various conditions – 'myeloproliferative disorders'- are all somewhat variable manifestations of proliferative activity of the bone marrow cells, perhaps due to a hitherto undiscovered stimulus. This may affect the marrow cells diffusely or irregularly with the result that various syndromes, either clear-cut or transitional, result." (DAMESHEK 1951)

Indeed, Dameshek's observations underscore a common MPN origin – the clonal expansion of an MPN HSC that results in myeloid hyperplasia, affecting one or multiple myeloid lineages. In many cases, a continuum of the disease sub-types can be observed, with many PV/ET patients progressing to secondary myelofibrosis. Furthermore, the pathologic boundaries between the disorders, especially ET and PMF, are difficult to delineate. This is reflected in the World Health Organization's revised 2016 diagnostic criteria (Arber et al. 2016).

The basis of Dameshek's observed clinicopathologic commonality in MPN was uncovered in 2005, when landmark genetic sequencing efforts identified recurrent somatic mutations in the cytosolic tyrosine kinase *JAK2*. The most frequent mutation observed in MPN is a guanine to thymine transversion event that results in the substitution of a valine for phenylalanine at position 617 in the JAK2 pseudo-kinase domain (Baxter et al. 2005; James et al. 2005; Kralovics et al. 2005; Levine et al. 2005). The Janus family of kinases (JAK) is involved in the transduction of cytokine-mediated signals in a number of cell types and regulates cytokine-dependent gene expression, in part by activating the signal

transducers and activators of transcription (STATs). The JAK-STAT pathway can also interact with the receptor tyrosine kinase (RTK)/RAS/MAPK pathway, resulting in parallel activation of the PI3K signaling pathway leading to complex biological consequences (Rane & Reddy 2000).

JAK/STAT pathway activating mutations are a molecular hallmark of MPN. *JAK2*^{V617F} collectively occurs in ~95% of PV cases and ~40-60% of ET/MF patients (Levine et al. 2007). Additional gain of function mutations in the SH2 domain of *JAK2* have also been identified in a small proportion of *JAK2*^{V617F}-negative PV cases (Scott et al. 2007), thus implicating *JAK2* mutations in almost 100% of PV. Furthermore, additional JAK/STAT pathway alterations, such as *MPL*$^{W515L/K}$, *CALR* mutations, and alterations in *LNK, CBL*, are observed in the majority of *JAK2*^{WT} MPN (Pikman et al. 2006; Nangalia et al. 2013; Klampfl et al. 2013; Oh et al. 2010; Aranaz et al. 2012; Grand et al. 2009; Schwaab et al. 2012). RNA-Seq (gene expression) analysis of MPN patients has also revealed that STAT5 activation downstream of these effectors is a defining hallmark of MPN, regardless of driver mutation status or clinical presentation (Rampal, Al-Shahrour, et al. 2014). With the exception of a few isolated cases of a subset of MDS with features of ET, known as refractory anemia with ring sideroblasts and thrombocytosis (RARS-T) (Szpurka et al. 2006), *JAK2*^{V617F} and other JAK/STAT pathway alterations are not frequently detected in MDS or de novo AML.

However, JAK/STAT alterations do not occur in isolation. Next-generation sequencing (NGS) and other analysis methods allowed for the identification of additional acquired mutations in MPN. These events include alterations in a variety of genes affecting a range

of cellular processes, including: *IDH1, IDH2, TET2, DNMT3A, SF3B1, EZH2, ASXL1, P53, KRAS, NRAS*, and many others. Targeted panel sequencing studies indicate that most patients present with multiple mutations, and these studies have allowed for the identification of high-risk patients (Vannucchi et al. 2013). Furthermore, many of these genes, especially those affecting epigenetic regulation and histone modifications, have also been implicated in the pathogenesis of MDS and AML. However, these mutations are not MPN-specific, and they are frequently detected in MDS and AML at a much higher frequency (Vainchenker & Kralovics 2017). This genetic overlap further highlights the pathogenic continuum linking MDS, AML, and MPN.

The goals of this thesis are two-fold: 1) to assess the impact of megakaryocytes on the initiation and phenotype of *JAK2*^{V617F}-driven myeloid neoplasia, and 2) to investigate how additional cooperating mutations, specifically loss of the myeloid tumor suppressor and histone modifier *ASXL1*, alter MPN stem cell function and expansion of the MPN clone.

JAK/STAT Pathway Activation Drives Myeloid Neoplasia

As previously mentioned, *JAK2*^{V617F} is the most frequently observed mutation in MPN. This gain of function event causes constitutive activation of JAK2, as well as downstream pathway effectors STAT3 and STAT5. *JAK2*^{V617F} is fairly unique among myeloid disease alleles, in that it is virtually restricted to MPN and not frequently observed in other hematologic pathologies. Below is a discussion of the broader biological role of JAK2, the

effect of the V617F mutation on the biochemical and cellular function of JAK2, and the role of $JAK2^{V617F}$ in myeloid cell transformation.

JAK2 AND CANONICAL JAK/STAT SIGNALING

JAK2 is one of 4 JAK family members, along with *JAK1, JAK3*, and *TYK2* (Wilks et al. 1991; Wilks 1991; Harpur et al. 1992; Takahashi & Shirasawa 1994; Krolewski et al. 1990). The JAK family of kinases is characterized by the presence of 2 highly homologous carboxy terminal domains: the catalytic kinase domain (JH1), and the pseudo-kinase (JH2) domain, which is largely assumed to have an auto-regulatory role (Kawamura et al. 1994) (**Figure 1.2A**). JAK kinases interact with Type I and Type II cytokine receptors and serve as the catalytic unit – allowing intracellular signal propagation following cytokine binding. Cytokine binding induces receptor hetero/homodimerization, which activates the associates JAK kinases via trans-phosphorylation. The activated JAKs then phosphorylate the receptors, which can then serve as docking sites for downstream signaling effectors (**Figure 1.2**). The canonical downstream effectors are the STAT family of transcription factors, which undergo hetero/homo-dimerization following phosphorylation by JAKs. These activated molecules can then translocate to the nucleus, where they mediate target gene transcription (**Figure 1.3**).

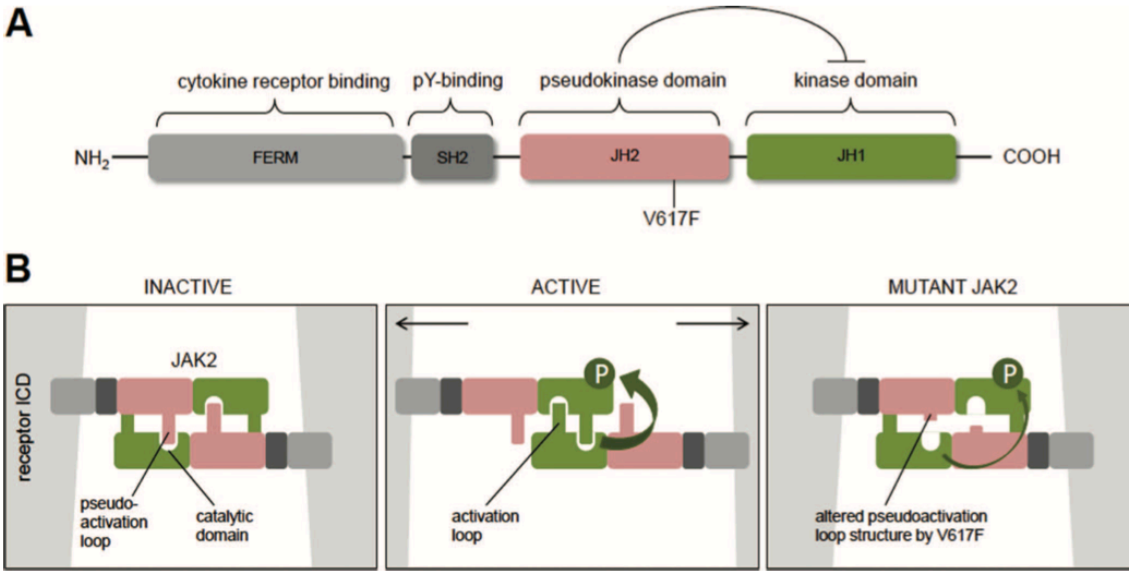

FIGURE 1.2: JAK2 STRUCTURE AND SIGNALING

(A) Domain structure of JAK2. JAK2 contains a tyrosine kinase domain (JH1), a pseudo-kinase domain (JH2), an SH2-like domain, and a FERM domain that is responsible for attachment to the intracellular domain of cytokine receptors. (B) Model for JAK2 activation at the cytokine receptor. Left, Intermolecular JH1–JH2 interactions keeps JAK2 in an inactive state. Center, Ligand binding induces increased separation of cytokine receptors and movement of JAK2 dimers leads to apposition of kinase domains of the 2 JAK2 molecules and facilitates mutual phosphorylation of specific tyrosine residues in trans. Consequences of the $JAK2^{V617F}$ mutation on the "sliding model" of JAK2 activation remains unclear but is likely to involve diminished repression of the catalytic activity of the JH1 domain due to decreased stability of JH1–JH2 interaction.

Republished with permission from the American Society Hematology. Image from: Chen, E. & Mullally, A. How does JAK2V617F contribute to the pathogenesis of myeloproliferative neoplasms? Hematology Am Soc Hematol Educ Program, 268–276 (2014). PMID: 25696866.

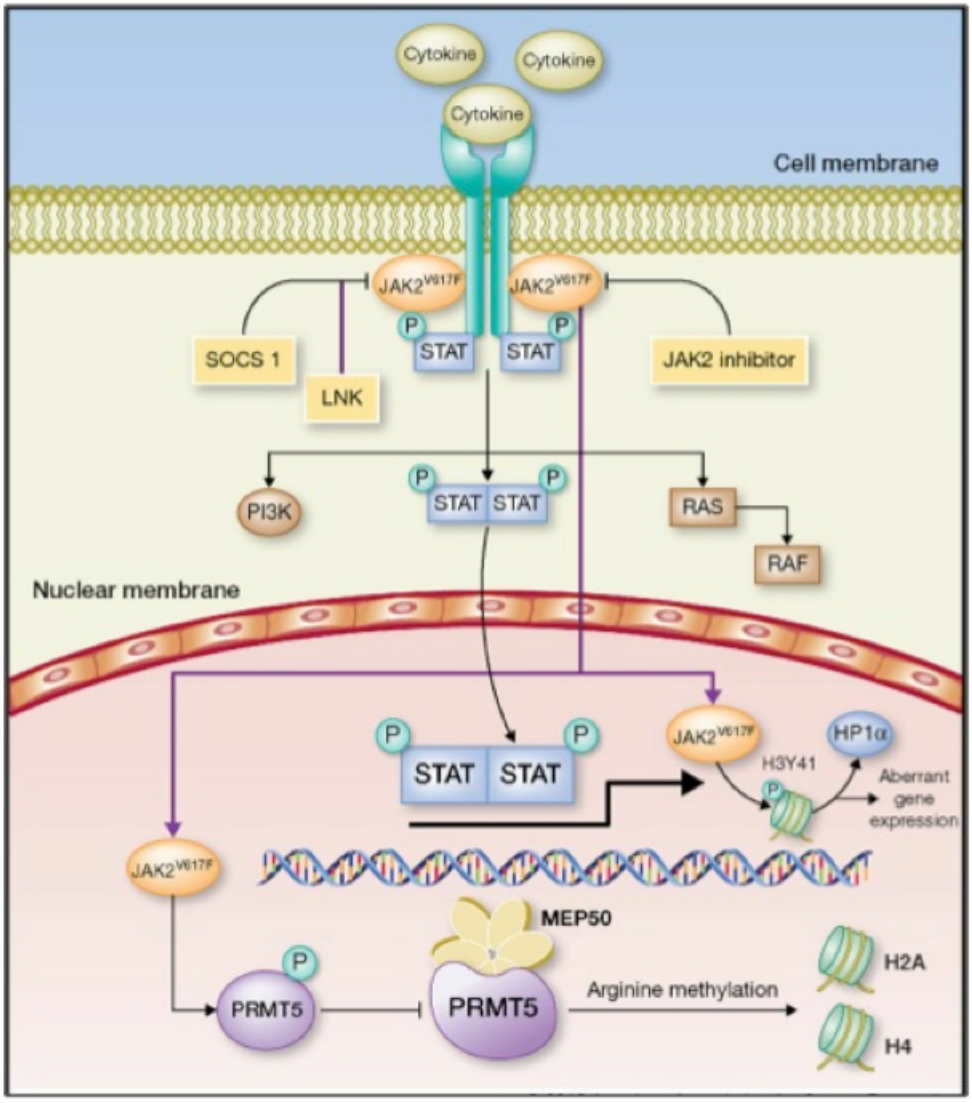

FIGURE 1.3: JAK-STAT SIGNALING IN MPN

In the presence of $JAK2^{V617F}$ mutations, the JAK/STAT pathway is constitutively activated, which leads to activation of the STAT family of transcription factors as well as activation of MAPK and PI3K pathways. The activity of the JAK2/STAT pathway is negatively regulated by SOCS1 and LNK. JAK2 can also localize to the nucleus and phosphorylate histone H3 (H3Y41), thus preventing its binding to the repressor HP1α. $JAK2^{V617F}$ also binds and phosphorylates the arginine methyltransferase PRMT5, which hampers its interaction with methylosome protein 50 (MEP50), thus decreasing global arginine methylation of histones H2A and H4.

Reprinted with permission from the American Association for Cancer Research. Image from: Quintás-Cardama A, Verstovsek S., Molecular pathways: JAK/STAT pathway mutations, inhibitors, and resistance. Clinical Cancer Research. 19(8), 1933-40 (2013). PMID: 23406773.

All *JAK* family members play critical roles in development and normal hematopoiesis (Rodig et al. 1998; Neubauer et al. 1998; Nosaka et al. 1995; S. Y. Park et al. 1995; Thomis et al. 1995; Karaghiosoff et al. 2000). Interestingly, JAK2 is the only JAK kinase that signals as a homodimer. It associates with single-chain cytokine receptors, including the erythropoietin receptor (EpoR), thrombopoietin receptor (TpoR), and granulocyte colony-stimulating factor receptor (G-CSFR). *Jak2*$^{-/-}$ cells do not respond to Tpo, IFNγ, or IL-3 stimulation, indicating that these cytokine receptors require JAK2. *Jak2* deletion in vivo is embryonic lethal; *Jak2*$^{-/-}$ mice die *in utero* due to defective erythropoiesis that phenocopies *Epo* or *EpoR* deletion (Neubauer et al. 1998). Cells from *Jak2*$^{-/-}$ mice also do not respond to Tpo, IL-3, GM-CSF, or IFNγ stimulation, further indicating a requirement of these receptors for Jak2 in propagating their signals (Parganas et al. 1998).

JAK2 ^{V617F}: A MYELOID LINEAGE ONCOGENE

Expression of *JAK2*^{V617F} results in constitutive phosphorylation of JAK2, as well as STAT3/5, and parallel activation of PI3K/AKT and MAPK signaling (Levine et al. 2005) (**Figure 1.3**). JAK2^{V617F} also promotes cytokine-independent growth and renders cells hyper-sensitive to cytokine stimulation. This mimics prior observations that erythroid progenitors from PV patients are hyper-sensitive to EPO stimulation (James et al. 2005; Ugo et al. 2004). Recent studies have shown that the V617F mutation abrogates the catalytic activity of the pseudo-kinase JH2 domain. The JH2 domain phosphorylates Ser523 and Tyr570, known negative regulatory sites in JAK2 (Ungureanu et al. 2011). JAK2^{V617F} is thus proposed to exert its activating effects in part via a loss of autoregulatory ability. Crystal structures of the wild-type (WT) and V617F-mutant JAK2 JH2 domain

revealed that the V617F mutation increased the rigidity of a critical helix that stabilizes a stimulatory interaction necessary for activation of the JH1 domain (Bandaranayake et al. 2012). The activating effect of V617F is therefore likely a net result of an enhanced stimulatory effect combined with loss of inhibitory function in the JH2 domain (**Figure 1.2**).

Expression of *JAK2*^{V617F} in vitro transforms hematopoietic cells, permitting cytokine-independent growth (Kralovics et al. 2005; Levine et al. 2005). Interestingly, *JAK2*^{V617F}-driven transformation is dependent on co-expression of a cognate receptor, such as EpoR, TpoR, or G-CSFR (Lu et al. 2008). *In vivo* expression of *JAK2*^{V617F}, either via retroviral overexpression in bone marrow transplantation (BMT) assays or using genetically-engineered mouse models (GEMMs), results ins a fully-penetrant myeloproliferative disease that resembles many of the canonical clinical hallmarks of MPN (summarized and discussed below **– Table 1.1** and

Table 1.2**).** Notably, the emergent phenotype and the severity varies widely across models. The basis of this variation remains poorly understood.

ADDITIONAL JAK/STAT PATHWAY ALTERATIONS IN MPN

The oncogenic effect of aberrant JAK2/STAT activation is also exerted by additional MPN-associated mutations in upstream signaling pathway effectors. *MPL*$^{W515L/K}$ mutations, as well as activating mutations in Calreticulin (*CALR*), are mutually exclusive with *JAK2*^{V617F} (Pikman et al. 2006; Nangalia et al. 2013; Klampfl et al. 2013). *MPL* encodes the thrombopoietin receptor (TpoR), and recurrent *W515L/K* mutations are seen in 3 to 5% of

ET/MF cases, respectively. These mutations arise in the amphipathic domain of MPL, which prevents spontaneous activation in the absence of ligand. Expression of $MPL^{W515L/K}$ in murine Ba/F3 and 32D cells leads to cytokine independent growth and constitutive phosphorylation of JAK2, in addition to downstream effectors, STAT5, STAT3, AKT and p44/42 MAPK in the absence of ligand stimulation. Retroviral overexpression of MPL^{W515L} *in vivo* in a BMT model results in a highly-aggressive myelofibrosis-like disease that also harbors since clinical features of ET (Pikman et al. 2006). Frameshift mutations in *CALR* are observed in the vast majority of *JAK2* and *MPL* wild-type PMF and ET. While Calreticulin is an endoplasmic reticulin chaperone protein, with no previously established connection to the JAK/STAT signaling cascade, several studies used elegant cellular and biochemical assays to demonstrate that these mutations promote TpoR/MPL stabilization by CALR (Chachoua et al. 2016; Pecquet et al. 2019; Pronier et al. 2018). This CALR-mediated stabilization potentiates abnormal MPL/JAK/STAT activation. Collectively, these observations further demonstrate the fundamental importance of JAK/STAT pathway activation in MPN pathogenesis.

Mouse Models of JAK2-Driven MPN

Numerous pre-clinical *JAK2*-mutant murine MPN models are reported in the literature (Bumm et al. 2006; Lacout et al. 2006; Wernig et al. 2006; Zaleskas et al. 2006; Akada et al. 2010; Li et al. 2010; Marty et al. 2010; Mullally et al. 2010). In addition to serving as essential tools for the identification and testing of novel therapeutic approaches, these models have and continue to provide invaluable insights into the molecular and cellular events in the initiation and evolution of *JAK2*-driven neoplasia. Each model utilizes

different genetic techniques to express mutant *JAK2/Jak2*, and the resulting disease phenotypes are as heterogeneous as the clinical diseases that they seek to model. These phenotypes are summarized in **Tables 1.1** and **Table 1.2**.

The effects on myeloid lineage output vary; some models report a mild increase (Mullally et al. 2010; Li et al. 2010) while other report more than 80-fold expansion of erythroid/myeloid precursors (Marty et al. 2010). Furthermore, the effect of each model on the HSPC compartment is inconsistent. Some models have increased stem cell fractions (Akada et al. 2010; Kubovcakova et al. 2013; Mullally et al. 2012), while others report a decrease or no change. However, all of these models demonstrate the ability of $JAK2^{V617F}$ to initiate myeloproliferation and hematopoietic cell transformation as a single event in vivo. Therefore, $JAK2^{V617F}$ is a bona fide oncogenic driver of myeloid malignancy.

The basis for the diverse range of murine JAK2-driven MPN phenotypes, which is also observed in the clinical context, is not completely clear. One explanation for the observed phenotypic heterogeneity is a correlation between $JAK2^{V617F}$ expression levels and phenotype: low levels are associated with a more ET-like phenotype, whereas higher expression levels (~30% of WT JAK2 or more) are associated with a more PV-like presentation (Tiedt et al. 2008). In one model, heterozygous knock-in of human $JAK2^{V671F}$ displays a very mild ET phenotype, while homozygous knock-in induced erythrocytosis more closely resembling PV (Li et al. 2010). The expression of mouse versus human $JAK2^{V617F}$ is also proposed as a possible explanation for the phenotypic variability seen across the murine models. The most common disease phenotype reported across the

murine models is a PV-like disorder that eventually progresses to MF (Mullally et al. 2010; Hasan et al. 2013).

While existing mouse models display PV, ET and mixed PV/ET-like disease, no model exists of *JAK2*^{V617F}-driven PMF. Several existing models progress from PV/ET to myelofibrosis after a marked latency period, but none exhibit MF outright. Additionally, no *JAK2* MPN model, in isolation without additional cooperating genetic events such as *P53* or *TET2* loss (Rampal, Ahn, et al. 2014; H. Chen et al. 2018), transforms to AML. How one mutation promotes such a diverse range of hematologic phenotypes still largely remains a mystery.

A. Retroviral overexpression and bone marrow transplantation models

V617F species	Recipient	Hct (%)		Platelets	WBC	MF	Reference
Mouse	BALB/c	73.7±6.5 (VF)	49.7±4.3 (WT)	~2-fold increase	~17-fold increase	Yes	Wernig et al., 2006
	C57Bl/6	72.5±3.8 (VF)	44.9±2.5 (WT)	Normal	~2-fold increase	No	
Mouse	C57Bl/6	61±7 (Group 1; VF) 57±7 (Group 2; VF)	Values not shown	Normal	Increased	Yes	Lacout et al., 2006
Mouse	BALB/c	~70 (mean; VF)	~40 (mean; WT)	Normal	Increased	Yes	Zaleskas et al., 2006
	C57Bl/6	~65 (mean; VF)	~47 (mean; WT)	Normal	Mild increase	Yes	
Mouse	BALB/c	~83 (median; VF)	–	Normal	Increased	Yes	Bumm et al., 2006

B. Transgenic models

V617F species	Construct	Activation	Hct (%)	Hb (g/l)	Platelets (×10⁹/l)	WBC (×10⁹/l)	MF	Reference
Mouse	*H2Kb* promoter	Not inducible	49.9±2.9[a] 42±4.5[b]	>180; 20% mice[a] 100 (mean)[b]	>1400; 35% mice[a] 2500 (mean)[b]	>20; 35% mice[a] 30 (mean)[b]	Yes NA	Shide et al., 2008
Human	*Vav* promoter	Not inducible	50.9±4.42[c] 48±2.87[d]	181±14[c] 165±5.9[d]	2708±712[c] 1278±215[d]	11.8±2.85[c] 9.14±2.63[d]	Yes No	Xing et al., 2008
Human	Minimal human *JAK2* promoter	*Vav*-Cre	47±1.67	164±5.93	3710±488.2	13.06±3.73	Yes	Tiedt et al., 2008
		Mx1-Cre:						
		pIpC ×6	49.33±9.87	161.3±32.33	8883±4461.7	28.63±21.08	Yes	
		pIpC ×3	51.09±6.35	182.2±19.71	2792±1267.2	14.12±8.00	Yes	
		pIpC ×1	61.60±9.10	196.0±42.07	5316±4315.6	35.62±35.57	Yes	

[a,b]Two different founder lines developed by Shide et al. (2008). [c,d]Two different founder lines developed by Xing et al. (2008). Hb, haemoglobin; Hct, haematocrit; MF, myelofibrosis; NA, not applicable; VF, V617F mutation; WBC, white blood cells; WT, wild type.

TABLE 1.1: SUMMARY OF RETROVIRAL OVEREXPRESSION, TRANSPLANTATION AND TRANSGENIC *JAK2* MOUSE MODEL PHENOTYPES.

Republished without modifications under Creative Commons license from Li, J., Kent, D. G., Chen, E. & Green, A. R. Mouse models of myeloproliferative neoplasms: JAK of all grades. Dis Model Mech 4, 311–317 (2011). PMID: 21558064.

Ref.	V617F species	Activation	Mouse background	Allele expression and validation	Animal survival	Het. V617F phenotype	Hom. V617F phenotype	Spleen
Akada et al., 2010	Mouse	pIpC induced	129Sv/C57Bl/6 mix	50% of WT expression; constitutive phosphorylation (Stat5, Erk, Akt)	Some death, unknown cause	PV-like (Hct ~80%; Plt ~1.5×10^{12}/l; WBC ~2- to 3-fold increase)	PV-like (Hct ~80%; Plt ~3.5×10^{12}/l; WBC, ~5- to 7-fold increase)	Enlarged
Mullally et al., 2010	Mouse	Constitutive	129Sv/C57Bl/6 mix	Expression lower than WT	Median survival = 146 days	PV-like (Hct ~80%; Plt, no significant change; WBC ~2-fold increase)	NA	Enlarged
Marty et al., 2010	Mouse	Constitutive	129Sv/C57Bl/6 mix	Expression similar to WT; constitutive phosphorylation (Stat5, Erk)	5 of 11 died (15±3 weeks)	PV-like (Hct ~70%; Plt ~4×10^{12}/l; WBC ~7.3-fold increase)	NA	Enlarged
Li et al., 2010	Human	pIpC induced	129Sv/C57Bl/6 mix	Expression similar to WT; no constitutive pStat5; hypersensitive to Epo	Normal unless transformed	ET-like (Hct ~60%; Plt ~1.6×10^{12}/l; WBC, mild increase; 10% mice transformed to PV or MF)	NA	Not enlarged

Table 2. Continued

Ref.	MF	Disease transplantability[a]	Effect on lineages	Colony formation	Effect on stem/progenitor cells	HSC function
Akada et al., 2010	Mild in het. BM; high in hom. BM; high in het. spleen; high in hom. spleen	Yes (D, backcrossed 4G; R, C57Bl6)	10-fold increased Ter119$^+$CD71$^+$ (20-fold in homozygous); 6- to 10-fold increased Mac1$^+$Gr1$^+$ (only observed in spleen)	Increased: GM (spleen); BFU-e (spleen and BM); GEMM (spleen); EECs (spleen)	2-fold increase LSK (BM and spleen); increased MEPs	NA
Mullally et al., 2010	None in BM or spleen (up to 6 months)	Yes (D, unknown number of backcrosses; R, C57Bl6)	2-fold increased Ter119$^+$CD71$^+$ (BM); 3-fold increased Ter119$^+$CD71$^+$ (spleen); no change in Mac1$^+$Gr1$^+$	Increased: BFU-e; EECs absent	No change LSK; increased L$^-$S$^-$K$^+$ (more MEP and pre-CFU-e)	No difference in competitive BMT (B6 recipients)
Marty et al., 2010	BM and spleen (~30 weeks)	NA	88-fold increase in erythroid precursors; 83-fold increase in myeloid precursors	Increased: G, M, BFU-e, CFU-e; EECs present	NA	NA
Li et al., 2010	None in BM or spleen (up to 6 months)	Yes (D, backcrossed 2G; R, 129SvEvBrd/C57Bl6 F1)	Mild increase in Ter119$^+$CD71$^+$; mild increase in Mac1$^+$Gr1$^+$ (only observed in BM)	Increased: G, M, BFU-e; EECs present	Reduced LSK in aged mice (normal in young)	Reduced function in competitive and non-competitive transplantations (129/B6 F1 recipients)

[a]Donor (D) and recipient (R) backgrounds are shown in parentheses. BFU-e, burst forming unit-erythroid; BM, bone marrow; BMT, bone marrow transplantation; CFU-e, colony forming unit-erythroid; D, donor; EECs, endogenous erythroid colonies; G, CFU-G (granulocytes); GEMM, CFU-GEMM (granulocyte, erythrocyte, macrophage, megakaryocyte); GM, CFU-GM (granulocyte, macrophage); Hct, haematocrit; Het., heterozygous; Hom., homozygous; M, CFU-M (macrophage); MF, myelofibrosis; NA, not applicable; Plt, platelets; R, recipient; WBC, white blood cell; WT, wild type.

TABLE 1.2: SUMMARY OF JAK2^{V617F} KNOCK-IN MOUSE MODELS.

Republished without modifications under Creative Commons license from: Li, J., Kent, D. G., Chen, E. & Green, A. R. Mouse models of myeloproliferative neoplasms: JAK of all grades. Dis Model Mech 4, 311–317 (2011). PMID: 21558064.

CLONAL HETEROGENEITY AND MPN PATHOGENESIS

Despite extensive genomic profiling efforts, the reason why *JAK2*^{V617F} is able to result in three distinct disease entities continues to puzzle investigators in the MPN field. MPN classification approaches reflect this uncertainty. MPN subtypes are diagnosed mainly on arbitrary decision variables based on blood count parameters (such as hemoglobin, hematocrit, or red cell mass). This makes patients with borderline count values difficult to diagnose and to predict the path of disease progression. This is particularly evident in patients presenting with isolated thrombocytosis and increased BM reticulin fibrosis. If they lack other ET/MF characteristics, then these patients can be diagnosed with neither disease despite evidence of a clinically advanced MPN (Beer et al. 2011).

Furthermore, the existence of three distinct disease entities itself is a topic of much debate: PMF could be a separate disease, or it could be an accelerated phase of previously undiagnosed PV or ET and it is not known if these two diseases have differences in pathogenesis or clinical outcome. PMF is clinically undistinguishable from post-ET MF, and the driver mutation frequencies are similar in ET and PMF (Campbell & Green 2006; Wilkins et al. 2008; Beer et al. 2011). Driver mutation status seems insufficient to describe or classify the pathogenesis of MPN on its own.

Disease progression, specifically transformation to AML, also cannot seemingly be attributed to specific genetic aberrations. Some mutations are commonly detected in secondary AML (*IDH1/2, TET2, ASXL1, LNK, TP53, EZH2, IKZF1,* and *RUNX1*).

However, only a handful are associated with worse prognosis in MF, such as: *IDH1/2*, *TET2, ASXL1*, and *TP53* (Abdel-Wahab et al. 2010; Lundberg, Karow, et al. 2014; Vannucchi et al. 2013). The latter are almost always detected in both primary MPN and secondary AML with a prevalence of ~20%. Interestingly, *ASXL1* mutations represent ~22% of MF, but only 5% of PV/ET (Cleary & Kralovics 2013). The frequencies of *TET2* and *IDH1/2* mutations in secondary AML are around 25% and 10% respectively (Abdel-Wahab et al. 2010), while *TP53* mutations are observed at a much higher frequency (45.5%) (Harutyunyan et al. 2011). Deeper molecular and cellular analysis is needed to understand how these genetic events contribute to MPN pathogenesis and disease progression.

MPN As A Model For Clonal Evolution

Mutant cells clonally expand as the result of acquiring hypersensitivity to or independence from mitogenic signals that regulate proliferation, differentiation, and/or survival. All MPNs, regardless of phenotype or driver mutation, share a common cell of origin: the long-term hematopoietic stem cell (LT-HSC). This was uncovered by clonogenity studies performed using primary MPN patient samples, which traced $JAK2^{V617F}$ and MPL^{W515L} mutations to the $CD34^{+}/CD38^{+}$ HSC compartment (Chaligné et al. 2007; Jamieson et al. 2006). BMT assays comparing the disease-propagating capacity of $Jak2^{VF/+}$ LT-HSCs versus short-term HSCs (ST-HSCs) (Mullally et al. 2012) further confirmed these observations.

Since HSCs by definition give rise to every blood cell type, the stem cell origins of MPN further imply that *JAK2*^{V617F} is present in all hematopoietic cell types. Therefore, it is possible that *JAK2*-mutant erythroid, myeloid, megakaryocytic, and even lymphoid (B, T, and Natural Killer) cells, could contribute to the expansion of the mutant clone. This has been borne out in sequencing studies of fractionated MPN patient samples and mouse models of *Jak2/JAK2*^{V617F}-driven disease. Interestingly, erythroid lineage-restricted *Jak2*$^{VF/+}$ expression is sufficient to potentiate aberrant erythroid cell proliferation (Mullally et al. 2012).

BLOODLINES: THE IMPACT OF LINEAGE ON JAK2^{V617F}-DRIVEN MPN

Several clinical studies have profiled the relative abundance of mutant *JAK2* across hematopoietic subsets in MPN patient samples. In many ET/PMF patients, *JAK2*^{V617F} manifests primarily in the megakaryocyte (Mk) lineage, with less significant involvement of erythroid and myeloid cells (Passamonti & Rumi 2009). Importantly, other studies reported impaired clinical outcomes and disease progression in a cohort of ET/MF patients with a relatively low fraction of mutant cells (Moliterno et al. 2006; Tefferi et al. 2008). However, these studies only determine the net effect of mutant HSC output, and no definitive conclusions can be made, as there are also reported cases of low *JAK2* allele burden PV (Tefferi et al. 2008).

This section will discuss several inter-related factors identified to date, beyond allele burden, that influence the phenotypic presentation of *JAK2*^{V617F}-mutant MPN.

JAK2^{V617F} Gene Dosage

Along with the discovery of *JAK2*^{V617F}, it was noted that while most cells in MPN patients are heterozygous for the mutation, a small proportion (of mostly PV cases) showed homozygosity for *JAK2*^{V617F}. For *JAK2*^{V617F}, homozygosity did not seemingly arise from classical loss of heterozygosity mechanisms. Instead, *JAK2*^{V617F} homozygosity arises from acquired uniparental disomy (Kralovics et al. 2005). Homozygous *JAK2*^{V617F} erythroid clones are observed in PV patient samples, and only rarely in ET (Scott et al. 2006). These data, concordant with observations in mouse models of homozygous versus heterozygous expression, suggest that *JAK2*^{V617F} gene dosage contribute to MPN heterogeneity by promoting a more predominant erythroid phenotype. While causal conclusions have been difficult to make, the expression level of *JAK2*^{V617F} across hematopoiesis seems to play a role in regulating disease presentation (Li et al. 2014).

Incidents of transformation of ET to PV are reported, most commonly in *JAK2*^{V617F}-mutant disease. This occurred in 5% of ET patients in a large patient cohort (Barbui et al. 2015). Evidence from murine studies suggests that this could be due to conversion from a *JAK2*^{V617F} heterozygous to homozygous state (Li et al. 2014), but the molecular basis of this conversion remains unknown. Furthermore, it is possible that the clinical cases of transformed ET could represent a “masked PV” state (Barbui et al. 2014), rather than a bona fide transformed disease. Collectively, these observations point to a hypothetical model where low levels of *JAK2*^{V617F} promote a more ET-like presentation, while higher levels are associated with PV and increased erythroid burden.

Downstream JAK2 Signaling

Mutant *JAK2* activates several signaling cascades, including MAPK, RAS, and PI3K, in addition to canonical STAT activation. In addition to gene dosage, collateral signaling pathway activation, and even differential STAT activation, could also contribute to drive the phenotypic diversity of MPN (**Figure 1.4**). Using clonally-derived MPN patient samples, Chen et al elegantly demonstrated that heterozygous $JAK2^{V617F}$-mutant erythroid colonies from PV and ET patients exhibited differential signaling responses (E. Chen et al. 2010). This study specifically pointed to a differential response via STAT1 – mainly, that an ET-like phenotype is accompanied by enhanced STAT1 activity resulting in increased megakaryocytic differentiation and a repression of erythroid differentiation. The role of additional downstream signaling moieties, specifically STAT5, has also been examined in relation to $JAK2^{V617F}$-mutant PV (Funakoshi-Tago et al. 2010; Yan et al. 2012; Walz et al. 2012). While STAT5 seems to be more crucial for potentiating PV, Stat1 and Stat3 activation is more relevant to ET pathogenesis (**Figure 1.4**). However, the precise mechanisms underlying differential STAT activation, as well as the downstream effects on transcription and HSPC differentiation/proliferation, remain unclear.

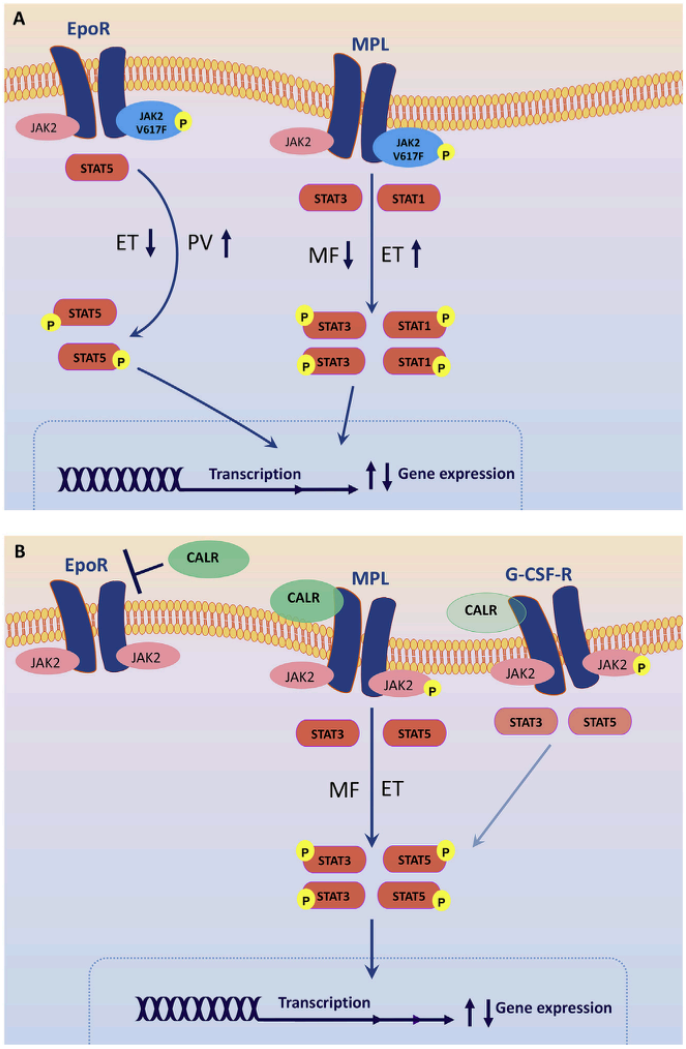

FIGURE 1.4: DIFFERENTIAL STAT ACTIVATION IN MPNS.

JAK2^{V617F}, when phosphorylated, activates STAT proteins. **(A)** In PV, JAK2^{V617F} binds to EPOR in the cytosol causing an increase in STAT5 activation. In ET, JAK2^{V617F} binding to MPL causes increased STAT1 and STAT3 but decreased STAT5 activation. In MF, reduced activation occurs in STAT3. **(B)** In *CALR*-mutant MPN, CALR binds directly to MPL, signaling through JAK2 to upregulate STAT3 and STAT5. It binds weakly to G-CSFR to activate these STAT proteins but does not bind to EPOR explaining only ET and MF phenotypes associated with CALR mutations.

Republished with permission from Elsevier. Image from: O'Sullivan, J. & Mead, A. J. Heterogeneity in myeloproliferative neoplasms: Causes and consequences. Adv Biol Regul 71, 55–68 (2019). PMID: 30528537.

Of One, Many: HSC Heterogeneity In MPN Pathogenesis

The "target" cell that acquires *JAK2*^{V617F} may also contribute to MPN heterogeneity. While clonality studies and successive accumulated evidence from both patients and mouse models have traced *JAK2*^{V617F} and other MPN driver mutations to the LT-HSC compartment, the effect of these mutations on HSC self-renewal and differentiation capacity is less straight-forward. Regardless of the effect of *JAK2*^{V617F} on normal HSCs, the disease-initiating potential (in transplantation models) is largely confined to the HSC compartment, as progenitor cell transplantation fails to recapitulate disease in secondary recipient mice (Mullally et al. 2012; Mullally et al. 2010).

However, the exact type of HSC that acquires *JAK2*^{V617F} might be important in disease pathogenesis. The HSC pool is highly heterogeneous, with many HSCs carrying inherent bias in their default lineage output (Eaves 2015). The acquisition of *JAK2*^{V617F} in a lineage-biased HSC, such as a platelet-biased HSC (Sanjuan-Pla et al. 2013), might result in ET, whereas acquisition in a more "balanced" or less-biased HSC might favor a PV phenotype (**Figure 1.5**). Initial evidence supporting this possibility comes from single-cell transplantation studies, which demonstrated that individual *JAK2*^{V617F}-mutant HSCs from a mouse model can induce a variety of different phenotypes upon transplantation into secondary recipients (Lundberg, Takizawa, et al. 2014). The effects of aging on mutant HSCs are also a potential source of variability, as platelet-biased HSCs increase with age, at least in mice (Grover et al. 2016; de Haan & Lazare 2018). Therefore, the lineage bias of the mutant HSC clone could influence MPN heterogeneity.

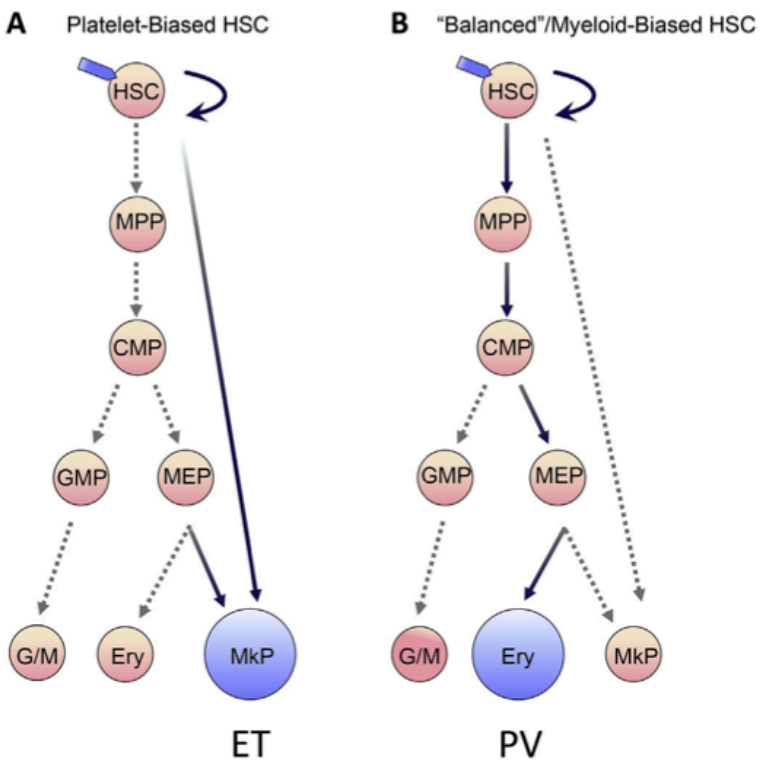

FIGURE 1.5: SCHEMATIC INFLUENCE OF "TARGET" HSCS ON DISEASE PHENOTYPE

(A) The disease-driving mutation is acquired in a platelet-biased HSC producing an excess of megakaryocytes and platelets producing an ET phenotype. **(B)** The disease-driving mutation is acquired in a myeloid-biased or "balanced" HSC with an expansion of erythroid progenitors producing a PV phenotype.

Republished with permission from Elsevier. Image from: O'Sullivan, J. & Mead, A. J. Heterogeneity in myeloproliferative neoplasms: Causes and consequences. *Adv Biol Regul* 71, 55–68 (2019). PMID: *30528537.*

SELECTIVE PRESSURE PROMOTES CLONAL EXPANSION

While *JAK2*^{V617F} clearly initiates MPN, the penetrance of this mutation in the general population is fairly low (Vainchenker & Kralovics 2017). Furthermore, recent studies of patients with clonal hematopoiesis reveal that a significant population of individuals with *JAK2*^{V617F} will never develop a fulminant MPN (Genovese et al. 2014; Jaiswal et al. 2014; Xie et al. 2014). This suggests that additional events, either intrinsic or extrinsic to the MPN clone, must co-occur to promote clonal expansion and disease initiation.

These observations favor a selective pressure model of MPN evolution. In this model (**Figure 1.6**), a single HSC acquires *JAK2*^{V617F} and gives rise to a rapidly growing clone that lacks inherent self-renewal capacity. Each cell in the mutant clone is then subject to selective pressure to acquire a self-renewal advantage to accommodate increased replicative stress. The *JAK2*^{V617F}-mutant clone would then proliferate and differentiate to create a large population of heterogeneous cells that could acquire additional secondary events. Furthermore, the mutant clone needs to establish a self-reinforcing bone marrow niche, to favor MPN stem cells over normal HSCs. The distinct disease presentation would thus be the net effect of the lineage biases displayed by the heterogeneous stem/progenitor pool that acquired a clonal advantage (Prick et al. 2014; Mead & Mullally 2017). However, one key limitation of this model as-written is the assumption that acquisition of *JAK2*^{V617F} occurs before any other genetic events.

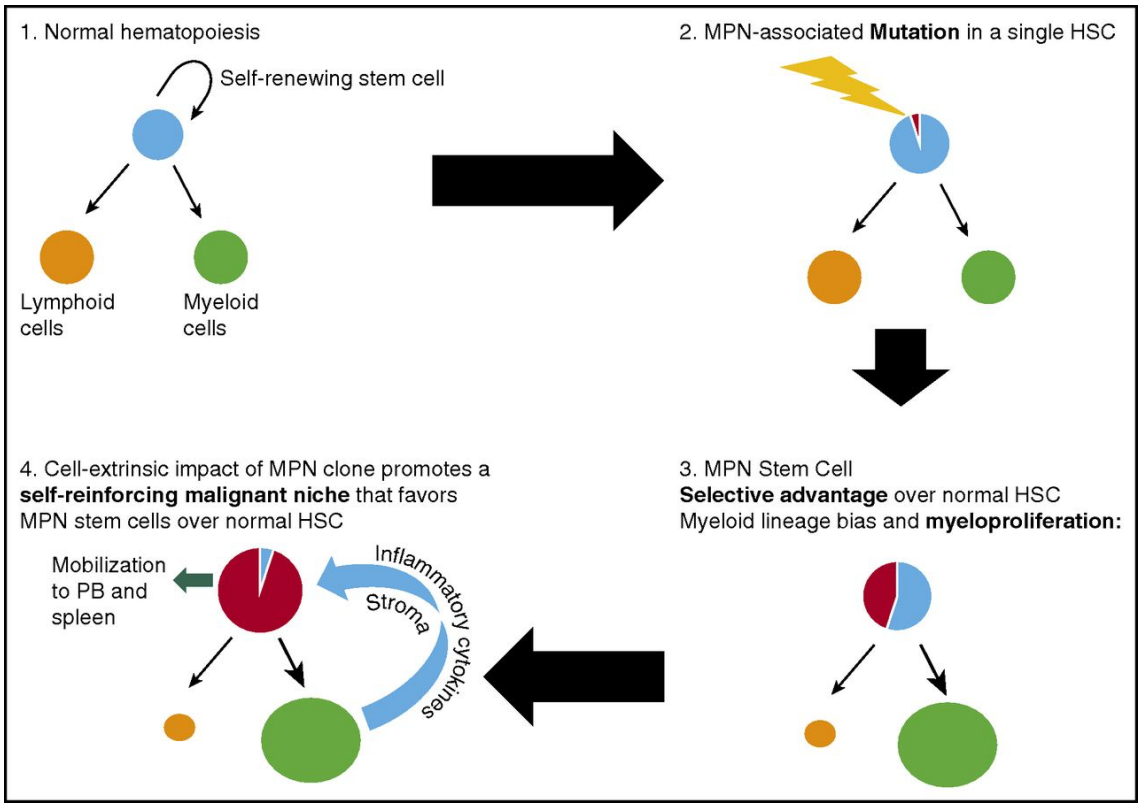

FIGURE 1.6: KEY STEPS DURING MPN DEVELOPMENT FROM NORMAL HEMATOPOIESIS FOLLOWING ACQUISITION OF AN MPN-INITIATING MUTATION IN A SINGLE HSC.

The mutant HSC acquires a selective advantage over normal HSC and also promotes myeloid differentiation, eventually leading to a myeloproliferative phenotype. The expanded, abnormal myeloid clone disrupts the bone marrow microenvironment, promoting a self-reinforcing malignant niche that favors MPN stem cells over normal HSC and leads to eventual mobilization of MPN HSC into the peripheral blood (PB).

Republished with permission from the American Society of Hematology. Image from: Mead A.J., Mullally A. Myeloproliferative neoplasm stem cells. Blood 129, 1607–1616 (2017). PMID: 28159736.

The work in this thesis is focused on addressing: 1) the role of mutant Mks in reinforcing a bone marrow niche that favors neoplasia, and 2) the role of co-occurring *ASXL1* mutations in conferring a selective advantage to *JAK2*^{V617F}-mutant stem cells. The rationale for each of these specific factors is addressed in the following sections.

INFLAMMATION PROMOTES CLONAL EXPANSION

All MPNs, and PMF in particular, are associated with a pathologic inflammatory state. High plasma levels of pro-inflammatory cytokines are observed in MPN patients, and anti-inflammatory therapies, including the type I JAK2 kinase inhibitor Ruxolitinib, are incredibly efficacious at alleviating the bulk constitutional symptoms of MPN (Tefferi 2005; Tefferi et al. 2011). Evidence in patient samples and MPN mouse models indicates that these cytokines are produced by both mutant and non-mutant hematopoietic cells, and this aberrant cytokine production is caused, at least in part, by aberrant JAK/STAT pathway activation (Kleppe et al. 2015). In MF, increased levels of proinflammatory cytokines (specifically TNF-α and TGF-β, which both negatively regulate HSCs) are elevated and produced by both the malignant clone and surrounding stromal cells (Pronk et al. 2011; Blank & Karlsson 2015). These observations raise the compelling idea that the *JAK2*-mutant clone interacts with and promotes the aberrant expansion of the wild type hematopoietic milieu.

THE BONE MARROW MICROENVIRONMENT AND MPN PATHOGENESIS

The BM microenvironment is essential for maintaining a healthy HSC pool (Calvi & Link 2015). Perturbation of the normal BM niche is known to promote the development of hematologic malignancies, and an increasing body of work is accumulating regarding the role of the microenvironment in MPN pathogenesis and heterogeneity (Schmitt-Graeff et al. 2015). A wide range of cell types comprise the niche, and clonal MPN HSCs are capable of re-wiring these interactions to allow further malignant expansion, creating a "self-reinforcing niche". A direct role of a malignant vascular niche in MPN propagation has been demonstrated, in a *Jak2*^{V617F}-mutant mouse model of mutant endothelial cells (Zhan et al. 2018). In this model, mutant endothelial cells express higher levels of CXCL-12 and SCF, which are essential for HSC survival. In this way, a mutant vascular niche can potentiate clonal expansion in MPN.

JAK2^{V617F}-mutant HSCs themselves can also produce niche remodeling factors. Mutant HSCs produce IL-1β, which results in neural damage and a reduction in Nestin-positive mesenchymal stem cells (Arranz et al. 2014), which permits the further clonal expansion of mutant HSCs in a self-perpetuating vicious cycle. Studies of patient samples have also indicated that the mesenchymal niche in MPN patients differs in its ability to support HSPC proliferation, versus healthy controls (Ramos et al. 2017).

These alterations to the niche not only promote disease progression overall, but also contribute to disease heterogeneity. This is evidence by the observation that PV and ET

patients have slightly different cytokine profiles, with TNF-α only elevated in *JAK2*^{V617F}-mutant patients (Pourcelot et al. 2014). Furthermore, bulk assessment of the BM niche in ET and PV cases has revealed several differences. Intravital microscopy detected that mutant HSCPs in ET and PV occupy distinct niches – ET HSPCs move faster and towards and endosteal niche than PV HSCPs (Korn et al. 2018). Furthermore, non-endosteal sinusoids where dilated in PV but not in ET. These observations suggest that different MPN niches impact the phenotypic heterogeneity of MPN. However, it is unclear if microenvironmental changes are a driver of MPN heterogeneity, or simply an epiphenomenon that reflects the underlying disease state.

MEGAKARYOCYTES AND THE HSC NICHE

Megakaryocytes (Mks) are rare, large, multinucleated cells that reside primarily in the bone marrow and give rise to discoid, anucleated platelets. These descendant platelets have well-studied essential roles on thrombosis and hemostasis in the periphery, but their parent Mks are increasingly appreciated as key components of the sinusoidal HSC niche.

BM Mks are intimately associated with BM sinusoidal endothelium, extending cytoplasmic protrusions into the sinusoids. Several studies suggested an indirect role for Mks in HSC regulation. These studies assessed BM/hematopoietic recovery after irradiation stress. One study found that HSCs reside preferentially near Mks after transplantation in to irradiated mice (Heazlewood et al. 2013). Furthermore, Mk inhibition impaired HSC engraftment in primary and competitive secondary transplantation experiments (Olson et

al. 2013). Mks are required for osteoblast expansion after irradiation, so it was initially suggested that Mks regulate HSC engraftment indirectly by expanding osteoblastic niches to make them more favorable (Olson et al. 2013).

Further studies have revealed a direct role for Mks in HSC regulation. Two concurrent studies revealed that Mks can regulate HSC quiescence in a paracrine manner (Bruns et al. 2014; M. Zhao et al. 2014; Nakamura-Ishizu et al. 2015). 20% of cells expressing HSC surface markers were directly adjacent to Mks. Both studies also selectively ablated $Pf4^+/Cxcl4^+$ cells (Cxcl4 is a chemokine that is highly enriched in Mks), which increased HSC cycling and overall frequency. While some differences were observed based on the analysis schema used, both studies reported that the frequency of HSCs with long-term repopulating capacity was the most strongly affected. Bruns et al showed that this effect was mediated directly by Mk-derived Cxcl4. Schwann cell-derived TGF-β was previously implicated in regulating HSC quiescence (Yamazaki et al. 2011); Zhao et al further showed that HSC-adjacent Mks are also contributing sources of TGF-β. Zhao et al also found that Mk-derived FGF1 induces HSC proliferation and enhances HSC recovery after myeloablative stress. Thus, Mks can produce a variety of factors that can both negatively (CXCL4 and TGF-β) and positively (FGF1) regulate HSC proliferation.

Earlier reports from our lab also revealed that *Jak2*-deficient Mks act as negative regulators of HSC expansion *in vivo* (Meyer et al. 2014). In *Pf4-Cre*$^+$*; Jak2*$^{-/-}$ mice, we observed a marked expansion of the HSPC compartment, in addition to paradoxical Mk expansion in the BM and thrombocytosis. These observations suggest that JAK2 activity

in Mks contributes to their HSC niche functions. Beyond their roles in normal hematopoiesis, Mks also have been implicated in disease states.

MEGAKARYOCYTES PROMOTE MYELOID NEOPLASIA

While Mks participate in MPN evolution directly by increasing platelet production (particularly in the setting of ET) , accumulating evidence points to an indirect role for this lineage in MPN pathogenesis. Abnormal Mks are a common feature of MPNs, regardless of driver mutation status or disease phenotype (Ciurea et al. 2007). A growing body of work indicates that megakaryocytic hyperplasia, and eventual dysplasia, plays a central role in MPN pathogenesis (summarized in **Figure 1.7**). While Mks can also affect inflammatory processes and osteogenesis, this thesis will focus on the role of Mks in niche remodeling and on HSC function as it relates to MPN pathogenesis.

The most well-studied role of Mks is in niche remodeling during MPN pathogenesis. Clonal Mks are known to produce VEGF and TNF-α, which promotes increased angiogenesis and fibroblast proliferation, ultimately potentiating the development of BM fibrosis (Di Buduo et al. 2015). Furthermore, Mk-derived TGF-β1 also contributes to the establishment of bone marrow fibrosis (Wen et al. 2015; Zahr et al. 2016).

Further studies have shown a direct role for mutant Mks in promoting the clonal expansion of the MPN stem cell pool. Additional work indicates that *JAK2*^{V617F}-mutant Mks can

directly promote hyper-proliferation of the *Jak2*^{WT} HSPC compartment (Zhan et al. 2016; Zhang et al. 2018). In these studies, Mk lineage-restricted expression of mutant *Jak2* (Tiedt et al. 2008) resulted in a myeloproliferative disorder that most closely resembled human ET. This MPD phenotype was accompanied by an expansion of the bulk HSPC compartment. Furthermore, they observed Mk hyperplasia and broad alterations to the composition and architecture of the BM vascular and sinusoidal niches. They also observed that mutant Mks (relative to wild type Mks) produced increased levels of several cytokines/chemokines with well-established functions in regulating HSC quiescence and proliferation. These include: CXCL12, FGF1, PF4, TGF-β1, and VEGF-α (Zhan et al. 2016).

A follow-up study revealed that mutant Mks promoted increased expansion and engraftment of mutant HSPCs in competitive transplantation assays, further suggesting that mutant Mks enable clonal expansion. These functions of mutant Mks were dependent on TPO/MPL signaling upstream of JAK2, as genetic deletion of either Tpo or its cognate receptor rescued both the myeloproliferative disorder and HSPC expansion (Zhang et al. 2018).

These studies collectively suggest the potential ability of *JAK2*-mutant Mks to promote disease evolution in a cell non-autonomous manner. They further imply that mutant Mks can promote the clonal expansion of both wild type and MPN stem cells during MPN initiation. This possibility was the objective of the studies in Chapter 3 of this dissertation.

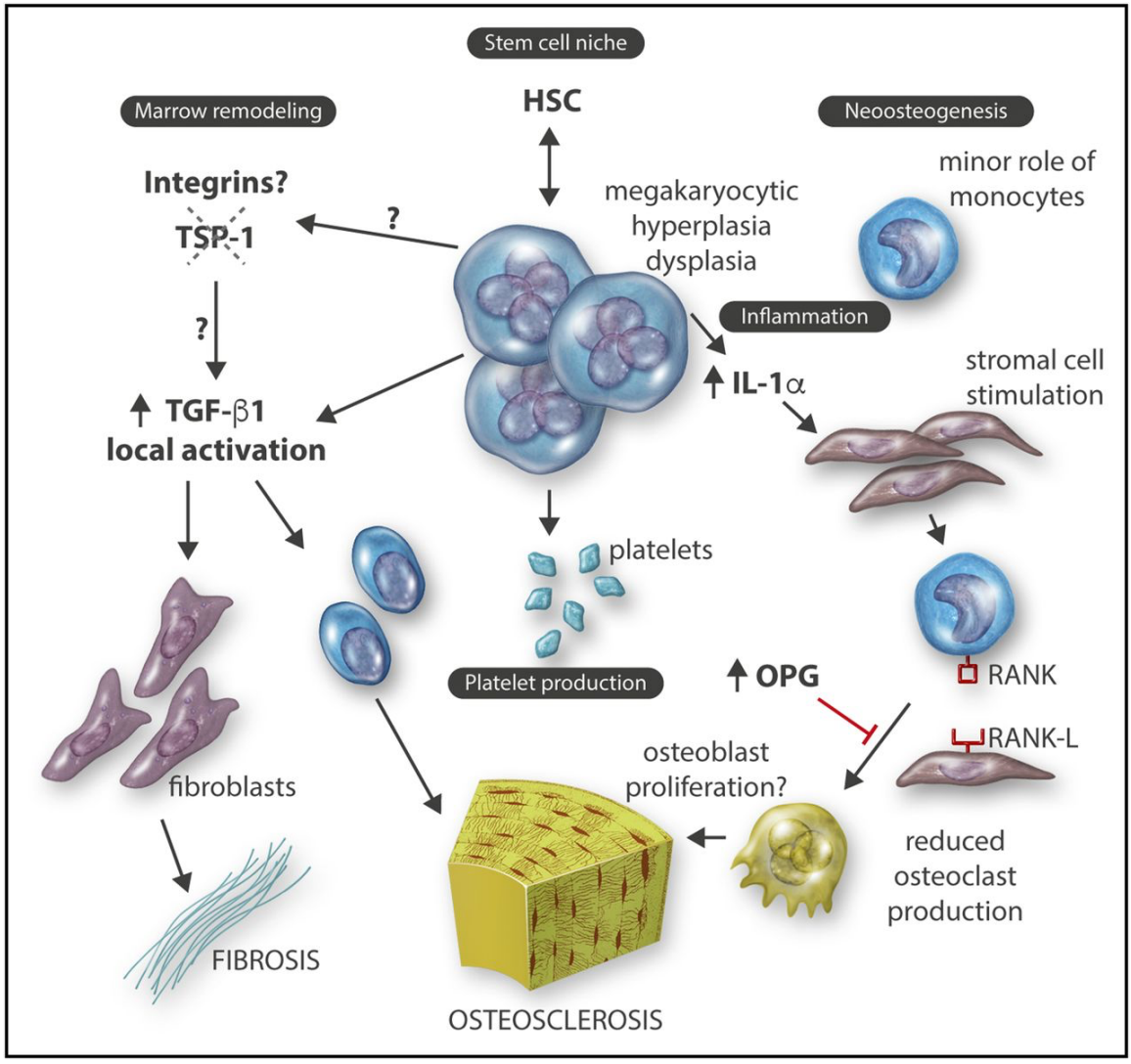

FIGURE 1.7: MEGAKARYOCYTES PLAY A CENTRAL ROLE IN MPN PATHOGENESIS

The MPL/JAK2 pathway is activated by the 3 MPN-restricted mutations (JAK2^{V617F}, CALR mutants, and MPL mutants) placing MK hyperplasia and eventually dysplasia as a central determinant in MPN. MKs are mainly involved in platelet production, and also play an important role in the hematopoietic niche by regulating HSCs, remodeling the marrow by secretion of TGF-β1 and other cytokines (platelet-derived growth factor [PDGF], vascular endothelial growth factor [VEGF]) which ultimately lead to MF, and also inducing a neo-osteogenesis by inducing an osteoblastic differentiation through TGF-β1 and inhibiting osteoclast differentiation through osteoprotegerin. Furthermore, MKs secrete numerous inflammatory cytokines such as IL1α. The mechanisms of local activation of TGF-β1 are poorly known.

Republished with permission from the American Society for Hematology. Image from Vainchenker, W. & Kralovics, R. Genetic basis and molecular pathophysiology of classical myeloproliferative neoplasms. Blood 129, 667 (2017). PMID: 28028029.

PARTNERS IN CRIME: CO-OCCURRING MUTATIONS PROMOTE DISEASE PROGRESSION AND EVOLUTION

The presence of additional somatic non-driver mutations also influences the biology of the MPN clone. These additional MPN disease alleles affect not only the manner in which the disease manifests, but they can also dramatically influence patient prognosis and overall outcome. Co-occurring mutations can confer myelodysplastic features and increase overall disease severity. A number of these events, such as loss of *TET2*, *DNMT3A*, or *EZH2*, and mutant *IDH1/2, P53*, or *SRSF2,* have been studied in great detail (Rampal, Ahn, et al. 2014; Stegelmann et al. 2010; Vannucchi et al. 2013). This thesis will focus on cooperating mutations that affect PRC2-mediated histone modifications and gene repression, specifically *ASXL1*.

ABERRANT PRC2 ACTIVITY PROMOTES PROGRESSION TO MYELOFIBROSIS

Loss-of-function mutations and cytogenetic lesions in *EZH2* and other PRC2 members (*SUZ12*, *JARID2*, *EED*) have been described in MPNs and across all myeloid malignancies (Ernst et al. 2010; Puda et al. 2012). EZH2 is one of the two histone methyltransferases that catalyzes activity of the Polycomb Repressive Complex 2 (PRC2), which is the primary "writer" of the repressive H3K27me3 histone mark. *EZH2* mutations occur in 5-10% of PMF, are closely associated with *JAK2*^{V617F} mutation status, and predict for worse patient prognosis (Guglielmelli et al. 2011).

Recent studies have investigated the consequences of concomitant *Ezh2* loss in *JAK2*^{V617F} mouse models (Sashida et al. 2016; Shimizu et al. 2016; Yang et al. 2016). All three of these models showed potent cooperativity between *Ezh2* loss and *Jak2*^{V617F} – survival was markedly reduced, and mice also showed rapid acceleration of the disease to myelofibrosis. *Ezh2* loss also facilitated MPN initiation by increasing the fitness of *Jak2*^{V617F}-mutant stem cells. These phenotypic changes were a consequence of altered PRC2 target gene expression. Collectively, these observations indicate that cooperating mutations in epigenetic regulators alter MPN pathogenesis by influencing stem cell differentiation and self-renewal capacity.

Addition Of Sex Combs-Like 1 (ASXL1)

The ASXL Family

ASXL1 encodes a chromatin binder and epigenetic regulator belonging to the human *ASXL* gene family. This family is comprised of three total members: *ASXL1, ASXL2,* and *ASXL3* (Fisher et al. 2003; Masuko Katoh & Masaru Katoh 2003; Masuko Katoh & Masaru Katoh 2004). The ASXL proteins all have a similar architecture of domains, including an N-terminal ASXH homology domain, central ASXM1 and ASXM2 domains, and a C-terminal plant homology domain (PHD) (M Katoh 2013). The ASXH domain is specific to the ASXL family and is similar to the Forkhead-box (FOX) domain that is predicted to have a role in DNA binding. Other data suggests that the N-terminal domain may also contain a unique DNA binding motif called the HARE-HTH (HB1, ASXL1, restriction endonuclease helix-turn-helix domain) (Aravind & Iyer 2012). The ASXH domain facilitates protein-

protein interactions, including the well-studied interaction of ASXL1 with Polycomb Deubiquitinase complex member BRCA1-Associated Protein 1 (BAP1) (Scheuermann et al. 2010; Sanchez-Pulido et al. 2012). The PHD domain is also unique to the ASXL family and is predicted to recognize histone H3 tails via methylated lysines. The central ASXM1 and ASXM2 domains are also hypothesized to serve as modulators of protein-protein interactions and may coordinate interaction with NCOA1 and nuclear hormone receptors (M Katoh 2013). The roles of these domains have not yet been fully elucidated. The sequence of ASXL1, ASXL2, and ASXL3 is divergent in regions not included in the conserved domain structures, and the level of functional redundancy between the human ASXL family members is still not known.

The ASXL family of proteins are mammalian homologs of *Drosophila Asx* (*Additional sex combs). Asx* knockout in *Drosophila melanogaster* results in posterior and anterior homeotic transformations which phenocopies deletion of repressive PcG (Polycomb) and activating Trithorax genes, respectively (Sinclair et al. 1992; Simon et al. 1992; Sinclair et al. 1998). These data led to the hypothesis that *Asx* can mediate both the repression and activation of homeobox genes. Several studies strongly suggest that mammalian ASXL1 primarily regulates Polycomb activity in hematopoietic cells (Abdel-Wahab et al. 2012; Davies et al. 2013; Abdel-Wahab et al. 2013; Wang et al. 2014). These studies do not exclude the possibility that ASXL1 could promote homeobox gene activation in other cellular contexts.

In mammalian systems, ASXL1 exerts a wide range of functions related to chromatin binding and gene expression and is capable of both activating and repressing gene

expression. Among its most well-studied interactions are with the Polycomb repressive complexes, which modify histones to regulate gene activation or repression. In myeloid cells, reports indicate that ASXL1 directly interacts with Enhancer of Zeste 2 (EZH2) to mediate the recruitment of Polycomb Repressive Complex 2 (PRC2) to target loci (Abdel-Wahab et al. 2012). In this context, ASXL1 depletion led to impaired PRC2 recruitment to target loci, and a concomitant decrease in the repressive H3K27me3 mark and elevated expression of PRC2 targets.

Another one of ASXL1's most-studied interacting partners is *BRCA1*-Associated Protein 1, or BAP1. Together, ASXL1 and BAP1 coordinate to remove the repressive H2AK119-Ubiquitin mark from chromatin (Machida et al. 2009; Sowa et al. 2009; Dey et al. 2012). H2AK119Ub is placed/written on chromatin by Polycomb Repressive Complex 1 (PRC1). This mark effectively "locks" chromatin in a repressive state (Scheuermann et al. 2010). Together, BAP1 and ASXL1 comprise a Polycomb Repressive Deubiqutinase Complex (PR-DUB), with BAP1 serving as the catalytic component, that removes H2AK119Ub to potentiate transcriptional activation. *ASXL1* knockdown studies show inconsistent decreases in global H2A119Ub levels in hematopoietic cells, however. Thus, the relevance of this particular ASXL1 function in myeloid cell transformation and leukemogenesis is not clear.

Proteomic studies also show that ASXL1 can also form a core complex with BAP1, composed of HCF-1, OGT, and other factors to influence transcription factor activity (Yu et al. 2010). The composition and net transcriptional effect of these complexes is highly cell type and cell state-specific. In non-hematopoietic contexts, ASXL1 also cooperates

with Heterochromatin Protein 1-α (HP1α) and Lysine-specific Histone Demethylase 1 (LSD1) to repress Retinoic Acid Receptor-α (RARα) and Peroxisome Proliferation Activity Receptor-γ (PPARγ) to inhibit lipogenesis (Cho et al. 2006; Lee et al. 2010; U.-H. Park et al. 2011).

Thus, *ASXL1* is an epigenetic regulator that can exert a diverse range of effects on gene expression, by either altering chromatin state via histone modifications or by altering transcription factor complex composition/activity.

ASXL1 Is A Myeloid Tumor Suppressor

Recurrent somatic mutations in *ASXL1* are detected across the spectrum of myeloid malignancies. This includes MDS, CMML, MF, MDS/MPN overlap disorders, and secondary AML transforming from MDS. *ASXL1* mutations occur in about 45% of CMML (Abdel-Wahab et al. 2011; Gelsi-Boyer et al. 2009), 35% of myelofibrosis (Abdel-Wahab et al. 2011), 15-20% of MDS (Gelsi-Boyer et al. 2009; Thol et al. 2011; Bejar et al. 2011), 40-60% of MDS/MPN overlap syndrome (Meggendorfer et al. 2013), 30% of AML transformed from MDS (Abdel-Wahab et al. 2010), and 6% of *de novo* AML cases (Metzeler et al. 2011; Patel et al. 2012). Numerous reports indicate that *ASXL1* mutations are associated with adverse overall survival (Vannucchi et al. 2013; Thol et al. 2011; Metzeler et al. 2011; Yonal-Hindilerden et al. 2015). In MF in particular, *ASXL1* mutant patients are at high-risk for leukemic transformation (Vannucchi et al. 2013).

The *ASXL1* mutations seen in myeloid malignancies are typically heterozygous frameshift or nonsense mutations which cluster in the C-terminal domain (Abdel-Wahab et al. 2011). It is largely accepted that these mutations lead to a truncated transcript that typically lacks the PHD domain and undergoes nonsense-mediated decay. Missense mutations in *ASXL1* are scattered across the protein, which strongly suggests that these mutations are largely loss of function events. This has led to the (still controversial) hypothesis that *ASXL1* is a myeloid tumor suppressor.

Since the majority of *ASXL1* mutations are frameshift or nonsense events, it is possible that these mutations could produce a truncated protein product with gain of function capabilities or altered function. Expression of a C-terminal truncated ASXL1 mutant in retroviral mouse BMT models yields an MDS-like phenotype (Inoue et al. 2013). Other work indicates that expression of truncated ASXL1 proteins in conjunction with BAP1 also results in an MDS-like disease. The authors propose that the C-terminal domain of ASXL1 has autoinhibitory capabilities, with deletion of the C terminus resulting in a hyperactive protein. About 88% of the ASXL1 mutations in the COSMIC database are frameshift mutations, and this enrichment could mean that it is advantageous to lose the C-terminus (Balasubramani et al. 2015).

Modeling *ASXL1* Loss

Murine *Asxl1* shares 81% sequence homology with human *ASXL1*, and the domain architecture is highly-conserved (Fisher et al. 2006). The first loss of function mouse model studying the role of *Asxl1* in normal hematopoiesis was generated by targeted insertion of

a neo cassette into the *Asxl1* locus. Constitutive deletion of *Asxl1* resulted in partial perinatal lethality. The remaining viable mice develop B and T cell abnormalities, and also display myeloid differentiation defects. However, hematopoietic repopulation experiments showed that *Asxl1* knock-out did not affect long-term hematopoietic reconstitution (Fisher, Pineault, et al. 2010; Fisher, Lee, et al. 2010). Homozygous germline *Asxl1* deletion (using *Ella-Cre*) caused embryonic lethality at embryonic day E19.5 (Abdel-Wahab et al. 2013). Knockout embryos all showed severe cranio-skeletal abnormalities, which were consistent with the presentation of Bohring-Opitz syndrome patients. Bohring Opitz syndrome is a congenital developmental disorder caused by de novo and germline *ASXL1* mutations (Hoischen et al. 2011).

Hematopoietic cell-specific *Asxl1* deletion in adult mice, using either *Vav*-Cre or *Mx1*-Cre, caused a progressive hematopoietic disorder with MDS-like features, including cytopenia. This effect is accelerated upon transplantation into secondary or tertiary recipients (Abdel-Wahab et al. 2013). In a follow-up model of constitutive *Asxl1* deletion, mice surviving to adulthood also developed a similar progressive hematopoietic malignancy (Wang et al. 2014).

Asxl1 deletion increases the frequency of HSPCs but impairs their self-renewal capacity (Abdel-Wahab et al. 2013; Wang et al. 2014). This is observed both *in vitro* in colony formation and serial replating assays, and *in vivo* in competitive BMT assays to assess long-term hematopoietic reconstitution capacity. However, this effect is relatively mild when *Asxl1* loss occurs in isolation. Cooperating events likely compensate for these effects on HSPCs in order to facilitate evolution to a fulminant neoplastic or dysplastic

state. Consistent with this, concomitant *Tet2* loss in Asxl1 knock-out mice rescues the stem cell self-renewal defect, but promotes worsened overall disease as compared to loss of either allele as a single event (Abdel-Wahab et al. 2013). Studies using *Asxl1* truncation mutants also demonstrate that *Asxl1* loss cooperates with *Tet2* loss to generate a worsened myelodysplastic state (Balasubramani et al. 2015).

In a massive sequencing study, 483 European patients and 396 Mayo Clinic primary myelofibrosis patient samples were assessed for mutation status and prognosis of the identified somatic alterations. *ASXL1* mutations were identified in about 22% of patients; *JAK2* activating mutations were found in about 60% of patients. *ASXL1* and *JAK2* mutations were the most common somatic alterations to co-occur in primary myelofibrosis patients (Vannucchi et al. 2013). Strikingly, a majority of these patients were determined to be high risk. In this large cohort of patients, the only significant indicator of poor prognosis was ASXL1 mutational status. These data have been validated by other studies.

While *ASXL1* clearly contributes to clonal evolution during MPN pathogenesis (**Figure 1.8**), its precise effect on $JAK2^{V617F}$ mutant stem cells remains poorly understood. Our efforts to better understand these effects are discussed in Chapter 4.

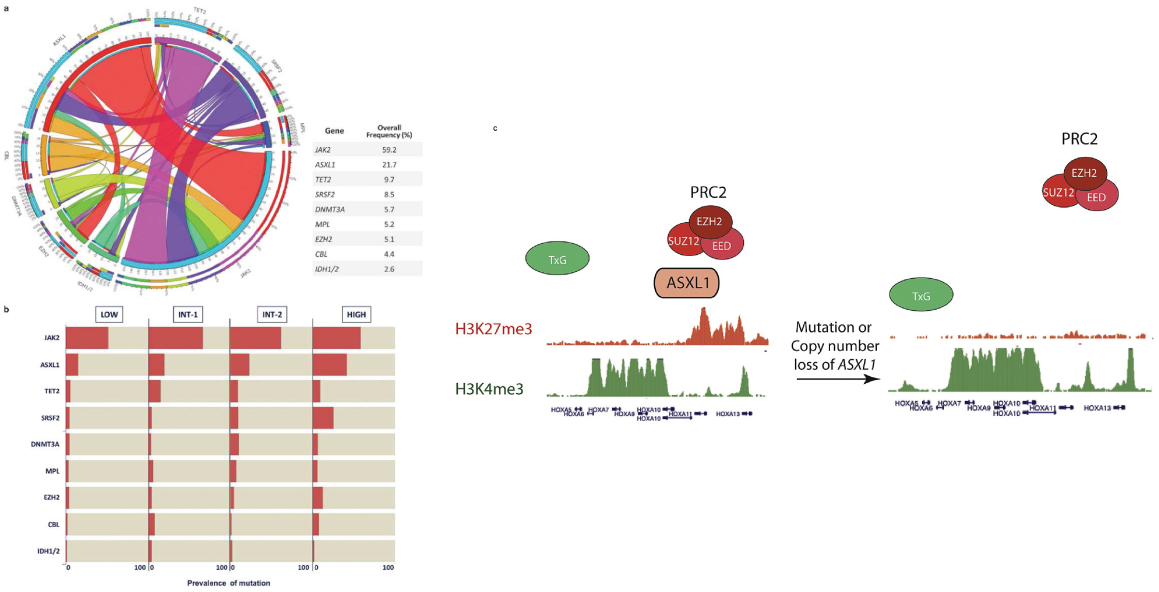

FIGURE 1.8: *ASXL1* LOSS COOPERATES WITH *JAK2*^{V617F}

(A) ASXL1 mutations are among the most frequently co-occurring mutations with JAK2^{V617F} in MF, and **(B)** frequently predict for high-risk disease. **(C)** ASXL1 loss promotes myeloid cell transformation, at least in part, by a loss of PRC2-mediated gene repression.

Reprinted with permission from Springer Nature and Elsevier. Image from: ***(A/B)*** *Vannucchi, A.M. et al. Mutations and prognosis in primary myelofibrosis. Leukemia 27, 1861–1869 (2013). PMID: 23619563.* ***(C)*** *Abdel-Wahab, O. et al. ASXL1 mutations promote myeloid transformation through loss of PRC2-mediated gene repression. Cancer Cell 22, 180–193 (2012). PMID: 22897849.*

SUMMARY

While the genetic determinants of MPN pathogenesis are well-described, there is a complex range of additional factors that influence the manifestation and course of *JAK2V617F*-mutant MPN. Existing pre-clinical models, while useful for identifying new therapeutic strategies, are limited. They rely on pan-hematopoietic $JAK2^{V617F}$ expression, and this context makes it difficult to discern the contributions of specific hematopoietic lineages (beyond HSCs) to MPN initiation, progression, and therapeutic response. The primary goal of this dissertation is to better model and understand the complex and dynamic forces that affect the initiation and progression of $JAK2^{V617F}$-driven myeloid malignancies.

In this dissertation, we generated several novel murine MPN models to investigate additional factors that modulate $JAK2^{V617F}$'s role in MPN pathogenesis. First, we sought to determine the impact of selective $JAK2^{V617F}$ expression in the megakaryocyte (Mk) lineage. This was accomplished by generating a murine model of Mk lineage-restricted *Jak2VF* expression. Our characterization revealed that mutant Mks (and their descendant platelets) contribute to MPN pathogenesis by promoting increased erythroid differentiation of *Jak2* wild-type hematopoietic stem/progenitor cell (HSPC) populations. This effect is mediated, at least in part, by increased production of Interleukin-6 (IL-6) by *Jak2*-mutant Mks. Furthermore, we demonstrated that mutant Mks contribute to MPN maintenance in vivo using diphtheria toxin receptor-mediated cell ablation in two bone marrow transplant (BMT) models of MPN. This work highlights a previously under-appreciated role of $JAK2^{V617F}$ in promoting MPN pathogenesis via cytokine-mediated expansion of the wild type hematopoietic compartment.

Next, we investigated how epigenetic deregulation via *ASXL1* loss cooperates with *JAK2*^{V617F} to promote myeloid cell transformation. To this end, we developed a compound *Jak2/Asxl1* mutant mouse model that allowed for simultaneous expression of mutant *Jak2* and *Asxl1* loss throughout the hematopoietic compartment and rigorously determined the phenotypic differences that *Asxl1* loss conferred to *Jak2*-driven MPN. These differences included accelerated disease onset, as well as increased bone marrow fibrosis and alterations to the HSPC compartment. Furthermore, *Jak2/Asxl1* double-mutant HSPCs showed continued expansion after JAK2 inhibitor treatment in vitro and in vivo, suggesting an important role for *ASXL1* loss in promoting JAK2 inhibitor persistence and disease progression.

Chapter 2 - MATERIALS AND METHODS

MOUSE MODELS

All mice used in this study were on the C57BL/6 background. For the Mk studies outlined in Chapter 3, heterozygous *Jak2*$^{VF/+}$ conditional knock-in animals (a gift of Dr. Ann Mullally (Mullally et al. 2010)) were bred with *Pf4-Cre* transgenic mice (a gift of Dr. Radek Skoda (Tiedt et al. 2007)) to induce *Jak2*^{V617F} expression in megakaryocyte lineage-committed cells. *Vav-Cre* (Stock# 008610) and *Mx1-Cre* (Stock# 003556) transgenic mice were purchased from Jackson Laboratory (Bar Harbor, ME) and bred with *Jak2*$^{V617F/+}$ mice to induce pan-hematopoietic *Jak2*^{V617F} expression. For Mk depletion studies, *iDTR* mice (which harbor a conditional Cre-inducible diphtheria toxin receptor (DTR) (Buch et al. 2005)) were obtained from Jackson Laboratory (Stock# 007900) and crossed to *Pf4-Cre*$^{+}$ mice. For lineage tracing studies, mTmG Cre switch reporter mice (Muzumdar et al. 2007) were obtained from Jackson Laboratory (Stock# 007676) and bred to *Jak2*$^{V617F/+}$*; Pf4-Cre*$^{+}$ mice to confirm lineage-specific Cre expression.

For the combinatorial *Jak2/Asxl1* model discussed in Chapter 4, *Asxl1* conditional knock-out mice (Abdel-Wahab et al. 2013) (a gift of Dr. Omar Abdel-Wahab) were crossed with *Jak2*$^{VF/+}$ conditional knock-in mice and *HSC-Scl-CreERT*$^{+}$ mice (Göthert et al. 2005) (also a gift of Dr. Omar Abdel-Wahab). To confirm Cre expression, these mice were further bred to a tdTomato-expressing Cre reporter mouse line purchased from the Jackson Laboratory (Stock # 007909).

All Cre, reporter, and conditional lines were genotyped using protocols and primers described in their attributed citations, using DNA processed from toe clips.

All animal work was done in compliance with MSKCC and Northwestern University's Internal Animal Care and Use Committee and the guidelines of the Federal Office of Laboratory Animal Welfare. Animals were house in the Research Animal Resources Center (RARC) of MSKCC. Full time veterinarians and technicians were staffed on site and took care of all routine husbandry procedures.

All mice were humanely sacrificed prior to use. Euthanasia was conducted in accordance with the *American Veterinary Medical Association Guidelines on Euthanasia*. Briefly, mice were sacrificed by asphyxiation with CO2 delivered into cages < 5 pounds per square inch per second. CO2 euthanasia stations are inspected regularly by the Internal Animal Care and Use Committee personnel (IACUC). Tissues were removed for experiments after confirmation of death.

TRANSGENE ACTIVATION

For studies using Mx1-Cre, transgene activation was induced by the administration of three intra-peritoneal injections of polyinositic:polycytidylic acid (pIpC; 200 μL of a 1 mg/mL solution). For studies using HSC-Scl-CreERT mice, Cre transgene expression was

induced by the Tamoxifen administration. Mice received two doses of Tamoxifen (TAM; 1 mg in 100μL of corn oil) by oral gavage 48 hours apart.

Two weeks after pIpC or TAM administration, peripheral blood was collected via cheek bleeding using heparinized microhematocrit capillary tubes (Thermo Fisher Scientific). Recombination was confirmed by either excision PCR or confirmation of Cre reporter expression by flow cytometry. Peripheral blood counts were obtained using a HemaVet according to standard manufacturer's instructions.

RUXOLITINIB ADMINISTRATION

Ruxolitinib was dissolved in citrate buffer with 20% Captisol. Dissolved drug was administered to symptomatic mice 4 weeks post-transplant, via oral gavage, at a dose of 60 mg/kg twice daily for 4 weeks.

IL-6 BLOCKADE

Age- and gender-matched symptomatic *Jak2*$^{V617F/+}$*; Pf4-Cre*$^{+}$ mice were randomized to receive an antibody against mouse IL-6 (R&D Systems, cat. # MAB406) at 0.3 mg/kg or PBS every other day by intraperitoneal (i.p.) injection for 6 weeks. *Jak2*$^{VF/+}$*; Pf4-Cre*$^{+}$ mice were classified as symptomatic if peripheral blood analysis indicated an elevated (>60%) hematocrit.

FLOW CYTOMETRY AND CELL SORTING

In brief, surface marker analysis was performed on freshly-harvested bone marrow and spleen cells. Staining for mature lineage markers (including mouse CD41, CD42b, Ter119, CD71, Gr1, and Mac1) was performed by incubating cells in antibodies diluted in PBS + 0.5% BSA for 30-60 minutes at 4ºC. FACS data were acquired using an LSR Fortessa flow cytometer (BD Biosciences) and analyzed using FlowJo software version 9.9.4 (Tree star; Ashland, OR).

STEM/PROGENITOR COMPARTMENT ANALYSIS

To characterize the myelo-erythroid stem/progenitor cell compartment, bone marrow cells were stained as follows: cells were first stained using a mouse hematopoietic progenitor enrichment kit (Stemcell Technologies; Vancouver BC) containing CD5, CD11b/Mac1, CD19, CD45R, Gr1, and Ter119. Cells were then incubated with Pacific Blue-conjugated streptavidin and simultaneously with antibodies against cKit, Sca1, FcγR, CD41, CD150, and CD105 as previously described (Pronk et al. 2007), and populations were gated accordingly. Sorting was performed using a FACS Aria (BD Biosciences) or SH800 (Sony). Red blood cell lysis was not performed, as this could potentially decrease the frequency of later-stage Mk/Erythroid progenitor populations.

Intracellular Phospho-Flow

Levels of phosphorylated Stat5 were determined according to a previously-established protocol (Mullally et al. 2010). For intracellular phospho-protein analysis, freshly isolated whole bone marrow cells were first resuspended in 1 mL RPMI + 1% BSA and incubated at 37°C for 1 hour. Cells were then stimulated with hEPO (1 U/mL) or hTPO (10 ng/mL) with or without mIL-3 (10 ng/mL) for 10 minutes. Labelling for surface antigens was performed at this time. After staining, cells were then fixed in 16% paraformaldehyde at room temperature for 10 minutes, washed twice with PBS + 2% BSA, and permeabilized in ice-cold 95% methanol for 10 minutes. Cells were then stained immediately with PE-conjugated phosphoStat5 antibody in the dark at room temperature for 20 minutes and immediately analyzed.

Immunoseparation Of $CD41^+$ Mks And $F4/80^+$ Macrophages

Immunoseparation of these populations was performed using the EasySep mouse PE Positive Selection kit from StemCell Technologies (Catalog # 17666).

BONE MARROW TRANSPLANTATION ASSAYS

DISEASE PROPAGATION TRANSPLANTS

In Chapter 3, to assess disease transplantability in *Jak2*$^{V617F/+}$*; Pf4-Cre*$^{+}$ mice, whole bone marrow cells were collected from *Jak2*$^{V617F/+}$*; Pf4-Cre*$^{+}$ mice (CD45.2) or wild type (WT) (CD45.1). Two million *Jak2*$^{V617F/+}$*; Pf4-Cre*$^{+}$ and WT bone marrow cells were transplanted into lethally irradiated two-month old WT mice at a ratio of 90:10 or 10:90.

In Chapter 4, the disease propagating capacity of LT- and ST-HSCs was performed following a previously established protocol (Mullally et al. 2012). In short, FACS-sorted CD150^{+}CD48^{-} LSKs (LT-HSCs) or CD150^{+}CD48^{+} LSKs (ST-HSCs) were combined with wild-type support BM from CD45.1^{+} B6.SJL-Ptprca/BoyAiTac mice (Taconic, Model # 4007), and transplanted into lethally-irradiated (11 Gy) WT B6 recipients. Engraftment was assessed by flow cytometry of peripheral blood samples obtained every 4 weeks. Peripheral blood parameters were assessed in parallel.

MPN BMT MODELS AND IDTR-MEDIATED MK/PLT ABLATION

Retroviruses were generated by transfecting Plat-E cells with either human *MPL*^{W515L} or *JAK2*^{V617F} in the MIGR1 retroviral expression vector using Fugene VI (Roche Life Sciences; Indianapolis, IN) according to the manufacturer's instructions. Viral supernatant was harvested at forty-eight hours post-transfection. cKit^{+} HSPCs were isolated from

mouse bone marrow by immunoseparation using cKit-conjugated microbeads (Cat# 130-091-224, Miltenyi Biotech Inc.; Auburn, CA), and transduced by mixing cells in viral supernatant with 8 μg/mL polybrene (Cat# TR-1003-G, MilliporeSigma, Burlington, MA) and centrifuging the mixture for 2,500 rpm for 90 minutes at 32°C. Transduced cells were cultured overnight, and transduction efficiency was confirmed by assessing GFP expression using flow cytometry. Three hundred thousand GFP^+ cells were transplanted in to lethally irradiated (11 Gy) *iDTR*$^+$*Pf4-Cre*$^+$ mice. Recipient mice were monitored for symptom onset every 2 weeks by assessing peripheral blood counts. Diphtheria toxin (DT; 10 μg/kg) was administered after establishment of overt MPN to initiate Mk depletion. Symptoms were then monitored weekly. Mice were sacrificed after 4 weeks for full histo-pathological and flow cytometric analysis of the resulting disease.

COMPETITIVE BONE MARROW TRANSPLANTATION

Competitive BMT assays were performed using 6-8-week-old recipient mice with the genotypes described. Mice were not treated with Tamoxifen prior to transplantation. Whole bone marrow was harvested, counted, and mixed 1:1 with whole bone marrow isolated from 6-8-week-old $CD45.1^+$ B6.SJL-Ptprca/BoyAiTac mice. At total of $1x10^6$ mixed BM cells were then transplanted into lethally-irradiated 6-8-week-old WT B6 recipient mice. Engraftment was monitored by peripheral blood sampling and flow cytometry every 2 weeks. Tamoxifen was administered 2 weeks post-transplantation to induce knock-out/knock-in cassette expression. Recombination/excision was confirmed, and recipients were monitored every 2 weeks. At 16 weeks, mice were sacrificed for a full assessment of the hematopoietic compartment, including BM and spleen chimerism.

For Ruxolitinib treatment in the competitive BMT setting, pre-recombined donor mice were used. Ruxolitinib treatment was commenced 8 weeks post-transplant, once recipient mice established overt disease. Equal engraftment was confirmed by flow cytometry prior to treatment.

COLONY-FORMATION ASSAYS

Myeloid colony formation was assessed by plating either 10,000 bulk bone marrow or splenocytes or FACS-sorted LSKs/MEPs in m3434 methylcellulose media (Stemcell Technologies) in triplicate. Colony formation was assessed after 7-10 days. For in vitro Ruxolitinib treatment, Ruxolitinib was dissolved in DMSO was added to m3434 at the indicated concentrations prior to plating.

Megakaryocyte colony formation was performed using Mega-Cult. For erythroid colony formation assays (BFU-E), mouse splenocytes were seeded at 50,000 cells per well in triplicate using m3436 media (Stemcell Technologies) supplemented with hEPO. In all assays, colony formation was scored at 7-10 days after plating.

EPO-dependent colony formation was assessed using cytokine-free methylcellulose-based media (Cat# m3234, Stemcell Technologies) supplemented with mSCF (10 ng/mL), hEPO (10 U/mL), and varying concentrations of mIL-6, mCxcl1, or mCxcl2. LSKs or MEPs

were sorted from 6-8-week-old WT C57Bl/6 mice and seeded at 3 000 cells per well in triplicate.

GENE EXPRESSION ANALYSIS (QPCR)

RNA was isolated from purified cell populations using Trizol reagent (Cat# 15596026, ThermoFisher Scientific), and cDNA was generated using a Verso cDNA synthesis kit (Cat# AB-1453/B, ThermoFisher Scientific). Relative quantification of transcripts was then performed with SYBR Green reagents (Cat# 4913850001, Sigma) or TaqMan reagents using an Applied Biosystems QuantStudio 7 real-time system. Analysis was performed using the comparative ΔΔCt method. Normalization was performed against *Gapdh*.

Relative levels of *Jak2*^{V617F} and *Jak2*^{WT} were measured using a previously-established protocol (Mullally et al. 2012). The following primer sequences were used:

Jak2^{WT} forward primer 5'- TTTGAATTATGGTGTCTGCG
Jak2^{V617F} forward primer 5'- TTTGAATTATGGTGTCTGCT
Jak2 common reverse primer 5'- CAGGTATGTATCCAGTGATCC

HISTONE EXTRACTIONS AND WESTERN BLOTTING

Histones were extracted overnight using the Active Motif Histone Extraction Minikit (40026). Histone Western blots were conducted with 3-5 µg of histones. Cells were lysed for Western blot and experiments in the following buffer: 150 mM NaCl, 20 mM Tris (pH

7.4), 5 mM EDTA, 1% Triton, protease arrest (EMD) and phosphatase inhibitors (Calbiochem). 40 µg of whole cell lysate was used for Western blotting.

CYTOKINE MEASUREMENTS

Levels of circulating cytokines were performed using a Luminex-based Mouse 32-Plex Cytokine Kit (Cat# MCYTMAG-70K-PX32, EMD Millipore, Billerica, MA). Analysis was performed on serum samples that were prepared according to Millipore's instructions. In brief, peripheral blood was collected and allowed to clot for 30 minutes. Afterwards, blood samples were centrifuged at 1000xg for 10 minutes. Serum samples were then aliquoted (~25 µL) in to clean tubes and frozen at -80°C until analysis. Before analysis, samples were diluted 1:2 in serum matrix and assayed according to the manufacturer's instructions. Data were acquired using the FlexMAP 3D system and xPONENT software (Luminex; Austin, TX), and analyzed using MILLIPLEX Analyst software (EMD Millipore) as previously described (Kleppe et al. 2015). Single-plex cytokine-specific ELISAs (R&D Systems), including Cxcl1 (Cat# MKC00B), Cxcl2 (Cat# MM200), Ccl11 (Cat # MME00) and IL-6 (Cat# M6000B), were then used to validate the changes observed in individual cytokines.

HISTO-PATHOLOGY

Tissues were fixed in 10% neutral buffered formalin, embedded in paraffin, and stained with hematoxylin and eosin to assess gross cellular histology or reticulin to assess fibrosis.

For VWF immunohistochemistry, antigen retrieval was achieved by incubating slides in 1X target retrieval solution (Cat# S1699, Dako North America; Carpinteria, CA) at 98°C for 30 minutes in a water bath. Sections were stained for VWF (Cat# GA52761-2, Dako North America) overnight at 4°C at a dilution of 1:200, then incubated with rabbit HRP (Cat# M4U534, Biocare Medical; Concord, CA) for 15 minutes before the addition of chromogen DAB (Cat # BDB2004; Biocare). Sections were then counterstained with hematoxylin. All slide images were obtained on a Leica (Wetzlar, Germany) DM4000B microscope equipped with a Leica DFC320 color digital camera.

STATISTICS

Different groups were reported as mean ± SEM or mean ± SD where specified and compared using unpaired two-sided Student's t-test. When multiple comparisons were necessary, one-way or two-way ANOVA with post-test Bonferroni correction was used. Statistical significance was established when $p < 0.05$, labeled as * $p < 0.05$, ** $p < 0.01$, *** $p < 0.001$, and **** $p < 0.0001$. All analysis was performed using GraphPad Prism. Statistical analysis of survival was performed via the Kaplan-Meier method, with significance determined using the Mantel-Cox long-rank test. Group sizes were determined by power calculation, to determine the sample size needed to achieve an 80% chance of detecting a significant different ($p < 0.05$) between groups. Analysis of flow cytometric data and histology was assessed in a blinded manner; investigators were not aware of sample genotype while analysis was being performed.

Chapter 3 - RESULTS I

JAK2^{V617F}-MUTANT MEGAKARYOCYTES PROMOTE AND SUSTAIN MYELOID NEOPLASIA IN A CELL NON-AUTONOMOUS MANNER

INTRODUCTION

The MPNs are clonal hematopoietic stem cell (HSC) disorders characterized by the expansion of mature myeloid elements. The most common genetic alteration is *JAK2*^{V617F}, which is found in > 95% of all patients with PV, and in 50-60% of ET/PMF cases (Baxter et al. 2005; James et al. 2005; Levine et al. 2005; Kralovics et al. 2005). Expression of this mutation in cell lines causes transformation to cytokine-independent growth and constitutive activation of downstream STAT signaling (James et al. 2005; Levine et al. 2005), and expression of *JAK2*^{V617F} in the hematopoietic compartment is sufficient to cause MPN in mouse models (Akada et al. 2010; Li et al. 2010; Marty et al. 2010; Mullally et al. 2010). These observations, along with gene expression studies in primary patient samples (Rampal, Al-Shahrour, et al. 2014), establish aberrant JAK/STAT signaling as a central molecular hallmark of MPN pathogenesis. Clonality studies using MPN patient samples have traced driver mutations, including *JAK2*^{V617F}, to the HSC compartment, regardless of clinical phenotype (Jamieson et al. 2006). Furthermore, *JAK2*^{V617F} can be detected across the hematopoietic ontogeny (Ishii et al. 2006; Delhommeau et al. 2007). This implies that *JAK2*^{V617F} can have differential effects on discrete cell types, such as progenitor cells versus mature lineage-committed cells (Mullally et al. 2012). However,

most studies performed to date have investigated the effects of *JAK2*^{V617F} when expressed across the hematopoietic ontogeny.

We initiated this study to explore the contributions of mutant megakaryocytes to MPN pathogenesis. In many ET/PMF patients, *JAK2*^{V617F} manifests primarily in the megakaryocyte (Mk) lineage, with less significant involvement of erythroid and myeloid cells as determined by mutant allele burden profiling (Passamonti & Rumi 2009) of specific hematopoietic subsets. Furthermore, aberrant megakaryopoiesis is a pathological hallmark of MPN, regardless of clinical subtype (Ciurea et al. 2007). These abnormal megakaryocytes are known to secrete increased levels of pro-inflammatory cytokines and other factors (such as TGF-β), which presumably contribute to various MPN-related pathologies, such as bone marrow fibrosis (Zahr et al. 2016; Wen et al. 2015). Megakaryocytes are also regulators of HSC quiescence (Bruns et al. 2014; M. Zhao et al. 2014), and Jak/Stat signaling in Mks negatively regulates stem/progenitor cell expansion *in vivo* (Meyer et al. 2014). These observations raise the possibility that *JAK2*^{V617F}-mutant Mks promote MPN pathogenesis, at least in part, by influencing the biology of non-clonal (*JAK2*^{WT}) cells. Indeed, earlier work has revealed that *Jak2*^{V617F}-mutant megakaryocytes promote hyper-proliferation of the stem/progenitor cell pool via the TPO/MPL signaling axis (Zhan et al. 2016; Zhang et al. 2018). However, it remains unclear if *Jak2*^{V617F}-mutant megakaryocytes can affect non-clonal hematopoietic cells, how they mediate these effects, and if *Jak2*^{V617F}-mutant megakaryocytes are required for maintenance of the disease state.

To explore these questions, we crossed a conditional *Jak2*^{V617F} knock-in mouse where mutant *Jak2* is expressed from the endogenous murine locus with *Pf4-Cre* transgenic

mice. This produces a murine model wherein *Jak2*^{V617F} is expressed specifically in megakaryocyte lineage-committed cells (Mullally et al. 2012; Tiedt et al. 2007). Steady-state megakaryopoiesis was significantly elevated, as expected. We were surprised to also observe that *Jak2*-mutant Mks/platelets significantly increased steady-state erythropoiesis and were thus capable of initiating a myeloproliferative disorder through cell non-autonomous mechanisms.

RESULTS

PF4-CRE RESTRICTS JAK2^{V617F} *EXPRESSION TO THE MK LINEAGE*

To study the role of megakaryocytes in MPN pathogenesis, we generated *Jak2*$^{V617F/+;}$ *Pf4-Cre*$^{+}$ mice. In this model, mutant *Jak2* is expressed from the endogenous *Jak2* locus and is controlled by expression of Cre recombinase under control of the megakaryocyte lineage-specific *Pf4* promoter (Mullally et al. 2010; Tiedt et al. 2007). This model is genetically distinct from prior studies, which employed a transgenic *Jak2V617F* model, where Jak2 is expressed at non-physiologic levels from a non-specific integration site (Zhan et al. 2016). Prior studies suggest that *Pf4* is expressed at low levels in HSPCs (Calaminus et al. 2012; Pertuy et al. 2015), which raises the possibility the Cre-mediated recombination (and subsequent *Jak2*^{V617F} expression) could occur prior to megakaryocyte lineage-commitment in our model. We took several approaches to confirm the lineage specificity of *Pf4-Cre* in this setting.

First, we performed allele-specific qPCR on sorted cell populations to assess *Jak2*^{V617} expression across hematopoietic ontogeny. We sorted long-term HSCs (LT-HSCs), bivalent Mk/erythroid progenitor cells (Pre-MegE), erythroid progenitor cells (Pro-ERY), Mk progenitors (MkP) as previously described (Pronk et al. 2007), in addition to whole bone marrow mononuclear cells (MNCs), CD41$^+$ Mks, and platelets from *Jak2*$^{V617F/+;}$ *Pf4-Cre*$^+$ mice and performed allele-specific qPCR for *Jak2*^{V167F}. We could not detect significant levels of *Jak2*^{V617F} in MNCs, LT-HSCs, Pre-MegEs, or Pro-ERYs, whereas we could detect significant expression of *Jak2*^{V617F} in MkPs. *Jak2*^{V617F} and *Jak2*^{WT} were detected at equal levels in CD41$^+$ Mks and platelets (**Figure 3.1A**). As *Jak2*^{V617F} could only be readily detected in megakaryocyte lineage-committed populations and was not present in earlier progenitor compartments or in erythroid lineage-committed cell types, we thus conclude that the Pf4 promoter drives Cre expression specifically in megakaryocyte lineage-committed cells.

We also employed the mTmG Cre switch reporter mouse to confirm the lineage-specificity of Pf4-Cre (Muzumdar et al. 2007). In this model, a double-fluorescent Cre reporter cassette is within the *Rosa26* locus. Prior to Cre-mediated recombination, the red fluorescent protein (RFP) tdTomato is expressed. In Cre-positive cells, the locus undergoes a recombination event that switches the cassette to express green fluorescent protein (GFP). Therefore, Cre-negative cells will be tdTomato$^+$/GFP$^-$, while Cre-positive cells will be tdTomato$^-$/GFP$^+$. We crossed *Jak2*$^{V617F/+;}$ *Pf4-Cre*$^+$ mice with *mTmG*$^{+/+}$ mice, which were then subjected to extensive flow cytometric analysis in order to survey reporter expression across hematopoiesis. No significant population of GFP$^+$ cells is detectable in the LSK compartment, in Mk/Erythroid progenitors (MEPs) or in CD71$^+$/Ter119$^+$ erythroid cells. The CD41$^+$ Mk compartment, as expected, was ~99% GFP$^+$ (**Figure 3.1B**).

Jak2^{V617F} causes constitutive downstream activation of Stat5 (Levine et al. 2005; Mullally et al. 2010). We therefore sought to further confirm *Jak2*^{V617F} expression at the functional level by assessing levels of phosphorylated Stat5 (pStat5) by intracellular flow cytometry. In CD41^{+} Mk cells from *Jak2*$^{V617F/+;}$ *Pf4-Cre*$^{+}$ mice, basal levels of pStat5 were similar to levels observed in hTPO-stimulated cells (with or without mIL-3) (**Figure 3.1C**). In contrast, basal pStat5 levels in *Jak2*$^{V617F/+;}$ *Pf4-Cre*$^{+}$ CD71^{+} erythroid cells were similar to levels observed in *Jak2*$^{+/+;}$ *Pf4-Cre*$^{+}$ CD71^{+} cells (**Figure 3.1D**). These observations provide compelling evidence that Pf4-Cre is active exclusively in megakaryocytes, and thus drives megakaryocyte lineage-restricted expression of *Jak2*^{V617F}.

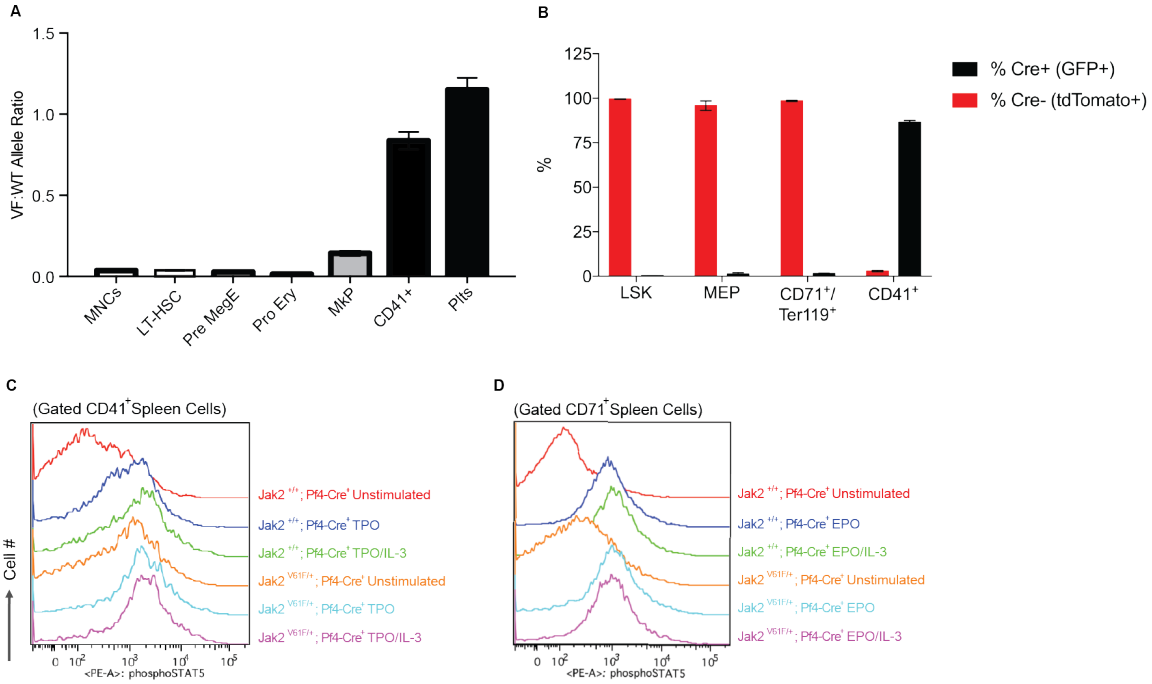

FIGURE 3.1: PF4-CRE DRIVES MEGAKARYOCYTE (MK) LINEAGE-RESTRICTED *JAK2*^{V617F} EXPRESSION.

(A) Allele-specific qPCR quantifying the ratio of VF mutant to WT Jak2 in either whole mouse bone marrow mononuclear cells (MNCs) after red cell lysis or sorted hematopoietic lineages from *Jak2*$^{VF/+;}$ *Pf4-Cre*$^{+}$ mice or age-matched *Jak2*$^{+/+}$ controls (n=4 mice per group). Sorted populations include LT-HSCs, Pre-MegEs, Pro-ERYs, MkPs, CD41^{+} Mks, and platelets. **(B)** Flow cytometric analysis of Cre reporter expression (% tdTomato^{+} (Cre^{-}) v. % GFP^{+}(Cre^{+}) in the LSK, MEP, erythroid (CD71^{+}/Ter119^{+}), and Mk (CD41^{+}) bone marrow compartments of *Jak2*$^{VF/+;}$ *Pf4-Cre*$^{+;}$ *mTmG*$^{+}$ mice (n=8 mice, aged 8-16 weeks). **(C-D)** Assessment of phospho-Stat5 levels by intracellular flow cytometry in stimulated and unstimulated **(C)** CD41^{+} and **(D)** CD71^{+} spleen cells from *Pf4-Cre*$^{+}$ mice.

Flow cytometry plots are representative of 4 independent experiments. N=3 animals per group, mice were 20 weeks old. Bar graphs depict mean +/- SD. **p < 0.01, by one-way ANOVA.

Reprinted with permission from the American Association for Cancer Research. Image from: Woods B. et al. Activation of JAK/STAT signaling in megakaryocytes sustains myeloproliferation in vivo. Clinical Cancer Research Jun 19 (2019) [ePub ahead of print]. PMID: 31217200.

JAK2^{V617F}-MUTANT MKS CONFER A PV-LIKE PHENOTYPE IN VIVO

Since the *Jak2^{V617F}* allele used in our model causes a distinct pan-hematopoietic phenotype from the transgenic allele used by previous studies (Tiedt et al. 2008; Zhan et al. 2016; Zhang et al. 2018), we assessed whether physiologic *Jak2^{V617F}* expression in Mks would induce myeloid neoplasia. We monitored the peripheral blood counts of *Jak2$^{V617F/+;}$ Pf4-Cre^{+}* mice for 200 days and observed progressive and significant increases in the hematocrit and hemoglobin levels in addition to the anticipated increase in platelet counts (**Figure 3.2A-C**). We were not able to detect a significant population of Cre^{+} (GFP^{+}) erythroid cells by flow cytometry (**Figure 3.1B**), and additional allele-specific qPCR on sorted CD71^{+}/Ter119^{+} cells confirmed that this population was *Jak2$^{+/+}$* (**Figure 3.2D**). Therefore, the aberrant erythropoiesis observed in this model is likely due to the interactions of *Jak2^{V617F}*-mutant Mks with the *Jak2^{WT}* hematopoietic milieu and is not a consequence of the clonal outgrowth of a rare subset of erythroid-biased HSPCs. This possibility is discussed at-length below.

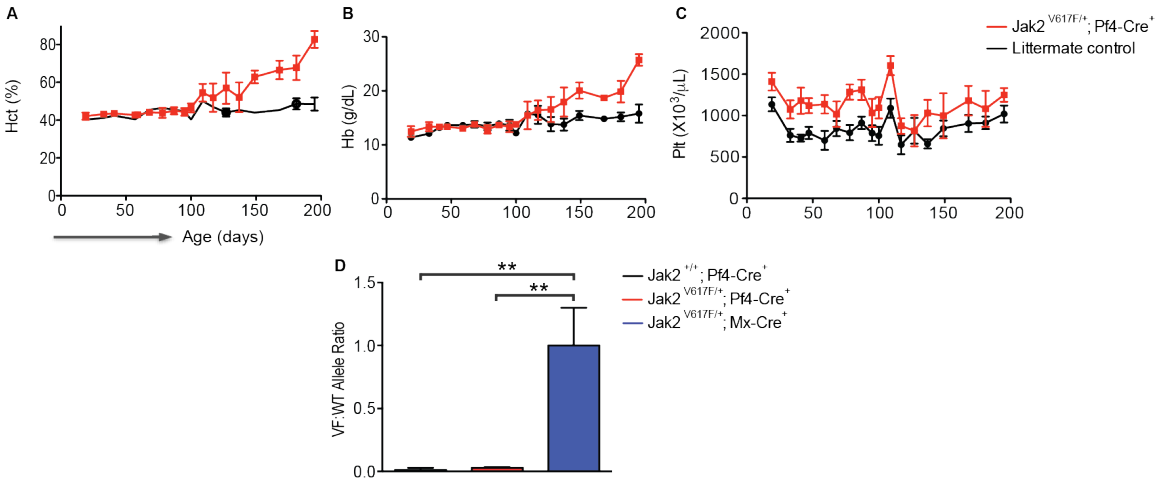

FIGURE 3.2: *JAK2*^{V617F}-MUTANT MKS PROMOTE INCREASED PERIPHERAL ERYTHROPOIESIS, IN ADDITION TO MILD THROMBOCYTOSIS

(A) Hematocrit, **(B)** hemoglobin, and **(C)** platelet counts in peripheral blood of *Jak2*$^{VF/+}$*; Pf4-Cre*$^{+}$ mice over a 200-day monitoring period ($p < 0.01$, by two-way ANOVA). **(D)** Allele-specific qPCR quantifying the ratio of mutant (V617F) to wild-type (WT) *Jak2* in sorted CD71^{+}/Ter119^{+} erythroid lineage-committed spleen cells from *Jak2*$^{VF/+}$*; Pf4-Cre*$^{+}$, *Jak2*$^{+/+}$*; Pf4-Cre*$^{+}$, and *Jak2*$^{VF/+}$*; Mx1-Cre*$^{+}$ mice. *Jak2*$^{VF/+}$*; Mx1-Cre*$^{+}$ mice showed an equal ratio of VF to WT *Jak2*, whereas the mutant allele could not be detected above background in cells sorted from *Pf4-Cre*$^{+}$ mice.

Results are representative of 2 independent experiments. Bar graphs depict mean ± SEM. n=3 mice per group (aged 20 weeks. *Jak2*$^{VF/+}$*; Mx1-Cre*$^{+}$ mice and *Jak2*$^{VF/+}$*; Pf4-Cre*$^{+}$ mice showed gross MPN symptoms, as determined by hematocrit levels in peripheral blood). ** $p < 0.01$ by one-way ANOVA.

Reprinted with permission from the American Association for Cancer Research. Image from: Woods B. et al. Activation of JAK/STAT signaling in megakaryocytes sustains myeloproliferation in vivo. Clinical Cancer Research Jun 19 (2019) [ePub ahead of print]. PMID: 31217200.

More detailed analysis of the hematopoietic compartment at 6 months revealed evidence of an overt myeloproliferative disease resembling PV. We observed splenomegaly (**Figure 3.3A, B**), along with marked changes in splenic architecture which include a profound increase in erythroid progenitors, white pulp expansion, increased megakaryocytes, and marked fibrosis (**Figure 3.3C-E**). We also observed impaired survival in *Jak2*$^{V617F/+}$*; Pf4-Cre*$^{+}$ mice relative to littermate controls (**Figure 3.3F**). The peripheral phenotype in our model emerged with a significantly longer latency than what is typically observed in models of pan-hematopoietic *Jak*^{V167F} expression. We thus compared *Jak2*$^{V617F/+;}$ *Pf4-Cre*$^{+}$ mice to *Jak2*$^{V617F/+;}$ *Vav-Cre*$^{+}$ mice (where *Vav-Cre* drives *Jak2*^{V617F} expression in HSPCs). While fully penetrant and similar, the disease phenotype of *Jak2*$^{V617F/+;}$ *Pf4-Cre*$^{+}$ was less severe overall (**Figure 3.4**). This suggests that additional *JAK2*^{V617F}-mutant lineages also contribute to the disease phenotype in pan-hematopoietic *JAK2*^{V617F} contexts.

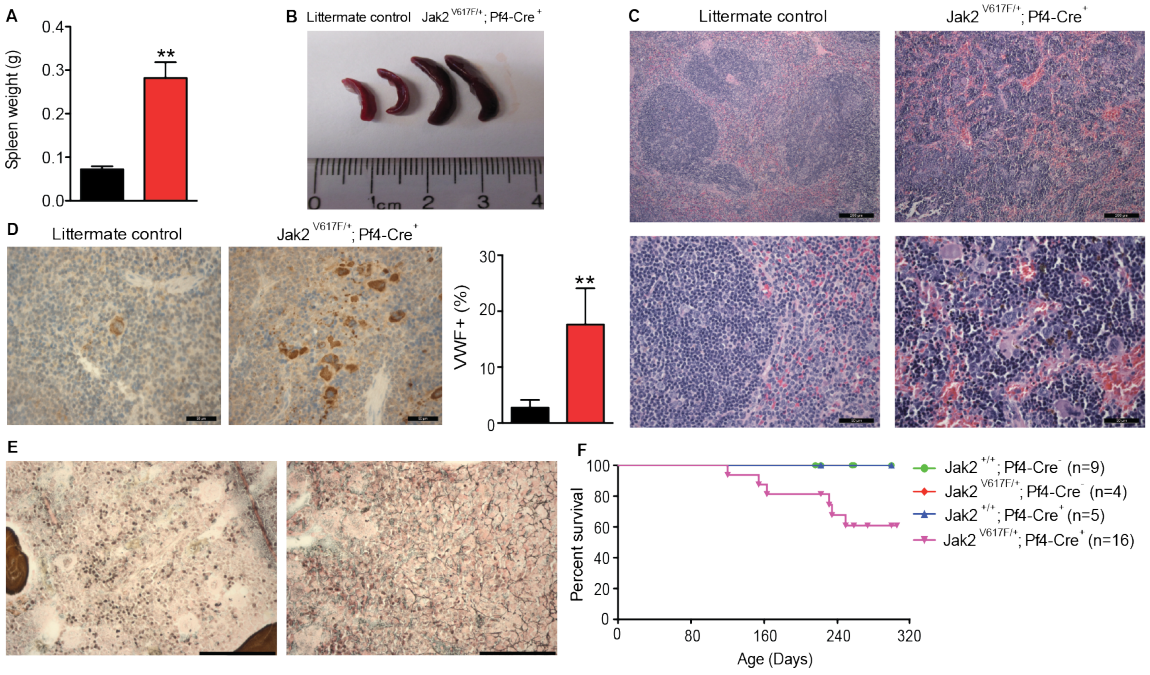

FIGURE 3.3: *JAK2*^{V617F}-MUTANT MKS INITIATE A FULMINANT MPN PHENOTYPE

(A-B) In addition to the change sin peripheral blood counts, *Jak2*$^{VF/+}$*; Pf4-Cre*$^{+}$ mice also displayed splenomegaly (increased spleen weight **(A)** and size **(B)**). **(C)** H&E staining revealed histopathological changes in splenic architecture (Scale bars depict 100 microns in the upper panel, 50 microns in the lower panel), as well as **(D)** increased VWF^{+} cells (Scale bars = 50 microns). **(E)** Reticulin staining revealed bone marrow fibrosis (Scale bars = 50 microns). **(F)** Kaplan-Meier survival curve (p=0.0374).

In **(A-E)**, mice were female and 6 months old. Results are representative of 2 independent experiments. N=6 animals per group. Bar graphs and line graphs depict mean ± SEM.

Reprinted with permission from the American Association for Cancer Research. Image from: Woods B. et al. Activation of JAK/STAT signaling in megakaryocytes sustains myeloproliferation in vivo. Clinical Cancer Research Jun 19 (2019) [ePub ahead of print]. PMID: 31217200.

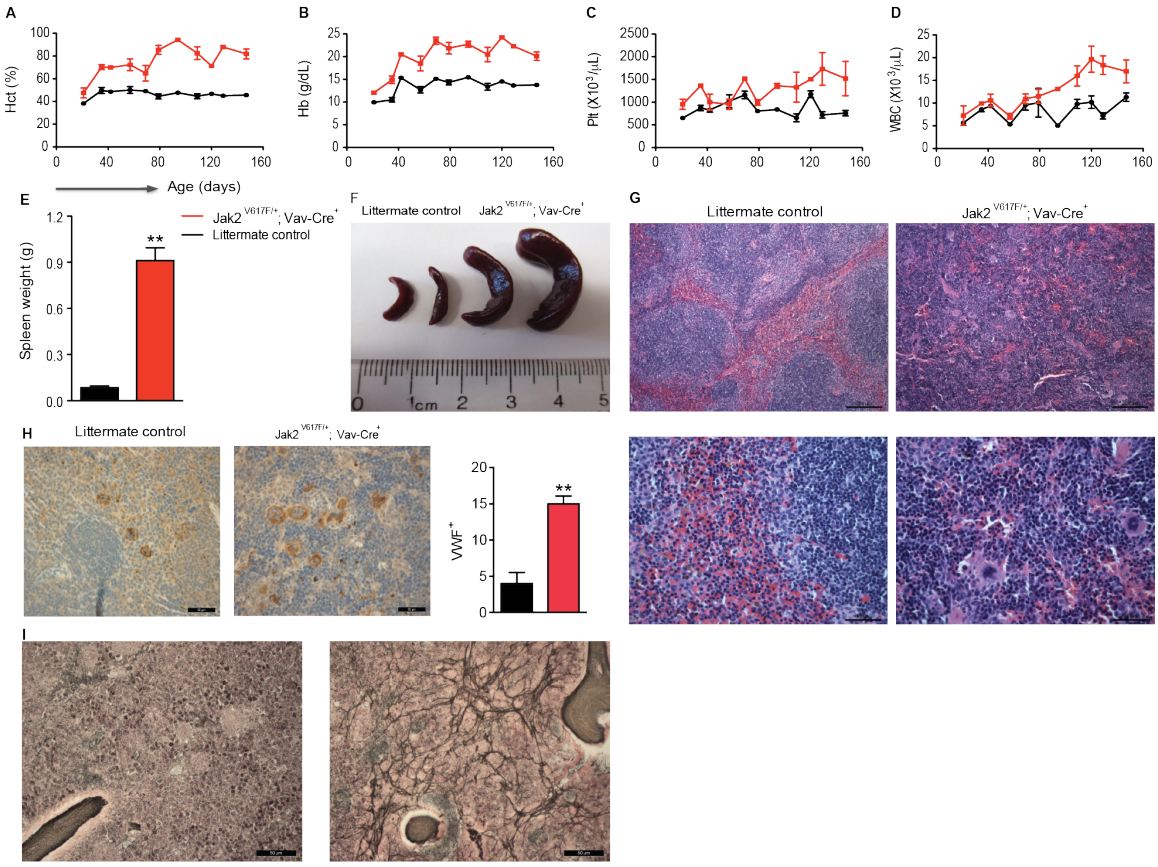

FIGURE 3.4: PAN-HEMATOPOIETIC *JAK2*^{V617F} EXPRESSION RAPIDLY INDUCES MPN

(A-D) *Jak2*$^{V617F/+}$*; Vav-Cre*$^{+}$ mice rapidly developed increased hematocrit, hemoglobin, platelets, and white blood cell counts relative to littermate controls. $p < 0.01$ by two-way ANOVA **(A-D)**. **(E, F)** Spleen weights (**$p < 0.01$ by unpaired two-sided Student's t test) and sizes were also increased. **(G)** H&E staining revealed marked disruption of splenic architecture. Scale bars depict 100 microns in the upper panel and 50 microns in the lower panel**. (H)** VWF staining (**$p < 0.01$ by unpaired two-sided Student's t test) by IHC was also increased, as were **(I)** reticulin fibers. Scale bars depict 50 microns in (**H, I**).

Results are representative of 2 independent experiments. n=6 animals per group. Bar graphs and line graphs depict mean ± SEM. Mice were 6 months old.

Reprinted with permission from the American Association for Cancer Research. Image from: Woods B. et al. Activation of JAK/STAT signaling in megakaryocytes sustains myeloproliferation in vivo. Clinical Cancer Research Jun 19 (2019) [ePub ahead of print]. PMID: 31217200.

Detailed flow cytometric analysis of symptomatic mice confirmed the histopathological observation of megakaryocytic expansion in the bone marrow and spleen (**Figure 3.5A, B** and **Figure 3.6A, B**). *Jak2*$^{V617F/+;}$ *Pf4-Cre*$^{+}$ mice displayed a robust expansion of *Jak2*^{WT} immature erythroid cells (Ter119^{low}/CD71^{high} R1 and Ter119^{high}/CD71^{high} R2 cells) (Socolovsky et al. 2001; Leung et al. 2007) in the spleen (**Figure 3.6C)** and in the R1 population in the bone marrow (**Figure 3.5C**). The mature CD11b^{+}/Gr1^{+} myeloid lineage is also expanded in both organs (**Figure 3.5D** and **Figure 3.6D**). Analysis of the HSPC compartment confirmed prior findings that *Jak2*^{V617F}-mutant Mks cause HSPC expansion. Lin^{-}Sca1^{+}cKit^{+} (LSK) HSPCs were expanded in bone marrow and spleen (**Figure 3.5E** and **Figure 3.6E**) (Zhan et al. 2016). Downstream myeloid progenitor populations were also expanded and skewed towards the Mk/erythroid lineage (**Figure 3.5F-H**, **Figure 3.6F-H**). This was confirmed at the functional level in *ex vivo* colony formation assays; whole bone marrow isolated from *Jak2*$^{V617F/+;}$ *Pf4-Cre*$^{+}$ mice also produced more BFU-E, CFU-Mk and CFU-Myeloid colonies than bone marrow harvested from littermate controls (**Figure 3.7**).

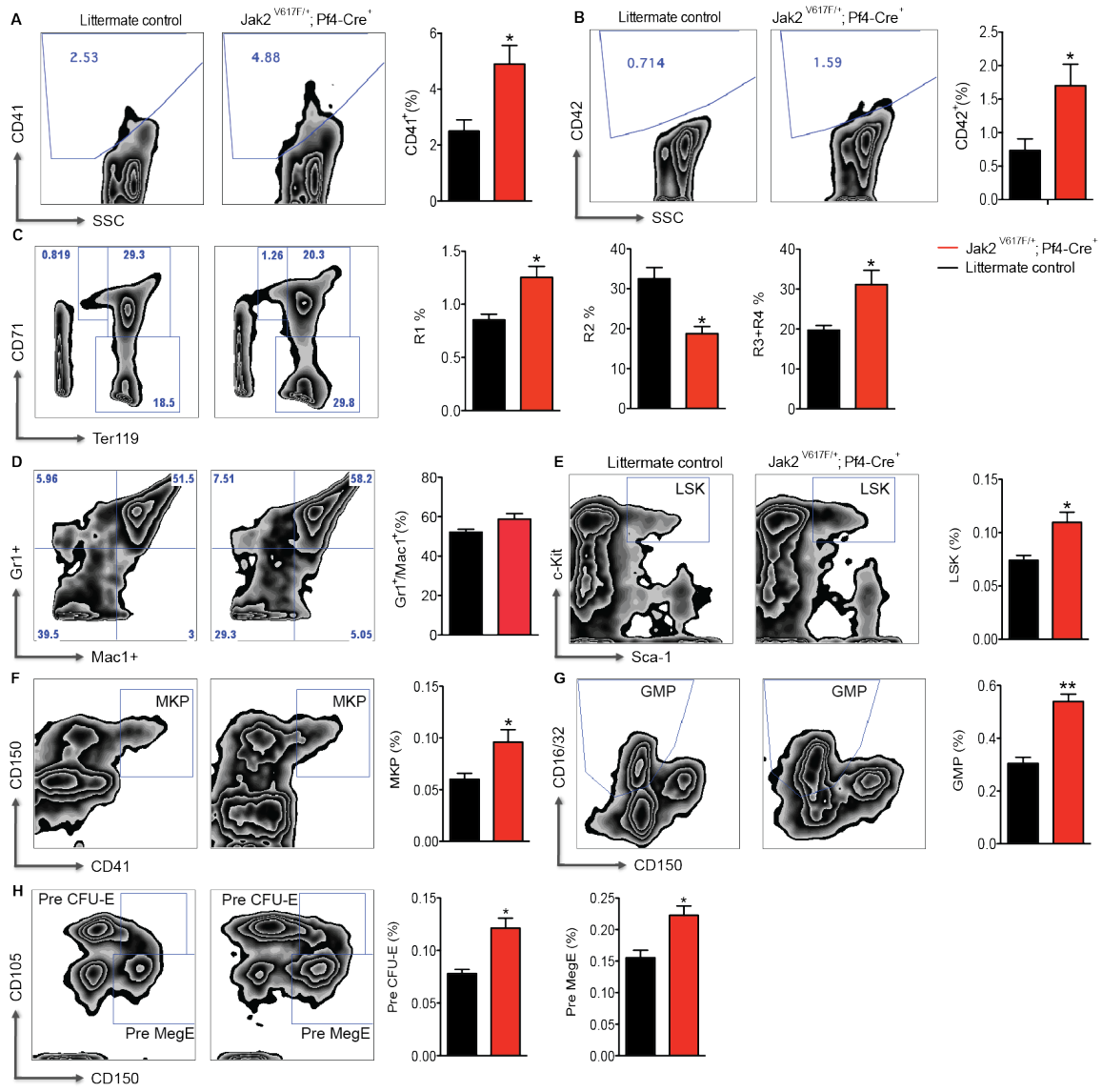

FIGURE 3.5: MK-RESTRICTED *JAK2*^{V617F} EXPRESSION PROMOTES TRI-LINEAGE HEMATOPOIETIC EXPANSION AND HSPC EXPANSION.

Flow cytometric analysis of the bone marrow compartment of symptomatic mice (6 months old) revealed the presence of increased **(A)** CD41$^+$ and **(B)** CD42$^+$ megakaryocytes, **(C)** erythroid cells, and **(D)** Mac1$^+$/Gr1$^+$ myeloid cells in the bone marrow of 6-month-old *Jak2*$^{VF/+}$*; Pf4-Cre*$^+$ mice relative to littermate controls. Further profiling of the stem/progenitor compartment indicated that the **(E)** LSK, **(F)** MkP, **(G)** GMP, **(H)** Pre CFU-E and Pre-MegE progenitor cell populations were also expanded.

Representative flow plots are shown, and results are representative of 2 independent experiments. n = 6 animals per group. Bar graphs depict mean ± SEM. *p < 0.05, ** p < 0.01, determined with unpaired two-sided Student's T-test.

Reprinted with permission from the American Association for Cancer Research. Image from: Woods B. et al. Activation of JAK/STAT signaling in megakaryocytes sustains myeloproliferation in vivo. Clinical Cancer Research Jun 19 (2019) [ePub ahead of print]. PMID: 31217200.

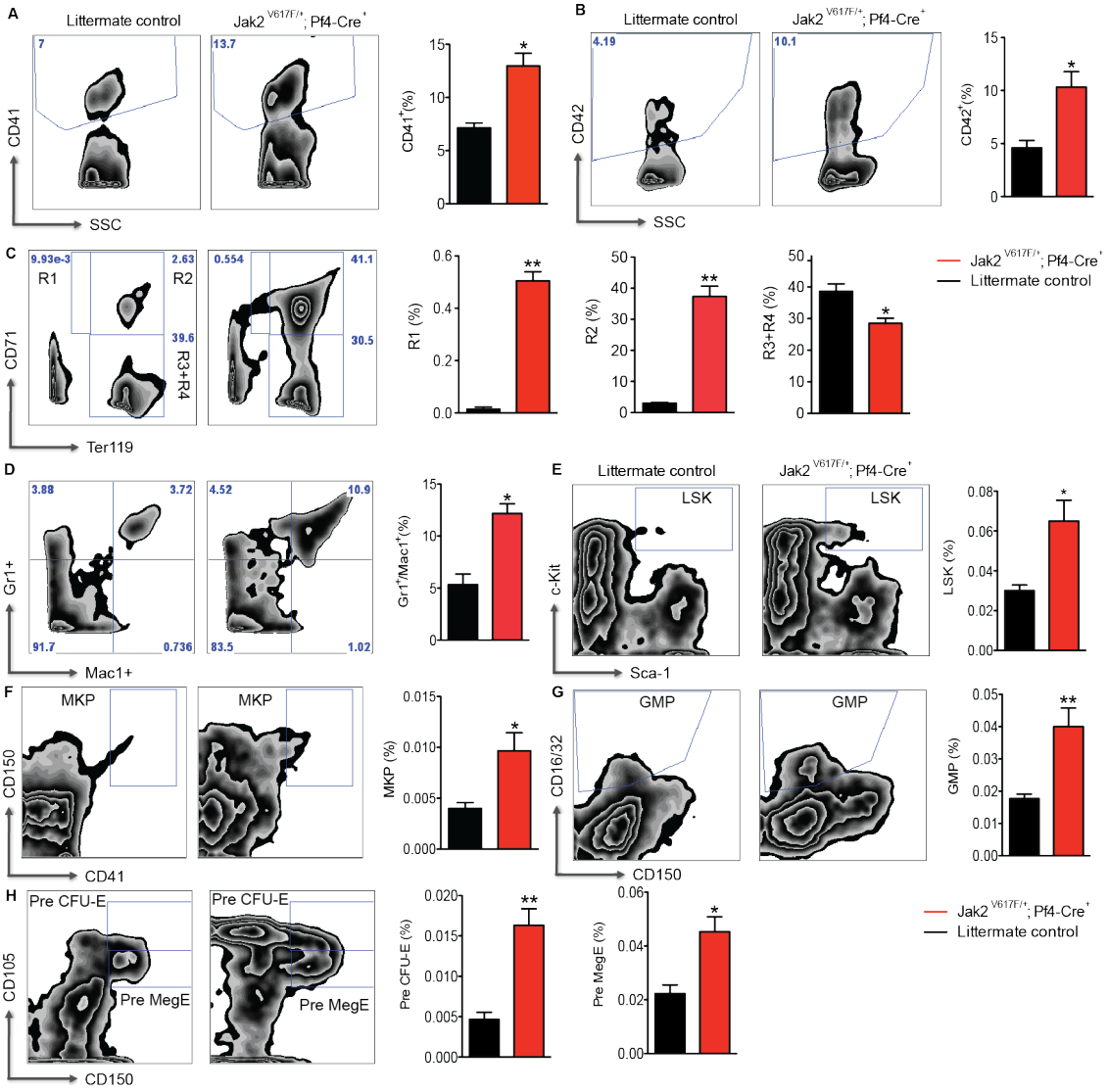

FIGURE 3.6: TRI-LINEAGE EXPANSION IS DETECTABLE IN THE PERIPHERY.

Flow cytometric analysis of spleens from 6-month-old *Jak2$^{VF/+}$; Pf4-Cre^{+}* mice revealed that *Jak2^{V617F}* expression in Mks increased **(A)** CD41^{+} and **(B)** CD42^{+} Mks, as well as (**C**) immature erythroid cells (R1 and R2 populations), and **(D)** Mac1^{+}/Gr1^{+} myeloid cells. Further profiling of the HSPC compartment showed increased **(E)** LSKs, **(F)** MkPs, **(G)** granulomonocytic progenitors (GMPs), as well as **(H)** Pre-CFU-E and Pre-MegEs in *Jak2$^{VF/+}$; Pf4-Cre^{+}* mice relative to littermate controls.

Representative flow plots are shown, and results are representative of 2 independent experiments. n=6 animals per group. Bar graphs depict mean ± SEM. * $p < 0.05$, ** $p < 0.01$ by unpaired two-sided Student's T-test.

Reprinted with permission from the American Association for Cancer Research. Image from: Woods B. et al. Activation of JAK/STAT signaling in megakaryocytes sustains myeloproliferation in vivo. Clinical Cancer Research Jun 19 (2019) [ePub ahead of print]. PMID: 31217200.

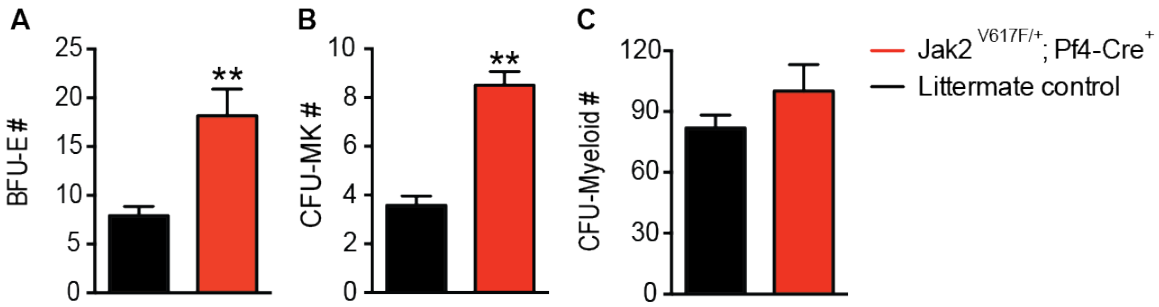

FIGURE 3.7: HSPCS ARE FUNCTIONALLY EXPANDED IN *JAK2$^{VF/+}$; PF4-CRE^{+}* MICE.

Bone marrow cells from 6-month-old *Jak2$^{VF/+}$; Pf4-Cre^{+}* mice and littermate controls were harvested and subjected to colony formation assays as described in materials and methods. *Jak2$^{VF/+}$; Pf4-Cre^{+}* bone marrow showed increased **(A)** BFU-E, **(B)** CFU-Mk, and **(C)** CFU-myeloid colony formation *in vitro*.

Bar graphs depict mean ± SEM. **p < 0.01 by unpaired two-sided Student's T-test. Results are representative of 2 independent experiments. n = 6 mice per group.

Reprinted with permission from the American Association for Cancer Research. Image from: Woods B. et al. Activation of JAK/STAT signaling in megakaryocytes sustains myeloproliferation in vivo. Clinical Cancer Research Jun 19 (2019) [ePub ahead of print]. PMID: 31217200.

THE EFFECT OF JAK2^{V617F}-MUTANT MKS IS CELL NON-AUTONOMOUS

Overt MPN appeared in the *Jak2$^{V617F/+;}$ Pf4-Cre^{+}* model after a relatively long latency period of ~20 weeks), whereas symptoms become apparent at 8-12 weeks on average in the setting of pan-hematopoietic *Jak2^{V617F}* expression (Mullally et al. 2010). We analyzed the composition of the hematopoietic compartment prior to the development of peripheral blood symptoms (elevated hematocrit). Young asymptomatic *Jak2$^{V617F/+;}$ Pf4-Cre^{+}* mice (~3 months old) only displayed signs of enhanced megakaryopoiesis. This was indicated by increased peripheral platelet counts (**Figure 3.8A**) and expansion of the CD41^{+} and CD42^{+} Mk compartment in both bone marrow (**Figure 3.9A**) and spleen (**Figure 3.10A**). Furthermore, no tissue abnormalities or fibrosis were apparent upon histological examination at these timepoints (**Figure 3.8G-I**). All other bone marrow and spleen compartments, especially the HSPC and erythroid compartments, at this earlier timepoint were comparable to littermate controls (**Figure 3.9** and **Figure 3.10**). These data suggest that the duration of exposure to *Jak2^{V617F}*-mutant Mks is an important factor to MPN development, and that the effect of mutant Mks on the HSPC niche is exerted gradually over time.

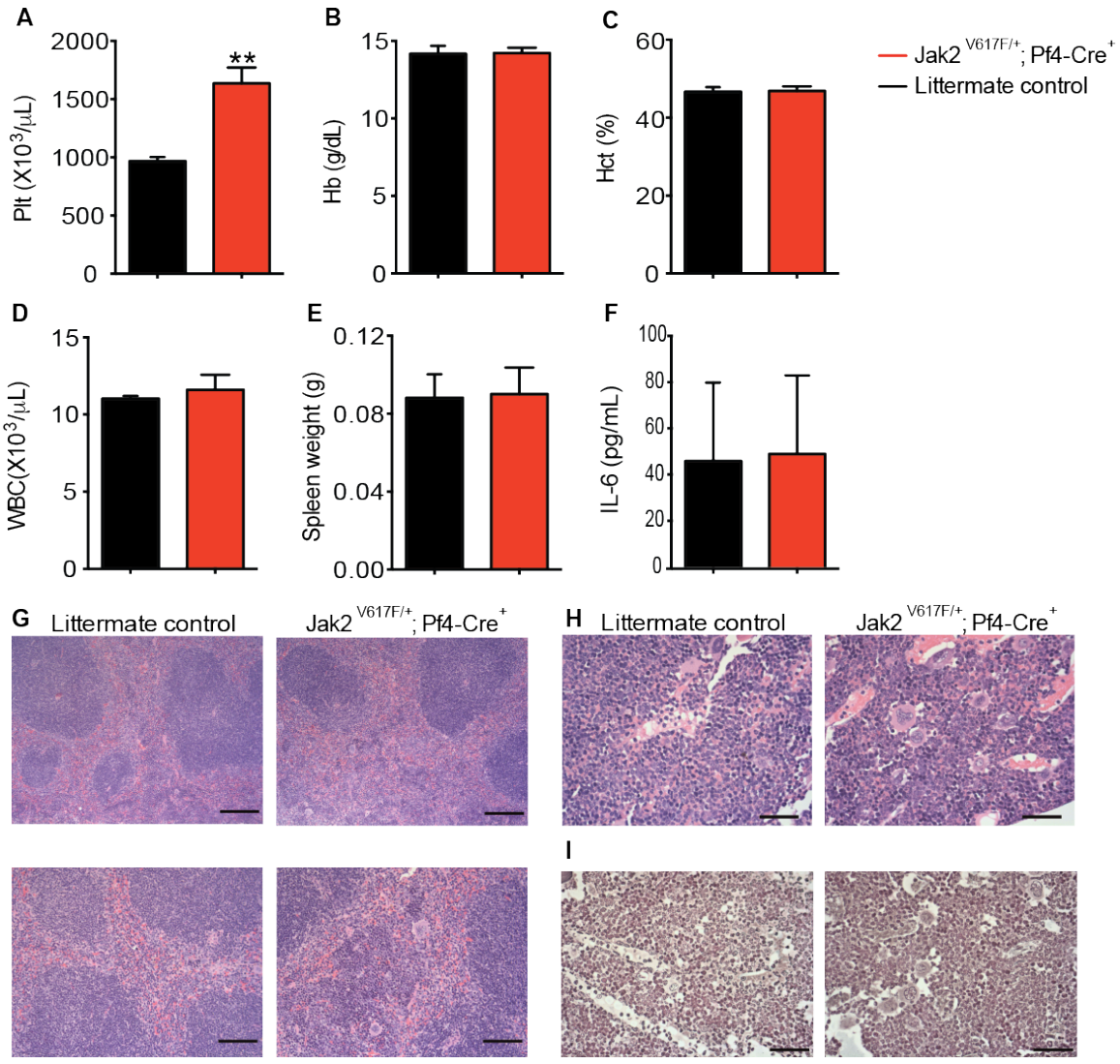

FIGURE 3.8: 3-MONTH-OLD *JAK2$^{V617F/+;}$ PF4-CRE^{+}* MICE DO NOT DISPLAY OVERT PV/MPN

Five pairs of 7-11-week-old *Jak2$^{V617F/+;}$ Pf4-Cre^{+}* mice and littermate controls were analyzed for signs of polycythemia. Compared to age-matched littermate controls, peripheral blood analysis of *Jak2$^{V617F/+;}$ Pf4-Cre^{+}* mice only showed an increase in **(A)** platelet counts. **(B)** Hemoglobin, **(C)** hematocrit, and **(D)** white blood cell counts were not changed. **(E)** Spleen weights and **(F)** serum IL-6 levels were also similar. H&E staining of **(G)** spleen and **(H)** sternum sections also revealed no alterations in tissue histology. **(I)** Reticulin staining of sternum sections also revealed no signs of fibrosis at this earlier time point. Scale bars depict 100 microns in upper panels of **(G)**, and 50 microns in lower panels of **(G)**, **(H)** and **(I)**.

Bar graphs depict mean ± SEM. ** $p < 0.01$ by unpaired two-sided Student's T test.

Reprinted with permission from the American Association for Cancer Research. Image from: Woods B. et al. Activation of JAK/STAT signaling in megakaryocytes sustains myeloproliferation in vivo. Clinical Cancer Research Jun 19 (2019) [ePub ahead of print]. PMID: 31217200.

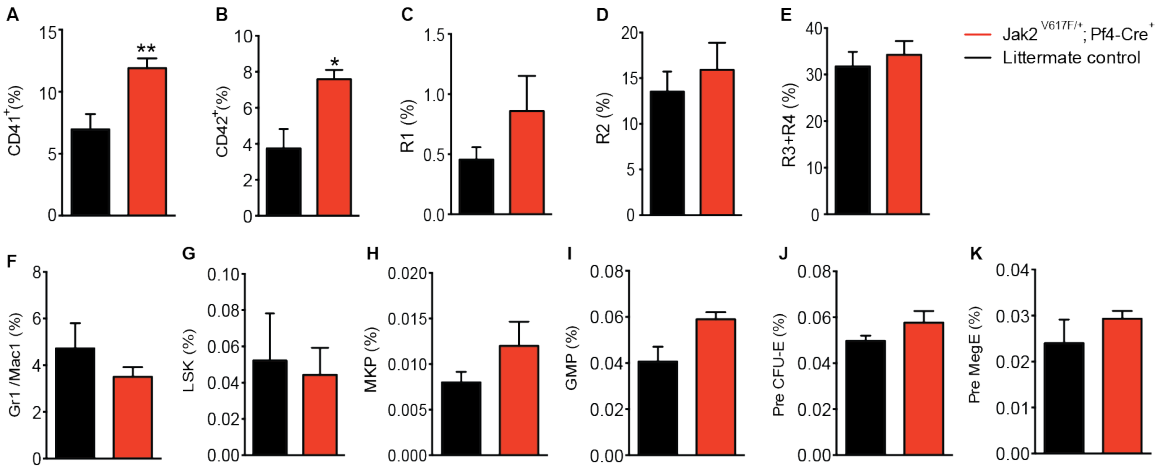

FIGURE 3.9: TRI-LINEAGE HYPERPLASIA IS NOT DETECTABLE IN THE BONE MARROW OF YOUNGER/ASYMPTOMATIC *JAK2$^{V617F/+}$; PF4-CRE^{+}* MICE.

The bone marrow of 5 pairs of 7-11-week-old *Jak2$^{V617F/+}$; Pf4-Cre^{+}* mice and littermate controls were analyzed by flow cytometry. Compared to littermate controls, *Jak2$^{V617F/+}$; Pf4-Cre^{+}* mice only show signs of increased megakaryopoiesis. This was indicated by increases in the frequency of **(A)** CD41^{+} and **(B)** CD42^{+} Mks. No differences were seen in the frequency of **(C-E)** erythroid cells, **(F)** Mac1^{+}/Gr1^{+} myeloid cells, or **(G-K)** progenitor cells between Jak2$^{V617F/+}$; Pf4-Cre^{+} mice and littermate controls.

Bar graphs depict mean ± SEM. * $p < 0.05$, ** $p < 0.01$ by unpaired two-sided Student's T test.

Reprinted with permission from the American Association for Cancer Research. Image from: Woods B. et al. Activation of JAK/STAT signaling in megakaryocytes sustains myeloproliferation in vivo. Clinical Cancer Research Jun 19 (2019) [ePub ahead of print]. PMID: 31217200.

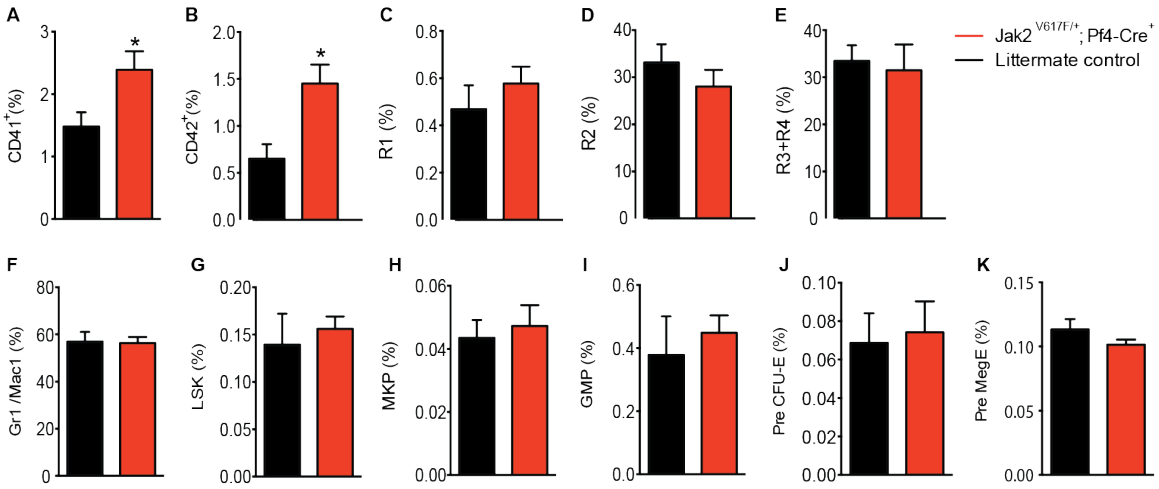

FIGURE 3.10: YOUNGER/ASYMPTOMATIC *JAK2$^{V617F/+}$; PF4-CRE^{+}* MICE ONLY SHOW INCREASED PERIPHERAL MEGAKARYOPOIESIS.

The spleens of 5 pairs of 7-11-week-old *Jak2$^{V617F/+}$; Pf4-Cre^{+}* mice and littermate controls were analyzed by flow cytometry. Compared to littermate controls, *Jak2$^{V617F/+}$; Pf4-Cre^{+}* mice only showed signs of increased megakaryopoiesis (also detected in bone marrow, **Figure 3.9**). This was indicated by increases in the frequency of **(A)** CD41^{+} and **(B)** CD42^{+} Mks. No differences were seen in the frequency of **(C-E)** erythroid cells, **(F)** Mac1^{+}/Gr1^{+} myeloid cells, or **(G-K)** progenitor cells between *Jak2$^{V617F/+}$; Pf4-Cre^{+}* mice and littermate controls.

Bar graphs depict mean ± SEM. * $p < 0.05$ by unpaired two-sided Student's T test.

Reprinted with permission from the American Association for Cancer Research. Image from: Woods B. et al. Activation of JAK/STAT signaling in megakaryocytes sustains myeloproliferation in vivo. Clinical Cancer Research Jun 19 (2019) [ePub ahead of print]. PMID: 31217200.

We next sought to confirm that *Jak2*-mutant Mks promote myeloproliferation in a cell non-autonomous manner. First, we transplanted lethally irradiated recipients with either 90% or 10% *Jak2*$^{VF/+}$*; Pf4-Cre*$^{+}$-derived bone marrow mixed with wild type support and monitored recipients for symptom onset. Only recipients receiving 90% *Jak2*$^{VF/+}$*; Pf4-Cre*$^{+}$-derived bone marrow showed signs of the disease phenotype (elevated hematocrits and hemoglobin, splenomegaly, expanded erythroid populations, expanded white pulp) observed in primary mice (**Figure 3.11**). Platelet counts were elevated over time in recipients receiving 90% *Jak2*$^{VF/+;}$ *Pf4-Cre*$^{+}$-derived bone marrow (**Figure 3.11C**), and neither group showed significant leukocytosis (**Figure 3.11D**). The disease phenotype emerged after a significant latency period, comparable to what is seen in primary mice, rather than emerging within 6-8 weeks post-transplantation like what is observed upon transplantation of purified *Jak2*^{V617F}-mutant LT-HSCs (Mullally et al. 2012).

Furthermore, LSK and MEP cells sorted from symptomatic *Jak2*$^{V617F/+;}$ *Pf4-Cre*$^{+}$ mice did not show EPO hypersensitivity, which is an established pathognomic feature of JAK2^{V617F}-mutant PV progenitor cells (**Figure 3.12**). This observation, combined with the latency periods observed in both primary and transplanted mice, strongly suggests that *Jak2*^{V617F}-mutant Mks require time to remodel the HSPC niche to potentiate a neoplastic state in a cell non-autonomous manner.

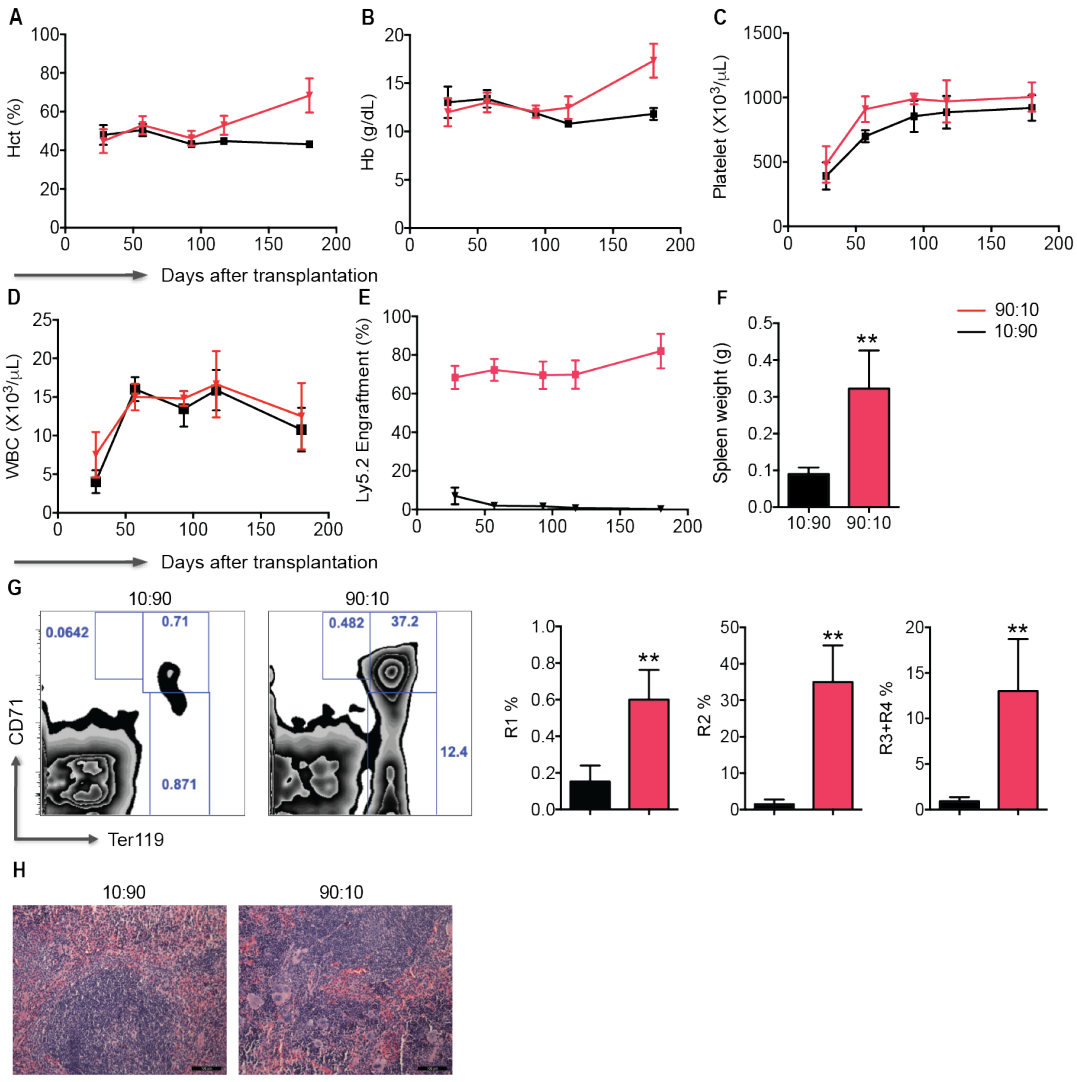

FIGURE 3.11: POLYCYTHEMIA CAUSED BY MK-RESTRICTED *JAK2*^{V617F} EXPRESSION IS TRANSPLANTABLE AFTER A LONG LATENCY PERIOD.

2 x 10^6 *Jak2*$^{V617F/+}$*; Pf4-Cre*$^+$ (CD45.2) and WT (CD45.1) total BM cells were transplanted into lethally irradiated female two-month old WT (CD45.1) mice at a ratio of 90:10 or 10:90. The *Jak2*$^{V617F/+}$*; Pf4-Cre*$^+$ donors were female six-month old mice with confirmed PV. **(A-E)** Hematological indices including **(A)** hematocrit, **(B)** hemoglobin, **(C)** platelet, and **(D)** white blood cell counts in peripheral blood and **(E)** CD45.2 cell chimerism were measured at indicated times. Line graphs depict mean ± SEM. 90:10 vs 10:90, $p < 0.01$ by two-way ANOVA (**A, B, C, E**). **(F)** Recipients of 90:10 bone marrow cells showed increased spleen weights. **(G)** Flow cytometric analysis showed that recipients of 90:10 cells had increased erythroid cells in the spleen. H&E staining of spleen sections from recipients of 90:10 bone marrow revealed disruption of splenic architecture **(H).** Scale bars depict 100 mm.

Bar graphs depict mean ± SEM. **$p < 0.01$ by unpaired two-sided Student's T-test. n=4 animals per group. Data are representative of 2 independent experiments.

Reprinted with permission from the American Association for Cancer Research. Image from: Woods B. et al. Activation of JAK/STAT signaling in megakaryocytes sustains myeloproliferation in vivo. Clinical Cancer Research Jun 19 (2019) [ePub ahead of print]. PMID: 31217200.

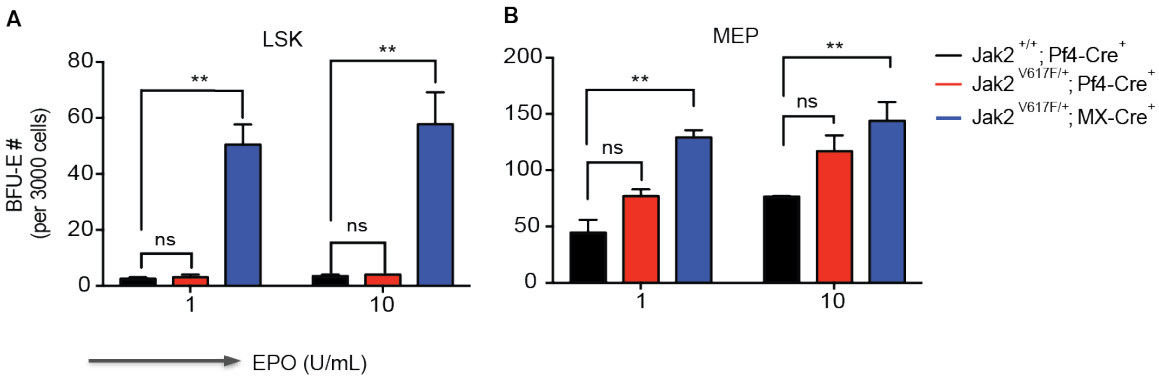

FIGURE 3.12: HSPCS FROM *JAK2$^{VF/+}$; PF4-CRE^{+}* MICE ARE NOT CYTOKINE HYPER-RESPONSIVE.

EPO-dependent colony formation was assessed on either sorted **(D)** LSKs or **(E)** MEPs from WT 6-8-week-old C57/B6 mice.

Bar graphs depict mean ± SEM. **p < 0.01 by two-way ANOVA. Results are representative of 2 independent experiments. n = 6 mice total per group.

Reprinted with permission from the American Association for Cancer Research. Image from: Woods B. et al. Activation of JAK/STAT signaling in megakaryocytes sustains myeloproliferation in vivo. Clinical Cancer Research Jun 19 (2019) [ePub ahead of print]. PMID: 31217200.

These observations collectively indicate that *Jak2*^{V617F}-mutant Mks promote MPN initiation in a cell non-autonomous manner. It is entirely possible that the observed MPN phenotype could potentially be due to the outgrowth of a very small erythroid-biased mutant HSC clone. Prior transplantation studies indicate that just one mutant LT-HSC is sufficient to initiate disease (Lundberg, Takizawa, et al. 2014). Numerous studies to date indicate that *Pf4* is expressed in a rare sub-set of Mk lineage-biased HSCs, and that *Pf4-Cre* transgenic mice show low levels of recombination in the HSC compartment (Calaminus et al. 2012; Pertuy et al. 2015). We could not detect a significant population of mutant/recombined cells in purified HSCs from symptomatic *Jak2*$^{VF/+}$*; Pf4-Cre*$^{+}$ mice. However, it is entirely possible that the methods that we used were not sufficiently sensitive to detect a rare clonal population. However, given that Pf4^{+} HSCs are mostly megakaryocyte-lineage biased while we observe erythroid lineage neoplasia this is likely not a primary contributor to the PV phenotype.

JAK2^{V617F}*-MUTANT MK-DERIVED IL-6 PROMOTES INCREASED ERYTHROPOIESIS*

Megakaryocytes secrete numerous cytokines and chemokines that regulate the behavior of other hematopoietic cell types, including HSPCs, in a paracrine manner (Bruns et al. 2014; M. Zhao et al. 2014; Nakamura-Ishizu et al. 2015; Storan et al. 2015; Domingues et al. 2017). We hypothesized that *Jak2*^{V617F}-mutant Mks secrete aberrant levels of cytokines or chemokines that influence the differentiation and/or proliferation of *Jak2*^{WT} HSPCs to promote neoplastic growth. Multi-plexed cytokine/chemokine profiling of serum from symptomatic *Jak2*$^{V617F/+;}$ *Pf4-Cre*$^{+}$ mice detected significant increases in the levels of

several cytokines/chemokines, including: Interleukin-6 (IL-6), Ccl11 (Eotaxin), Cxcl1 (KC), and Cxcl2 (MIP-2) in symptomatic *Jak2*$^{V617F/+;}$ *Pf4-Cre*$^{+}$ mice relative to age-matched littermate controls (**Figure 3.13A**). Single-plexed ELISA measurements validated a four-fold increase in IL-6 (**Figure 3.13B**), as well as significant increases in Ccl11, Cxcl1, and Cxcl2 (**Figure 3.13C-E**).

We next sought to determine if any of these factors could independently promote increased erythropoiesis, and thus contribute to the PV-like disease observed in our model. We cultured *Jak2*^{WT} HSPCs (either LSKs or MEPs sorted from wild-type mice) in methylcellulose under erythroid colony promoting conditions (cytokine-free methylcellulose supplemented with EPO and SCF). Only exogenous IL-6 treatment increased EPO-dependent colony formation, whereas Cxcl1/Cxcl2 showed no effect (**Figure 3.14**). Interestingly, LSKs showed a > 15-fold increase in colony formation whereas MEPs only responded approximately 2-fold. This suggests that more primitive LSKs are the cells that respond to IL-6, rather than the more lineage-restricted MEP compartment. Therefore, (Mk-derived) IL-6 likely exerts its effect by promoting increased erythroid differentiation of *Jak2*^{WT} HSCs and increased proliferation of committed erythroid progenitors.

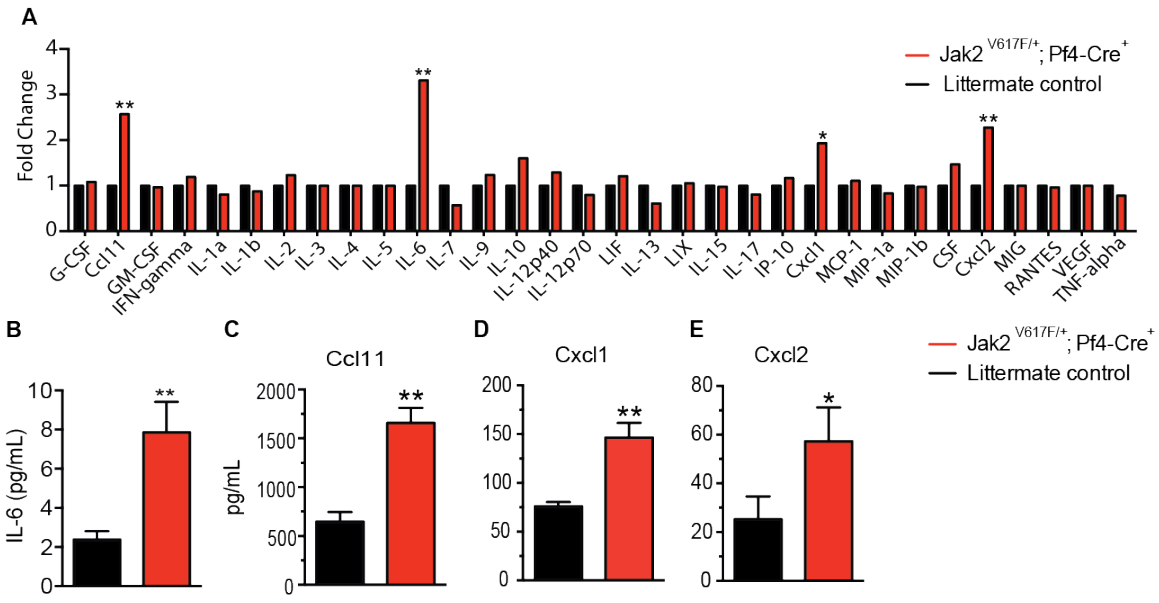

FIGURE 3.13: MK-RESTRICTED *JAK2*^{V617F} EXPRESSION INCREASES PRO-INFLAMMATORY CYTOKINES/CHEMOKINES.

(A) Multiplexed serum profiling (Luminex cytokine assay) of 32 cytokines/chemokines in sera from 5-month-old *Jak2*$^{VF/+}$*; Pf4-Cre*$^{+}$ mice and littermate controls showed significant increases in Ccl11 (Eotaxin), Cxcl1 (KC), Cxcl2 (MIP-2), and IL-6. Data shown are representative of 2 independent experiments. **(B-E)** Single-plex ELISA confirming the increase in serum IL-6 levels observed in *Jak2*$^{VF/+}$*; Pf4-Cre*$^{+}$ mice.

N = 4 mice per group. * p<0.05, **p<0.01 by unpaired Student's T-test.

Reprinted with permission from the American Association for Cancer Research. Image from: Woods B. et al. Activation of JAK/STAT signaling in megakaryocytes sustains myeloproliferation in vivo. Clinical Cancer Research Jun 19 (2019) [ePub ahead of print]. PMID: 31217200.

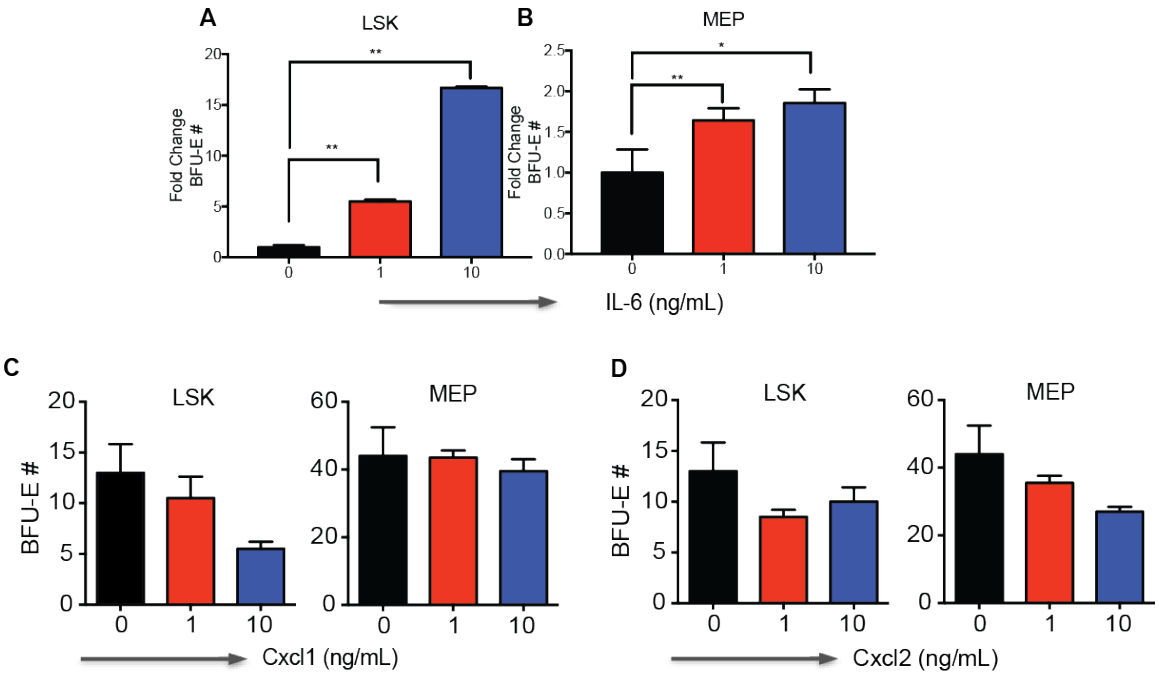

FIGURE 3.14: IL-6 PROMOTES EPO-DEPENDENT COLONY FORMATION OF *JAK2*^{WT} HSPCS.

(**A, B)** IL-6 increases BFU-E formation from wild type HSPCs. **(A)** LSKs and **(B)** MEPs in a dose-dependent manner. LSK/MEP populations were FACS sorted from 6-8-week-old WT C57BL/6 mice. Unlike IL-6, WT HSPCs (FACS-sorted LSKs and MEPs from 6-8-week-old C57BL/6 mice) did not show increased erythroid colony formation in the presence of either exogenous **(C)** Cxcl1 or **(D)** Cxcl2.

Results are representative of 3 independent experiments. Bar graphs depict mean ± SEM. Results were determined to be non-significant ($p > 0.05$) by one-way ANOVA with Bonferroni correction.

Reprinted with permission from the American Association for Cancer Research. Image from: Woods B. et al. Activation of JAK/STAT signaling in megakaryocytes sustains myeloproliferation in vivo. Clinical Cancer Research Jun 19 (2019) [ePub ahead of print]. PMID: 31217200.

We next sought to determine if elevated IL-6 potentiates the disease phenotype observed in our model. We accomplished this by treating symptomatic *Jak2*$^{V617F/+;}$ *Pf4-Cre*$^{+}$ mice with an IL-6 antibody to block IL-6 activity *in vivo*. The antibody was well-tolerated; treated animals showed no significant weight loss or hematopoietic toxicities. IL-6 antibody treatment was not enough to change peripheral blood cell counts (**Figure 3.15**). However, upon further analysis, we observed IL-6 blockade did suppress earlier stages of erythropoiesis.

IL-6 blockade significantly reduced the frequency of erythroid progenitors, including the Pre-MegE and Pre-CFUe compartments in symptomatic *Jak2*$^{V617F/+;}$ *Pf4-Cre*$^{+}$ mice (**Figure 3.16A, B**). IL-6 blockade also decreased the proportion of immature R1 and R2 erythroid populations. This was further demonstrated in vitro – treated splenocytes formed fewer BFU-E colonies *ex vivo* (**Figure 3.16C**). While IL-6 blockade was insufficient to reverse erythroplasia, it is sufficient to inhibit erythroid progenitor cell expansion. In parallel, age- and gender-matched *Jak2*^{WT} littermate controls were also treated in order to assess if IL-6 contributes to erythropoiesis in steady-state erythropoiesis. Interestingly, we observed a similar effect on wild type erythroid progenitors (**Figure 3.17**). This indicates that increased levels of IL-6 significantly contribute to the aberrant expansion of *Jak2*^{WT} erythroid cells in our model.

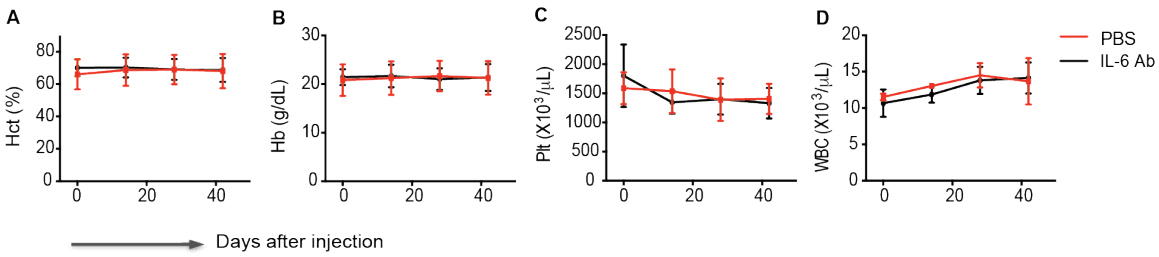

FIGURE 3.15: IL-6 BLOCKADE DOES NOT NORMALIZE PERIPHERAL BLOOD COUNTS IN *JAK2*$^{V617F/+}$; *PF4-CRE*$^{+}$ MICE.

Symptomatic *Jak2*$^{V617F/+}$; *Pf4-Cre*$^{+}$ mice (16-20 weeks old) treated with an antibody against IL-6 for 6 weeks showed no changes in peripheral blood counts. Peripheral blood was analyzed at 0, 14, 28, and 42 days after starting treatment. Reported are **(A)** hematocrit, **(B)** hemoglobin, **(C)** Platelet, and **(D)** leukocyte/white blood cell counts over time.

$p > 0.05$ by two-way ANOVA. Results are representative of 2 experiments, n=3 animals per group. Line graphs depict mean ± SEM.

Reprinted with permission from the American Association for Cancer Research. Image from: Woods B. et al. Activation of JAK/STAT signaling in megakaryocytes sustains myeloproliferation in vivo. Clinical Cancer Research Jun 19 (2019) [ePub ahead of print]. PMID: 31217200.

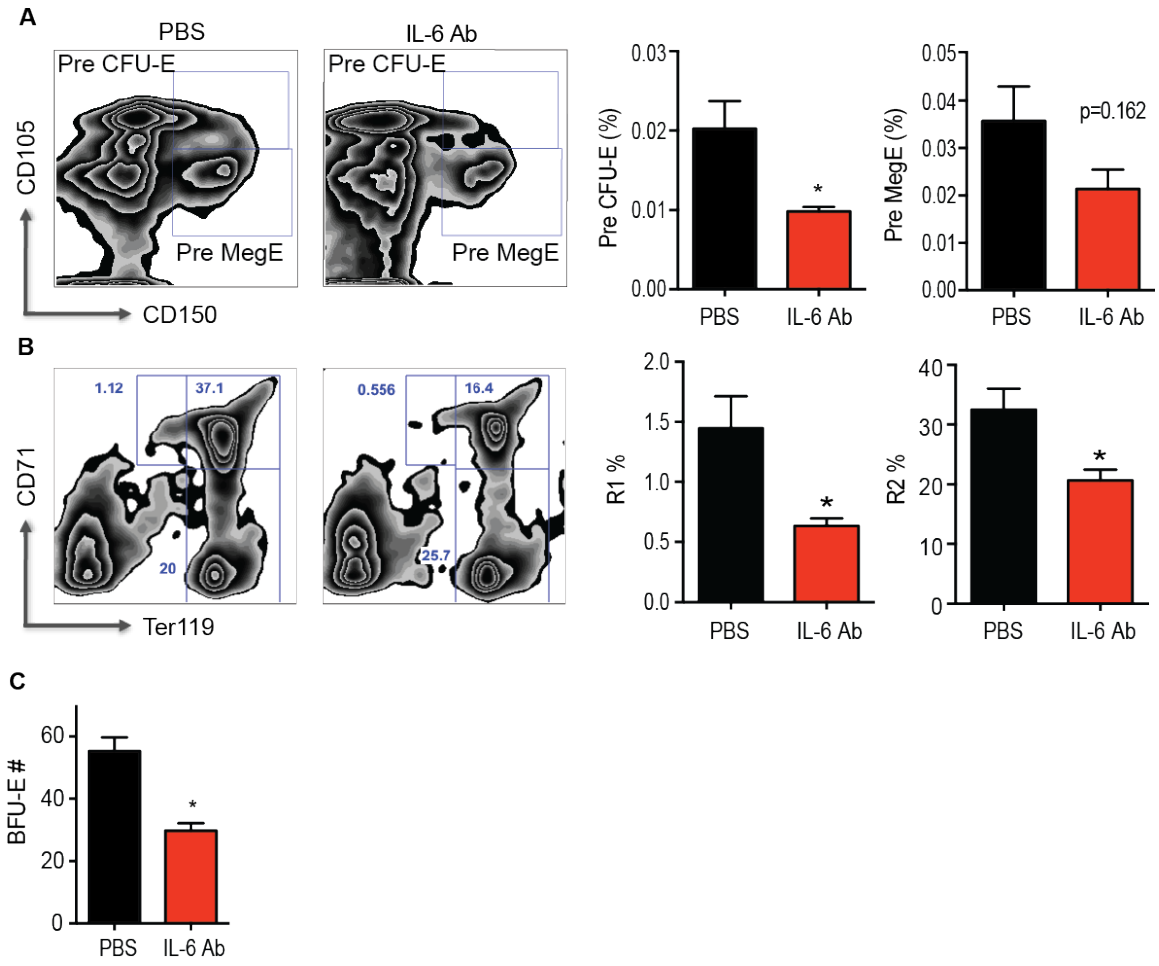

FIGURE 3.16: IL-6 BLOCKADE SUPPRESSES ABERRANT ERYTHROPOIESIS.

3 pairs of 16-20-week-old male or female *Jak2*$^{VF/+;}$ *Pf4-Cre*$^{+}$ mice were treated with either an antibody against IL-6 or PBS for 6 weeks. Decreases in the splenic erythroid progenitors **(A)** Pre-CFU-E and Pre-MegE populations and **(B)** immature erythroid (R1 and R2) populations were also observed by flow cytometry. **(C)** IL-6 blockade markedly reduced BFU-E formation by splenocytes in vitro.

Results are representative of 2 independent experiments. * $p < 0.05$, ** $p < 0.01$ by unpaired two-sided Student's T-test.

Reprinted with permission from the American Association for Cancer Research. Image from: Woods B. et al. Activation of JAK/STAT signaling in megakaryocytes sustains myeloproliferation in vivo. Clinical Cancer Research Jun 19 (2019) [ePub ahead of print]. PMID: 31217200.

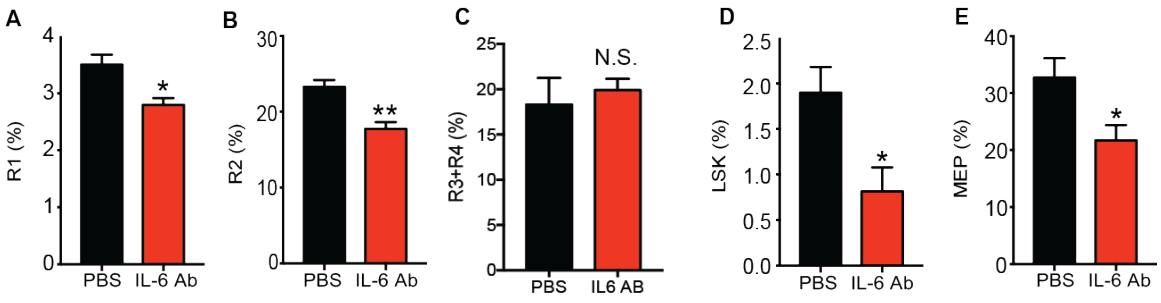

FIGURE 3.17: IL-6 BLOCKADE DISRUPTS NORMAL ERYTHROPOIESIS.

(A-D) 4-month-old wild type littermate controls were treated in parallel. IL-6 antibody treatment significantly reduced the immature erythroid (R1 and R2) populations, as well as the frequency of LSKs and MEPs in the bone marrow, as determined by flow cytometry. The frequency of mature erythroid cells (R3+R4) was not significantly decreased.

Bar graphs depict mean ± SEM. *p < 0.05 and **p < 0.01 by unpaired two-sided Student's T-test. N=4 mice per group (2 males and 2 females).

Reprinted with permission from the American Association for Cancer Research. Image from: Woods B. et al. Activation of JAK/STAT signaling in megakaryocytes sustains myeloproliferation in vivo. Clinical Cancer Research Jun 19 (2019) [ePub ahead of print]. PMID: 31217200.

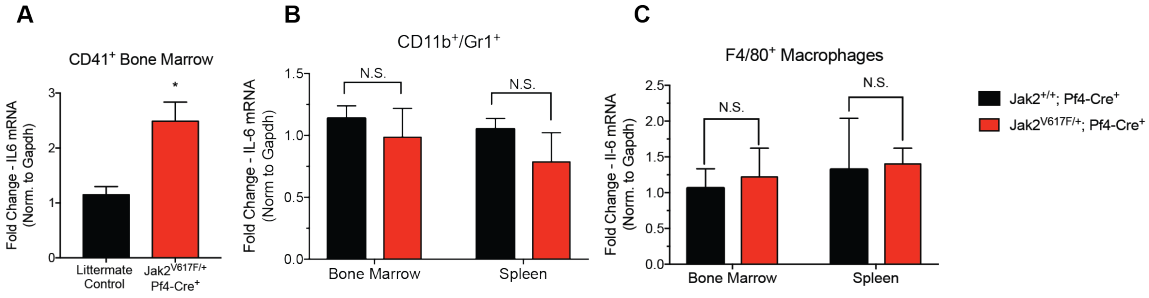

FIGURE 3.18: *JAK2*^{V617F}-MUTANT MKS ARE A SOURCE OF ELEVATED IL-6.

(A) IL-6 mRNA expression is elevated in CD41+ megakaryocytes sorted from *Jak2*$^{VF/+}$*; Pf4-Cre*$^{+}$ mice relative to littermate controls but is not elevated in sorted **(B)** mature myeloid CD11b^{+}/Gr1^{+} cells or **(C)** F4/80^{+} macrophages. IL-6 transcript levels were normalized to *Gapdh*.

N = 4 mice per group. Results are representative of 2 independent experiment. * p < 0.05, ** p < 0.01 by unpaired two-sided Student's T-test. Bar graphs depict mean ± SEM.

Reprinted with permission from the American Association for Cancer Research. Image from: Woods B. et al. Activation of JAK/STAT signaling in megakaryocytes sustains myeloproliferation in vivo. Clinical Cancer Research Jun 19 (2019) [ePub ahead of print]. PMID: 31217200.

The observations above, along with observations in human PV patients, strongly suggest that *Jak2*^{V617F}-mutant Mks are a primary source of IL-6 (Wickenhauser et al. 1999). Mutant Mks isolated from symptomatic *Jak2*$^{V617F/+}$*; Pf4-Cre*$^{+}$ mice did show marked increases in IL-6 expression (**Figure 3.18A**). However, this does not preclude the possibility that additional cell types could contribute additional IL-6. Circulating platelets could promote elevated IL-6 levels indirectly, by collateral activation of mature myeloid cells or erythroblastic island macrophages. In order to determine if mature myeloid cells or macrophages could serve as contributing IL-6 sources, we also examined IL-6 transcript levels in FACS-sorted F4/80^{+} macrophages or Mac1^{+}/Gr1^{+} mature myeloid cells from the spleens of symptomatic *Jak2*$^{V617F/+}$*; Pf4-Cre*$^{+}$ mice. IL-6 expression was not significantly increased in these populations (**Figure 3.18B, C**). This suggests that *Jak2*^{V617F}-mutant Mks are the primary contributors of increased IL-6 in this model.

MEGAKARYOCYTES ARE REQUIRED FOR MPN MAINTENANCE

Given that *Jak2*^{V617F}-mutant Mks are sufficient to cause aberrant erythropoiesis and HSC expansion (Zhan et al. 2016; Zhang et al. 2018), we next sought to determine if the megakaryocyte lineage is necessary for maintenance of the neoplastic state. To accomplish this, we crossed a Cre-inducible Diphtheria toxin receptor transgenic mouse with *Pf4-Cre*$^{+}$ mice to generate a murine model for selective depletion of *Pf4*$^{+}$ megakaryocytes (Buch et al. 2005; Tiedt et al. 2007). We then retrovirally transduced cKit^{+} progenitor cells from either *iDTR*$^{+/-}$*; Pf4-Cre*$^{+}$ or *iDTR*$^{+/-}$*; Pf4-Cre*$^{-}$ mice with *Jak2*^{V617F} and transplanted infected cells into lethally-irradiated recipients.

Retroviral overexpression of *Jak2*^{V617F} in bone marrow transplants leads to a PV-like phenotype that is characterized by elevated hematocrit and hemoglobin levels. As expected, *Jak2*^{V617F}-transplanted mice developed a characteristic PV-like phenotype (**Figure 3.19A**). Diphtheria toxin (DT) treatment significantly reduced platelet counts and the frequency of Mks in *iDTR*$^{+/-}$*; Pf4-Cre*$^{+}$ mice (**Figure 3.19A, B, C**). Mk/platelet depletion was further accompanied by a significant decrease in several disease indicators.

Notably, the erythroid lineage was markedly impacted by Mk depletion. Hematocrit and hemoglobin levels were decreased (**Figure 3.19A**). We also observed significant reductions in the terminally-differentiated mature erythroid R3+R4 populations in both the bone marrow and spleen (**Figure 3.19D, E**). White blood cell counts were not affected by Mk depletion (**Figure 3.19A**). However, white blood cell counts are only modestly increased in this model at baseline. Mk depletion also led to a significant reduction in serum IL-6 levels (**Figure 3.19H**), further implicating Mk-derived IL-6 as a central mediator of the aberrant erythropoiesis associated with *Jak2*^{V617F}-driven MPN.

We next sought to investigate the larger relevance of Mks to MPN maintenance, by assessing the effects of Mk depletion on an additional MPN murine model: the *MPL*^{W515L} BMT model. Retroviral overexpression of *MPL*^{W515L} results in a rapid (~17-21 days post-BMT), fully penetrant, and lethal myeloproliferative disease that is characterized by splenomegaly, thrombocytosis, leukocytosis, and fibrosis without evident polycythemia or an overt erythroid presentation (**Figure 3.20**) (Pikman et al. 2006). In addition to the expected decreases in Mk frequency and platelet counts, leukocyte counts, and spleen weights were also significantly reduced (**Figure 3.20A, B, C**). Mk depletion also reversed

myeloid progenitor expansion and markedly restored the histological architecture of the spleen (**Figure 3.20E, F**). These observations correspond to a reduction in overall disease burden in this MPN model. Therefore, combined with the results of Mk depletion in the *Jak2*^{V617F} BMT model, the Mk lineage contributes significantly to the general maintenance of myeloid neoplasia, regardless of driver mutation or even disease phenotype.

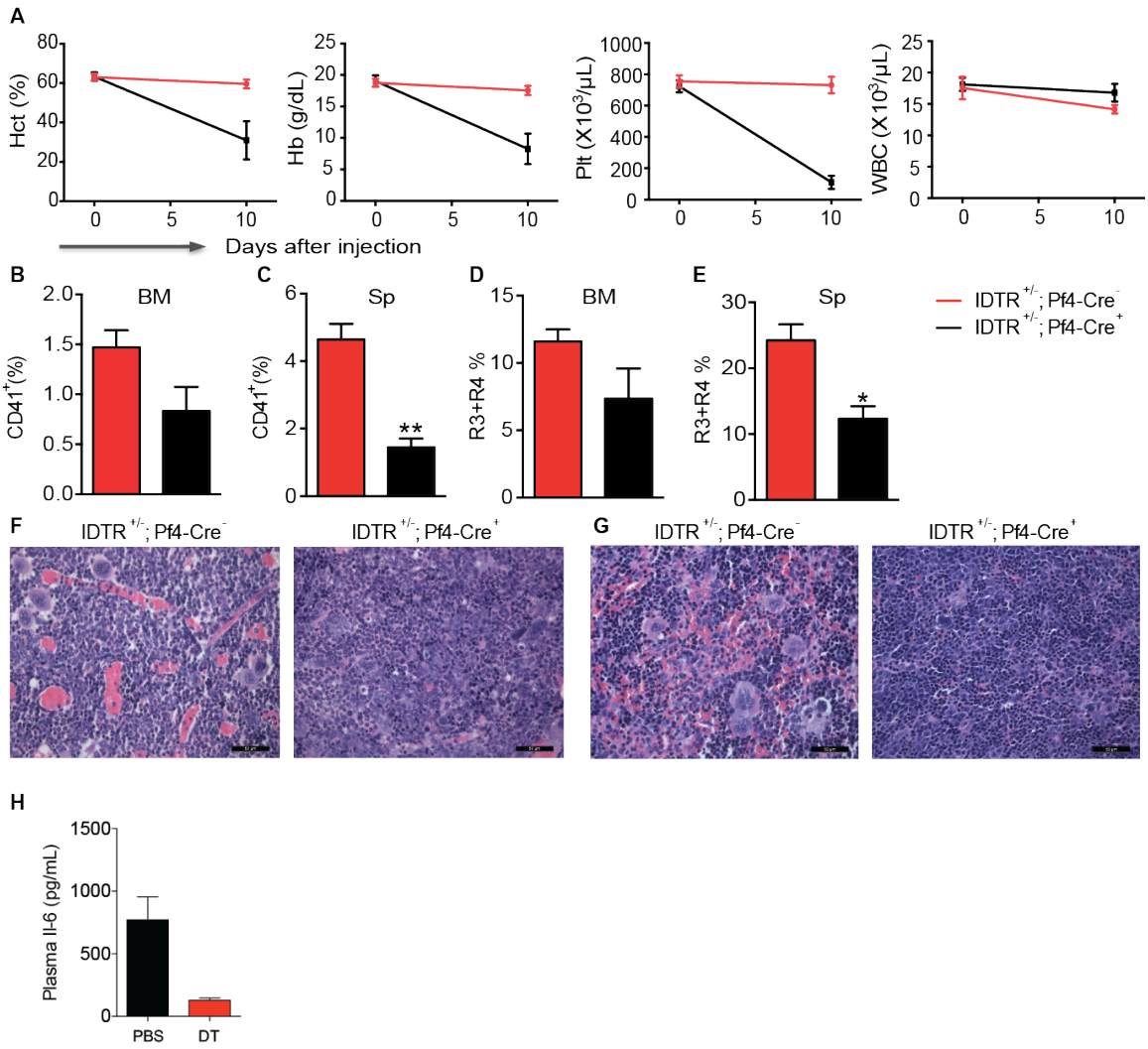

FIGURE 3.19: MK DEPLETION ATTENUATES MPN IN THE JAK2^{V617F} BMT MODEL.

(A) Mk depletion significantly decreased platelet counts, hematocrit, and hemoglobin in peripheral blood ($P < 0.01$ by two-way ANOVA), while white blood cell counts were unaffected. **(B-E)** Mk depletion significantly reduced the CD41+ Mk compartment and terminally-differentiated mature erythroid compartment (R3+R4 populations) in bone marrow (BM) and spleen (Sp). H&E staining of **(F)** bone marrow and **(G)** spleen sections after Mk ablation showed markedly fewer Mks and restoration of splenic architecture. **(H)** Serum IL-6 levels were also decreased.

Scale bars depict 50 microns; n=5 iDTR+/-; Pf4-Cre- controls and 3 iDTR+/-; Pf4-Cre+ mice. Bar graphs and line graphs depict mean ± SEM.

Reprinted with permission from the American Association for Cancer Research. Image from: Woods B. et al. Activation of JAK/STAT signaling in megakaryocytes sustains myeloproliferation in vivo. Clinical Cancer Research Jun 19 (2019) [ePub ahead of print]. PMID: 31217200.

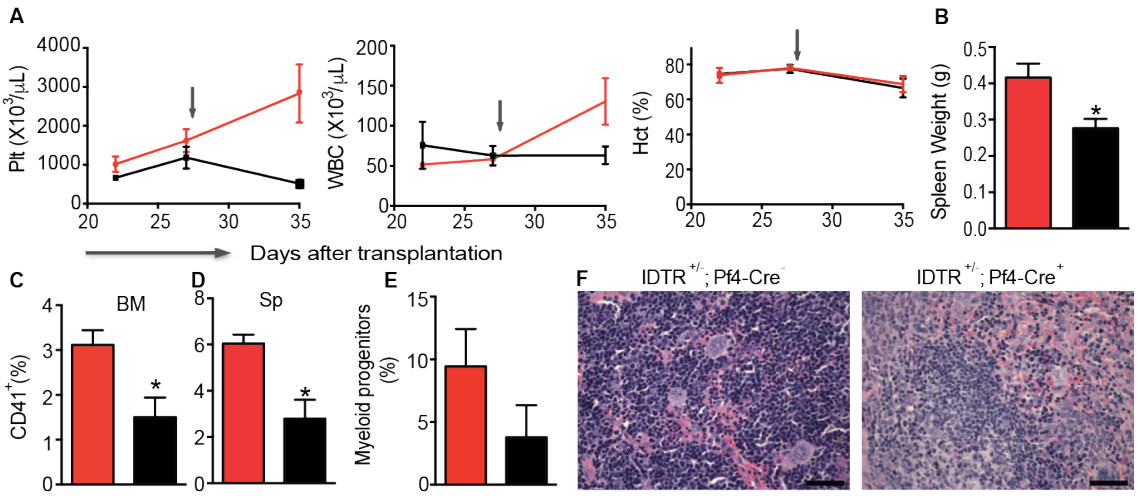

FIGURE 3.20: MK DEPLETION ATTENUATES MPL^{W515L}-DRIVEN MF.

(A-F) DT (10 μg/kg) was administered to MIGR1-*MPL*^{W515L}-GFP recipients 28 days post-transplant to initiate Mk depletion in the setting of myelofibrosis. **(A)** Mk ablation significantly reduced platelets and white blood cell counts in this model ($p < 0.01$ by two-way ANOVA), while hematocrit was unchanged. **(B)** Spleen weights were also significantly reduced following Mk depletion in *iDTR*$^{+/-}$*; Pf4-Cre*$^{+}$ mice compared to *iDTR*$^{+/-}$*; Pf4-Cre*$^{-}$ controls. **(C-E)** DT treatment decreased the frequency of CD41^{+} megakaryocytes in both the bone marrow and spleen, as well as the frequency of cKit^{+} myeloid progenitor cells in the spleen of *iDTR*$^{+/-}$*; PF4-Cre*$^{+}$ mice. **(F)** H&E stained spleen showed DT treatment reduced megakaryocytes and partially restored the normal splenic architecture in *iDTR*$^{+/-}$*; PF4-Cre*$^{+}$ mice.

Scale bars depict 50 microns. n=6 animals per group. Mice were sacrificed 7 days after initiation of DT treatment. Bar graphs and line graphs depict mean ± SEM. *$p < 0.05$, **$p < 0.01$. Results shown are representative of 2 independent experiments.

Reprinted with permission from the American Association for Cancer Research. Image from: Woods B. et al. Activation of JAK/STAT signaling in megakaryocytes sustains myeloproliferation in vivo. Clinical Cancer Research Jun 19 (2019) [ePub ahead of print]. PMID: 31217200.

DISCUSSION

In these studies, we investigated the contributions of *Jak2*^{V617F}-mutant Mks to MPN pathogenesis by developing novel murine models of megakaryocyte lineage-restricted *Jak2*^{V617F} expression. Our observations are consonant with previous studies of megakaryocyte lineage-specific *Jak2*^{V617F} expression, in demonstrating that mutant Mks promote expansion of the *Jak2*^{WT} hematopoietic milieu to initiate a myeloproliferative state *in vivo* (Zhan et al. 2016; Zhang et al. 2018). As with previously reported models, we observed a significant expansion of both the *Jak2*^{V617F}-mutant megakaryocyte lineage and the *Jak2*^{WT} HSPC compartment. However, there are several distinct differences between the model reported by Zhan et al and the model described in this thesis, with regards to both the general *Jak2/JAK2* expression strategies and salient features of the disease phenotypes that they generate.

The 2016 and 2018 studies using *Pf4-Cre* to drive Mk-restricted *JAK2*^{V617F} expression used an inducible human JAK2 Flip-Flop transgenic model, where human *JAK2*^{V617F} is expressed at supra-physiologic levels under the control of a minimal human *JAK2* promoter element (Tiedt et al. 2008). This mouse line carries nine copies of a bacterial artificial chromosome (BAC) (containing human JAK2 exons 1–12 with the 5′ regulatory region) followed by a cDNA fragment (exons 13–25 with SV40 polyA, encoding the mutant human JAK2 kinase domains) placed in the inverse orientation and flanked by antiparallel lox66 and lox71 sites. When crossed to Cre recombinase mouse lines to induce transgene expression, this model gives rise to variable levels of *JAK2*^{V617F} expression that is dependent on the levels of Cre recombinase activity and expression. As such, the resulting

disease phenotype varies with the strategy used to activate the transgene. Use of *Vav-Cre* results in the expression of lower levels of *JAK2*^{V617F} compared to endogenous mouse *Jak2* and results in an ET-like phenotype characterized by elevated platelet counts, moderate effects on WBCs, and no discernable effect on the erythroid lineage. Use of *Mx1-Cre*, however, results in higher *JAK2*^{V617F} expression levels and promotes a heterogeneous MPN phenotype with increased erythropoiesis as well as thrombocytosis. Use of either *Cre* transgenic line also promotes myelofibrosis, indicating that this aspect of the disease phenotype is likely dictated by factors other than oncogene expression levels. Flip-flop transgene expression via *Pf4-Cre* leads to a transplantable ET-like phenotype that presents with thrombocytosis (and expansion of the CD41^{+} Mk compartment), splenomegaly, and broad expansion of the HSPC pool (Zhan et al. 2016). While similar to the results described above, our model presents with distinct differences.

Our model uses a mouse *Jak2*^{V617F} allele that is expressed at physiologic levels via knock-in to the endogenous mouse *Jak2* locus (Mullally et al. 2010). This conditional knock-in allele was engineered to have a point mutation in exon 13 of mouse *Jak2* and, upon Cre recombination, mouse *Jak2*^{V617F} is expressed under the control of endogenous mouse *Jak2* regulatory elements. Pan-hematopoietic expression of this allele using either *Vav-Cre* or *Mx1-Cre* results in a PV-like phenotype that can eventually progress to myelofibrosis (Mullally et al. 2010). Our model of Mk-restricted *Jak2*^{V617F} expression is characterized by a very strong PV-like phenotype, along with impaired overall survival, splenomegaly, and aberrant erythropoiesis (elevated hemoglobin/hematocrit, and erythroid progenitor cell expansion). The erythroid phenotype, while characteristic of PV in general, is markedly less pronounced than what is observed upon pan-hematopoietic expression. The latency period is also far longer, with the erythroid expansion becoming

apparent in peripheral blood after almost 16-20 weeks, compared to just 8 weeks (Mullally et al. 2010). Fibrosis, albeit mild, was also apparent.

Therefore, we conclude that *Jak2*^{V617F}-mutant Mks are sufficient to generate a myeloproliferative state that most closely resembles human PV. *Jak2*^{V617F}-mutant Mks also promote cell non-autonomous myelo-erythroid expansion, which likely contributes to MPN in concert with clonal expansion of mutant cells in different lineages. These observations are consistent with genetic and clinical correlative studies in a cohort of MPN patients with low *JAK2*^{V617F} allele burden. These studies reported impaired clinical outcome and disease progression in a cohort of ET/MF patients, even though their hematopoietic compartment was comprised of a relatively low fraction of *Jak2*^{V617F}-mutant cells (Moliterno et al. 2006; Tefferi et al. 2008). Additional studies suggest that *JAK2*^{V617F} allele burden shows little to no correlation with disease phenotype.

Pro-inflammatory cytokines and chemokines are frequently elevated in MPN patients, and this is typically associated with adverse survival. This cytokine-driven inflammatory state is most likely driven by JAK/STAT pathway hyper-activation and is hypothesized to be the key contributing cause of the constitutional symptoms of MPN. This led us to hypothesize that *Jak2*^{V617F}-mutant Mks (and possibly platelets) could potentiate a myeloproliferative state by the aberrant production of pro-inflammatory cytokines/chemokines, which could in turn promote the neoplastic expansion of *Jak2*^{WT} lineages. Indeed, we observed that *Jak2*^{V617F}-mutant Mks/platelets led to a significant elevation in serum levels of 4 discrete factors: IL-6, Ccl11, Cxcl1, and Cxcl2. Of these factors, only IL-6 supported increased

erythroid differentiation *in vitro*, which implicates this classical mediator of inflammatory response as a key promoter of MPN pathogenesis.

Consistent with our observations, elevated IL-6 levels in MPN patients are correlated with splenomegaly, overall survival, and *JAK2* mutation status (Tefferi et al. 2011). Furthermore, the improvement in constitutional symptoms seen upon JAK2 inhibitor treatment correlates with reductions in serum IL-6 levels. A previous report also implicated IL-6 in the myeloproliferative syndrome observed in miR-146a knock-out mice (J. L. Zhao et al. 2013). $Jak2^{V617F}$-mutant Mks, in our model, showed increased IL-6 expression by qPCR, thus implicating mutant Mks as primary contributing sources of IL-6.

A previous *in vivo* study revealed that exogenous IL-6 treatment in rats causes a transient erythroid hyperplasia (Ulich et al. 1991). However, a link between IL-6 and erythroid differentiation is still not fully established. We show above that IL-6 synergizes with EPO *in vitro* to promote EPO-dependent colony formation by HSPCs. Furthermore, IL-6 blockade significantly impedes erythropoiesis, either in the setting of $Jak^{VF/+}$*; Pf4-Cre*$^{+}$-mediated disease or during steady-state hematopoiesis. These observations suggest that chronically elevated IL-6 levels support MPN pathogenesis by promoting erythroid neoplasia/hyperplasia. This effect could be exerted on either the mutant MPN clone or wild type HSPCs to promote MPN initiation and maintenance.

Mutant Mks and platelets could promote aberrant erythropoiesis either directly, via increased IL-6 production which then acts on HSPCs or erythroid progenitors, or indirectly,

by recruiting and activating myeloid cells. Activated platelets aggregate with leukocytes and monocytes in the periphery, leading to their subsequent activation and cytokine secretion, and platelets are increasingly recognized as having a role in innate immune responses (Weyrich & Zimmerman 2004; Suzuki et al. 2013). Furthermore, macrophages are key central components of erythroblastic "island" niches, reservoirs of immature erythroblasts that are activated during stress hematopoiesis (Chasis & Mohandas 2008). Mature myeloid cells were not significant contributors of IL-6 in our model. However, given that we observe both an increase in platelet-WBC aggregates in *Jak2*$^{VF/+}$*; Pf4-Cre*$^{+}$ mice and histological signs of low-grade inflammation (data not shown), it is likely that these populations could contribute to the observed neoplastic state via additional factors.

We also established a broader role for Mks in MPN maintenance by employing Mk ablation in two established MPN models. Mk depletion in both the *JAK2*^{V617F} and *MPL*^{W515L} bone marrow transplant MPN models significantly blunted the polycythemia and leukocytosis phenotypes of either model respectively, and significantly reduced disease burden overall. This demonstrates that Mks are broadly necessary for the maintenance of a myeloproliferative state in vivo. It also suggests that the contributions of Mks are not driver mutation-specific. Instead, they are a broader consequence of JAK/STAT pathway hyper-activation.

Collectively, our findings confirm and provide further mechanistic insight in to the role of the megakaryocyte lineage in MPN pathogenesis. We demonstrate that mutant Mks are directly involved in MPN initiation and maintenance in vivo, and that Mks can promote the heterotypic expansion of wild type HSPCs via aberrant cytokine production. These data

support a novel model for MPN pathogenesis, in which MPN manifests as a genetically and phenotypically heterogeneous hematopoietic disorder, with both mutant and wild type cells contributing to the pathogenic ecosystem. We expect that similar mechanisms underlie the development of other myeloid neoplasms as well as in non-hematopoietic malignancies, where malignant transformation is driven by a complex interplay between discrete clonal cell populations. While *JAK2*^{V617F} expression levels are still likely relevant in determining the emergence of a PV or ET phenotype in MPN patients, these observations suggest that lineage balance plays a more determinant role.

These findings also contribute to the collective understanding of how MPN patients with a relatively small MPN clone (defined by a small fraction of driver mutation-harboring cells) can present with fulminant disease. They also highlight the therapeutic potential of targeting these cellular interactions (such as Mks and the HSPC niche) to achieve improved therapeutic benefit in MPN.

Chapter 4 - RESULTS II

COORDINATE REGULATION OF MYELOID CELL TRANSFORMATION BY JAK2^{V617F} AND ASXL1 LOSS

INTRODUCTION

The results in Chapter 3 describe a cell non-autonomous role for *JAK2*^{V617F}-mutant cells in promoting the expansion and increased erythroid differentiation of *Jak2*^{WT} HSPCs. However, while *JAK2*^{V617F} is capable of initiating MPN on its own, single *Jak2*^{V617F} mutant HSCs can only propagate MPN at a very low frequency in transplantation assays (Lundberg, Takizawa, et al. 2014). Furthermore, *JAK2*^{V617F} rarely occurs in isolation. Additional non-driver somatic mutations are present in MPN patients, and affect cellular processes including: epigenetic regulation, splicing, metabolism, and parallel signaling cascades. In contrast to the specificity of canonical driver mutations, most of these mutations are detected in other hematologic malignancies. Mutations affecting genes involved in epigenetic regulation are the most prevalent in MPN, and many of these factors modify the disease phenotype and contribute to disease transformation, in addition to altering HSC self-renewal and alter cellular responses to JAK2 inhibitors.

Co-occurring mutations affecting PRC2 function, mainly loss of function mutations in *ASXL1* and *EZH2*, are more commonly found in MF than in PV and ET. In mouse models, *Ezh2* loss synergizes with *Jak2*^{V617F} to enhance MPN development and promote fibrotic progression (Shimizu et al. 2016; Yang et al. 2016). Furthermore, both *ASXL1* and *EZH2*

loss can function as disease-initiating events, both occurring in the LT-HSC compartment in PMF. In mouse models, *Ezh2* loss increased MPN stem cell fitness and repopulation capacity. *Ezh2* loss also increased fibrosis. Collectively, these studies demonstrate that loss of PRC2-mediated gene repression confers an advantage to *Jak2*^{V617F}-mutant MPN stem cells to promote clonal expansion and disease progression.

Heterozygous *ASXL1* frameshift and nonsense mutations frequently co-occur with *JAK2*^{V617F} and confer worsened overall prognosis in Primary Myelofibrosis (PMF). These same alterations in *ASXL1* are also detected across the spectrum of myeloid malignancies. Asxl1 deletion on its own results in a lethal myelodysplastic syndrome in mice and is accepted as a myeloid tumor suppressor that also transforms myeloid cells at least in part via deregulation of PRC2 target genes. Both ASXL1 and EZH2 mutations are associated with increased engraftment capacity of PMF samples in xenografts (Triviai et al. 2019). Therefore, both *ASXL1* and *EZH2* loss contribute to MPN pathogenesis by promoting clonal expansion of MPN stem cells. However, as discussed in the introduction, ASXL1 loss might have additional PRC2-independent roles. 79% of *EZH2*-mutant patients also had concurrent *ASXL1* mutations in one study (Triviai et al. 2019). While these two histone modifiers have overlapping roles in chromatin modification, it is possible that *ASXL1* loss contributions to MPN pathogenesis through PRC2 independent mechanisms.

Here, we sought to determine how *Asxl1* loss modulates *JAK2*^{V617F}-mutant MPN stem cells to alter disease initiation and progression. Furthermore, most studies to date have only investigated the effects of homozygous *Asxl1* loss on hematopoiesis, while most patients present with heterozygous *ASXL1* mutations. We hypothesized that monoallelic *Asxl1* loss

would be sufficient to alter HSC function and promote clonal expansion in *Jak2*^{V617F}-driven MPN. To this end, we generated compound mutant *Jak2*$^{VF/+}$*; Asxl1*$^{-/+}$ or $^{-/-}$ mice and induced simultaneous *Jak2*^{V617F} expression and Asxl1 loss in hematopoietic cells using *HSC-Scl-CreERT* transgenic mice. We demonstrate that loss of one or both copies of *Asxl1* accelerates *Jak2*^{V617F}-driven polycythemia and fibrotic onset and impairs overall survival. *Asxl1* loss also enhanced the fitness of MPN HSCs in vitro and in vivo, and also enhanced JAK2 inhibitor persistence. Heterozygous *Asxl1* loss was also sufficient to affect stem cell function, which suggests a haploinsufficient role for *Asxl1* in myeloid transformation. Our preliminary gene expression studies also suggest a cooperative effect of Jak2^{V617F} and *Asxl1* in regulating a gene expression program that promotes these phenotypes. Collectively, these findings identify a stem cell-centric role for *Asxl1* in promoting expansion and evolution of the MPN clone.

RESULTS

MODELING SIMULTANEOUS ASXL1 LOSS IN JAK2^{V617F}*-DRIVEN MPN*

We used *HSC-Scl-CreERT* transgenic mice to induce simultaneous *Jak2*$^{VF/+}$ expression and *Asxl1* loss in HSCs during adult hematopoiesis. *HSC-Scl-CreERT* transgenic mice contain a tamoxifen-inducible *CreERT* transgene under transcriptional control of an *Scl* enhancer element that is active exclusively in HSCs (Göthert et al. 2005). In our model, Cre recombinase is expressed in HSCs after Tamoxifen treatment, and can go on to recombine the two floxed loci (**Figure 4.1A**). In order to confirm Cre-mediated

recombination at both target loci, excision product PCRs were performed before and after Tamoxifen on genomic DNA harvested from peripheral blood of *Scl-CreERT*$^{+}$*; Jak2*$^{VF/+}$*; Asxl1*$^{-/+}$ mice, *Scl-CreERT*$^{+}$*; Jak2*$^{VF/+}$*; Asxl1*$^{-/-}$ mice, *Scl-CreERT*$^{+}$*; Jak2*$^{+/+}$*; Asxl1*$^{-/+}$ mice, and *Scl-CreERT*$^{+}$*; Jak2*$^{+/+}$*; Asxl1*$^{-/+}$ mice. PCRs were performed using previously established primer sequences that recognize the sequence of the recombined locus. No excision product was detectable before tamoxifen induction. After tamoxifen treatment, excision bands were detectable for both alleles (**Figure 4.1B, C**). These results confirm that *HSC-Scl-CreERT* efficiently induces the simultaneous recombination of multiple Cre-targeted alleles.

In order to quantify the recombination efficiency after Tamoxifen treatment, mice were bred to a *Rosa26-LSL-tdTomato* Cre reporter mouse strain. This transgenic allele uses a LoxP-flanked STOP cassette placed ahead of a *tdTomato* transgene knocked in to the *Rosa26* locus. In the presence of Cre, the STOP cassette is removed and *tdTomato* is expressed. Therefore, Cre^{+} cells can be readily detected by flow cytometry or other similar approaches. While some tdTomato expression could be seen prior to Tamoxifen treatment in some animals, this small population is likely an artifact of transcriptional read-through, rather than a recombined population as this was rarely but occasionally observed in *HSC-Scl-CreERT*$^{-}$ *Rosa26-LSLtdTomato*$^{+}$ controls. Our Tamoxifen induction protocol induced efficient recombination, with >97% of *HSC-Scl-CreERT*$^{+}$*Rosa26-LSLtdTomato*$^{+/+}$ peripheral blood cells appearing tdTomato^{+} by flow cytometry 6 weeks after TAM (**Figure 4.2A**). Furthermore, recombination efficiency was not affected by genotype, since tdTomato levels were comparable in *Asxl1*, *Jak2*, and *Jak2/Asxl1* mice (**Figure 4.2B**). These studies confirm that *HSC-Scl-CreERT* induces efficient Cre expression across the hematopoietic compartment.

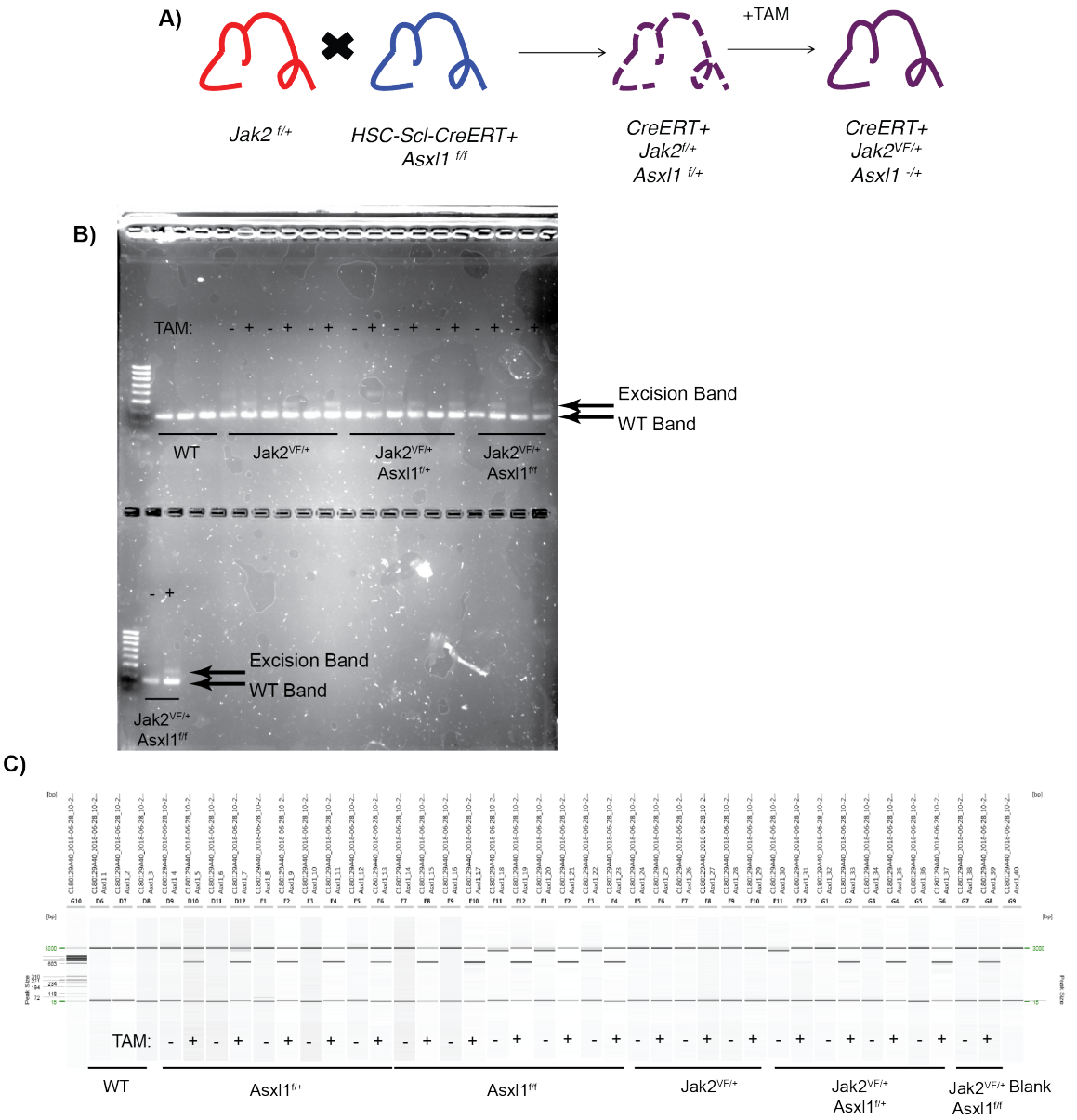

FIGURE 4.1: HSC-SCL-CREERT EFFICIENTLY RECOMBINES AT BOTH TARGET LOCI.

(A) Schematic representation of the breeding strategy for simultaneous induction of *Jak2*^{VF} and *Asxl1* deletion in HSCs. **(B)** Gel electrophoresis of *Jak2*^{VF} excision PCR products on peripheral blood DNA samples obtained from *HSC-Scl-CreERT*$^{+}$ mice before and 2 weeks after TAM. **(C)** Gel electrophoresis of *Asxl1* excision PCR products on peripheral blood DNA samples obtained from *HSC-Scl-CreERT*$^{+}$ mice before and 2 weeks after TAM.

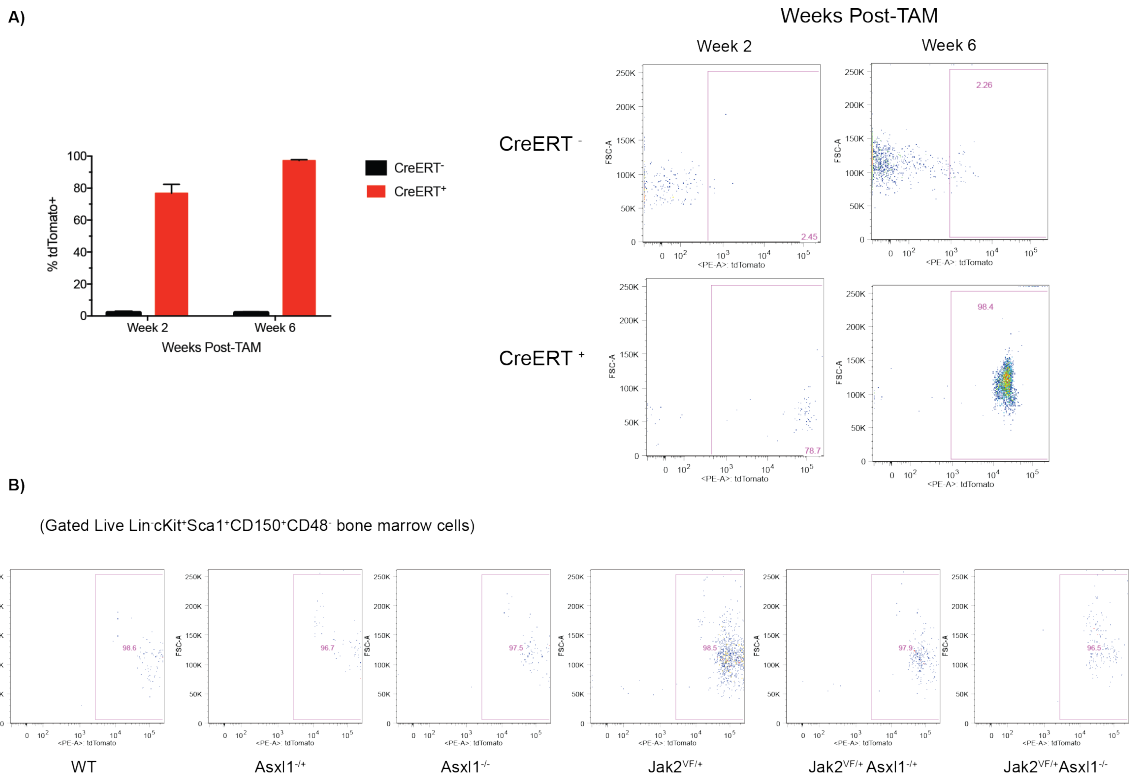

FIGURE 4.2: *HSC-SCL-CREERT* PROMOTES EFFICIENT INDUCTION IN LONG-TERM HSCS.

(A) tdTomato expression in peripheral blood at 2 weeks v. 6 weeks post-TAM in *HSC-Scl-CreERT*$^{+}$*; Rosa26LSLtdT*$^{+}$ mice, as assessed by flow cytometry. **(B)** Representative FACS plots of tdTomato reporter expression in gated LT-HSCs in *HSC-Scl-CreERT*$^{+}$*; Rosa26LSLtdT*$^{+}$ mice 6 weeks post-TAM.

n=4 animals per group. Mice were sacrificed 2 or 6 weeks after initiation of TAM treatment. Bar graphs and line graphs depict mean ± SEM. Results shown are representative of 2 independent experiments.

ASXL1 LOSS ACCELERATES JAK2^{V617F}-DRIVEN MPN

We next sought to investigate the effect of mono- or biallelic *Asxl1* loss on MPN initiation and progression. We monitored a cohort of *HSC-Scl-CreERT^{+}; Jak2$^{VF/+}$; Asxl1$^{+/+}$, HSC-Scl-CreERT^{+}; Jak2$^{VF/+}$; Asxl1$^{-/+}$*, and *HSC-Scl-CreERT^{+}; Jak2$^{VF/+}$; Asxl$^{-/-}$* mice for 16 weeks after Tamoxifen treatment. Peripheral blood counts were monitored over time, and mice were sacrificed at 16 weeks for full assessment of terminal disease. In parallel, a second cohort was monitored for overall survival. *Asxl1* loss accelerated polycythemia, as evidenced by increased hemoglobin and hematocrit levels at 4 weeks post-TAM. At 16 weeks, no overall changes in peripheral blood counts were apparent between *Scl-CreERT^{+}; Jak2$^{VF/+}$; Asxl1$^{-/+}$* or *HSC-Scl-CreERT^{+}; Jak2$^{VF/+}$; Asxl1$^{-/-}$* mice and *HSC-Scl-CreERT^{+}; Jak2$^{VF/+}$; Asxl1$^{+/+}$* mice (**Figure 4.3A**). Spleen weights were also not significant increased at 16 weeks (**Figure 4.3B**). Concordant with studies of MPN patients, overall survival was significantly decreased by loss of even one copy of *Asxl1* (**Figure 4.3C**). These observations indicate that *Asxl1* loss accelerates the onset of *Jak2^{V617F}*-driven PV.

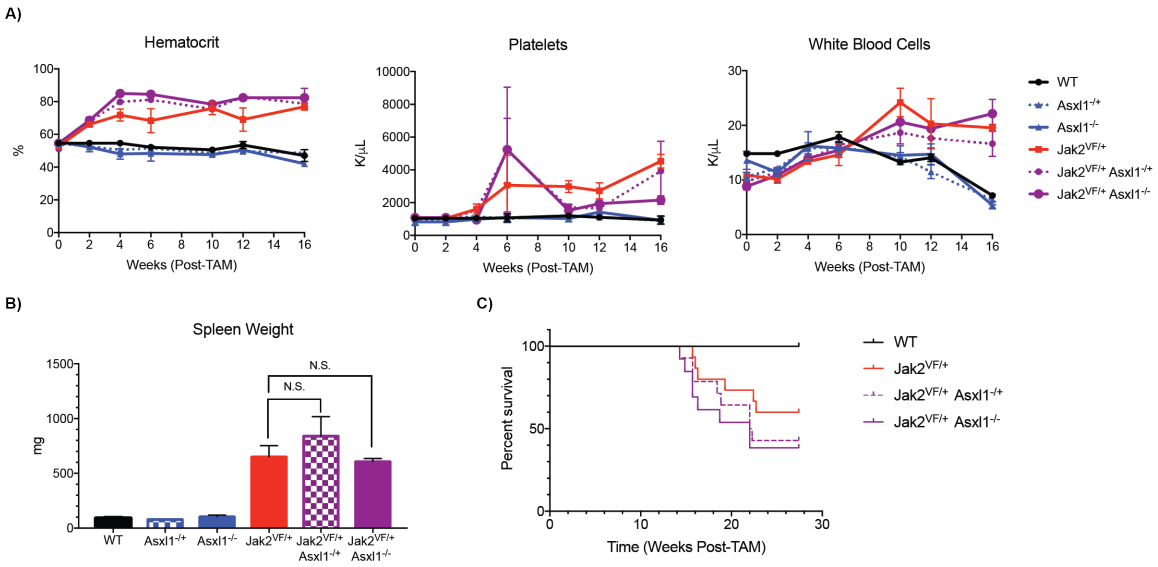

FIGURE 4.3: *ASXL1* LOSS ACCELERATES *JAK2*-DRIVEN PV.

(A) Assessment of PB counts over time in *HSC-Scl-CreERT*$^{+}$ mice post-TAM. **(B)** Spleen weights at 16 weeks post-TAM. **(C)** Kaplan-Meier survival curve of *HSC-Scl-CreERT*$^{+}$ mice post-TAM. p= 0.0198 by Mantel-Cox Log-Rank test.

n=8 mice per group. Bar graphs and line graphs depict mean ± SEM. Results shown are representative of 2 independent experiments.

Several remarkable histopathological differences could be observed between *Jak2*$^{VF/+}$ mice and *Jak2*$^{VF/+}$*; Asxl1*$^{-/+ \text{ or } -/-}$ mice at 16 weeks (**Figure 4**). These differences include: megakaryocyte hyperplasia, left-shifted myeloid progenitors, and low-level bone marrow fibrosis in the bone marrow (**Figure 4.4A, B**). These gross histologic changes were also observed in the spleen (**Figure 4.4C**). We observed increases in circulating levels of myelofibrosis-associated cytokines (Kleppe et al. 2015), including TNF-α, IL-6, and IL-12p40 upon *Asxl1* loss at 16 weeks (**Figure 4.4D**). Overall, these findings are indicative of a phenotypic shift upon *Asxl1* deletion from neoplasia towards a more aggressive MPN/MDS overlap syndrome. These observations indicate that loss of just one copy of *Asxl1* is sufficient to cooperate with *Jak2*^{V617F}, and that *Asxl1* loss shifts *Jak2*^{V617F}-mutant PV to a more aggressive MPN/MDS overlap syndrome. While the *Jak2*$^{VF/+}$ model used in this study does develop fibrosis, the onset is latent and varies greatly between animals. We were thus very surprised and intrigued by the increase in detectable fibrosis in double-mutant mice at 16 weeks after disease induction.

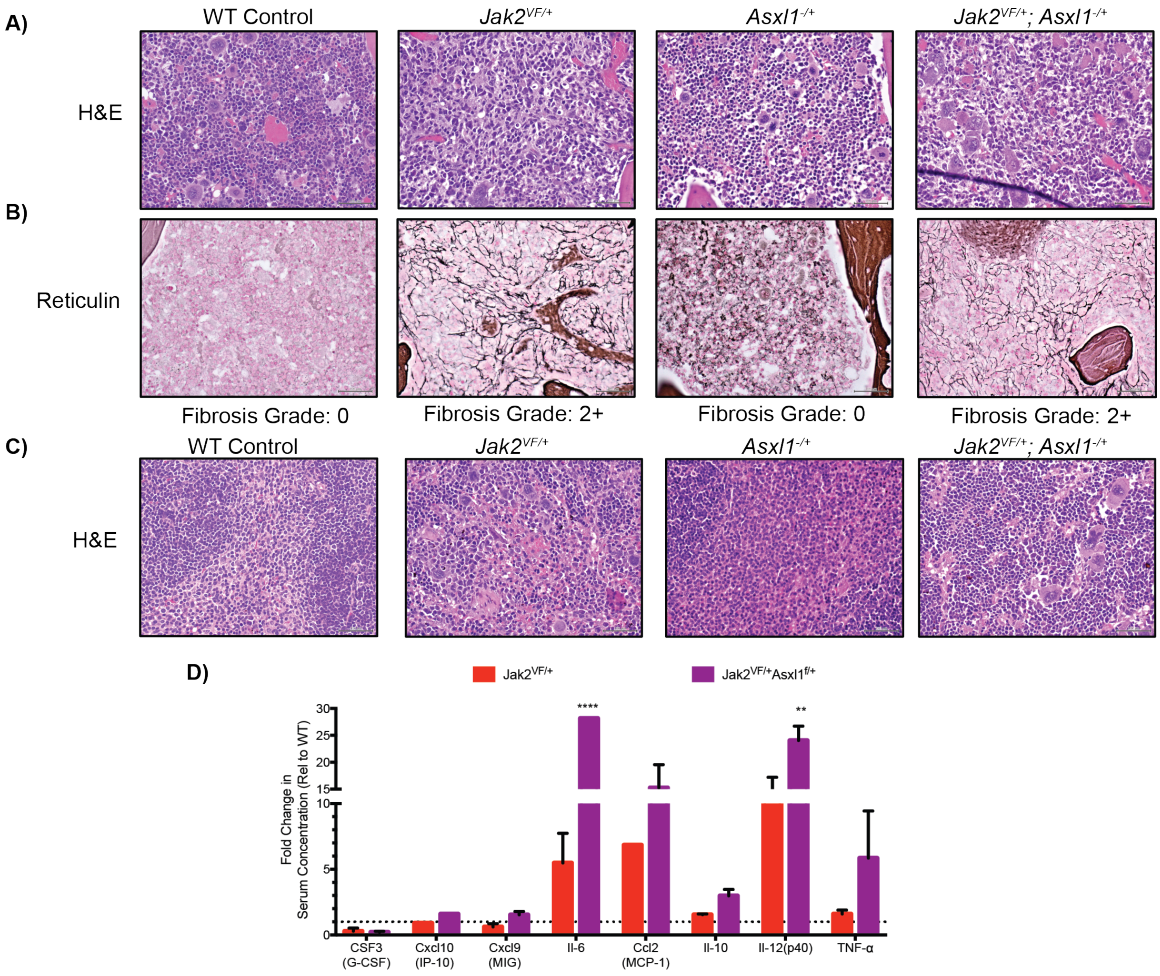

FIGURE 4.4: *ASXL1* LOSS ACCELERATES FIBROTIC PROGRESSION AND PROMOTES DYSPLASIA.

Representative slide images **(A)** H&E staining and **(B)** reticulin staining of BM sections in *HSC-Scl-CreERT*$^{+}$ mice 16 weeks post-TAM for gross tissue histology and fibrosis. **(C)** H&E staining of spleen sections. **(D)** Multiplexed serum profiling (Luminex cytokine assay) of 32 cytokines/chemokines in sera from *HSC-Scl-CreERT*$^{+}$ mice 16 weeks post-TAM.

Scale bars depict 50 microns in (**A, B, C**). Results are representative of 2 independent experiments. n=6 animals per group. Bar graphs and line graphs depict mean ± SEM. *p < 0.05, **p < 0.01, ***p < 0.001, ****p < 0.0001.

ASXL1 LOSS ENHANCES MPN STEM CELL FITNESS

Asxl1 loss on its own impairs HSC self-renewal and differentiation (Abdel-Wahab et al. 2013; Wang et al. 2014). While HSCs are expanded and hyper-proliferate upon *ASXL1* loss, progenitor cell differentiation is markedly impaired. This ultimately potentiates a lethal MDS-like phenotype in mouse models.

Given the accelerated disease onset and dysplastic morphological changes that we observed in terminally-ill mice (described above), we next sought to determine the effect of *Asxl1* loss on *Jak2*$^{VF/+}$-mutant stem cells. The LSK compartment in bone marrow and spleen, as expected, was significantly expanded in *Jak2*$^{VF/+}$ mice at 16 weeks post-TAM. *Asxl1* loss did not promote a further expansion of this population compared to *Asxl1* heterozygosity, however (**Figure 4.5A, B**). Deeper analysis of the bone marrow LSK compartment, however, revealed a skewing towards a more short-term HSC (ST-HSC) immune-phenotype, characterized by a decrease in the overall frequency and number of CD150^{+}CD48^{-} LT-HSCs, (**Figure 4.5C, E**). No significant change in either the ST-HSC (CD150^{+}CD48^{+} LSKs) or MPP (CD150^{-}CD48^{+}) populations was detected (**Figure 4.5D, E**). Therefore, *Asxl1* deletion alters the overall composition of the MPN stem/progenitor cell compartment. Specifically, *Asxl1* loss skews the stem cell compartment to favor ST-HSCs at the expense of LT-HSCs.

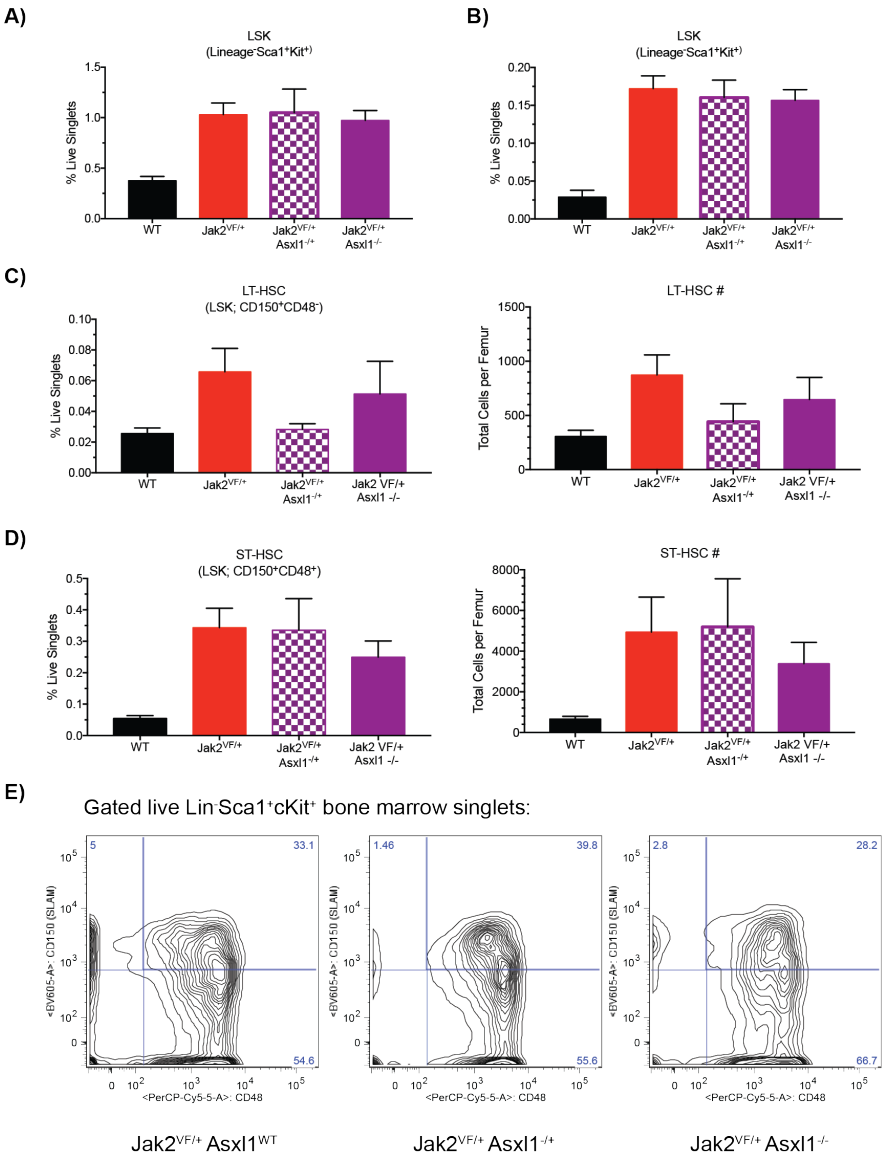

FIGURE 4.5: *ASXL1* LOSS ALTERS THE MPN STEM CELL COMPARTMENT.

(A, B) Frequency of BM **(A)** and Sp **(B)** LSKs. **(C)** Frequency and number of LT-HSCs (LSK; $CD150^{+}CD48^{+}$), **(D)** ST-HSCs (LSK; $CD150^{+}CD48^{-}$). Representative flow plots of gated LSKs are shown in **(E)**

Results are representative of 2 independent experiments. n=6 *HSC-Scl-CreERT*$^{+}$ animals per group, 16 weeks post-TAM. Bar graphs and line graphs depict mean ± SEM.

We next investigated the effect of *Asxl1* loss on downstream myeloid lineage-committed (lineage$^-$Sca1$^-$cKit$^+$) hematopoietic progenitor cells. Downstream *Jak2*$^{VF/+}$ myeloid progenitor populations, such as granulo-myeloid progenitors (GMPs) and bivalent megakaryocytic-erythroid progenitors (MEPs) were both affected by *Asxl1* loss. Interestingly, the effect on each compartment differed.

Asxl1 loss decreased the frequency of bone marrow GMPs and increased the frequency of bone marrow MEPs (**Figure 4.6A, B**). Further analysis of erythroid or megakaryocyte lineage-committed progenitor/precursor cells by flow cytometry revealed that while Asxl1 loss did not increase the frequency of MkPs (**Figure 4.6C**), while erythroid precursors were more frequent (**Figure 4.6D**). This observation indicates that, in addition to influencing the composition of the MPN stem cell compartment, *Asxl1* loss can influence lineage commitment or differentiation potential of MPN stem/progenitor cells.

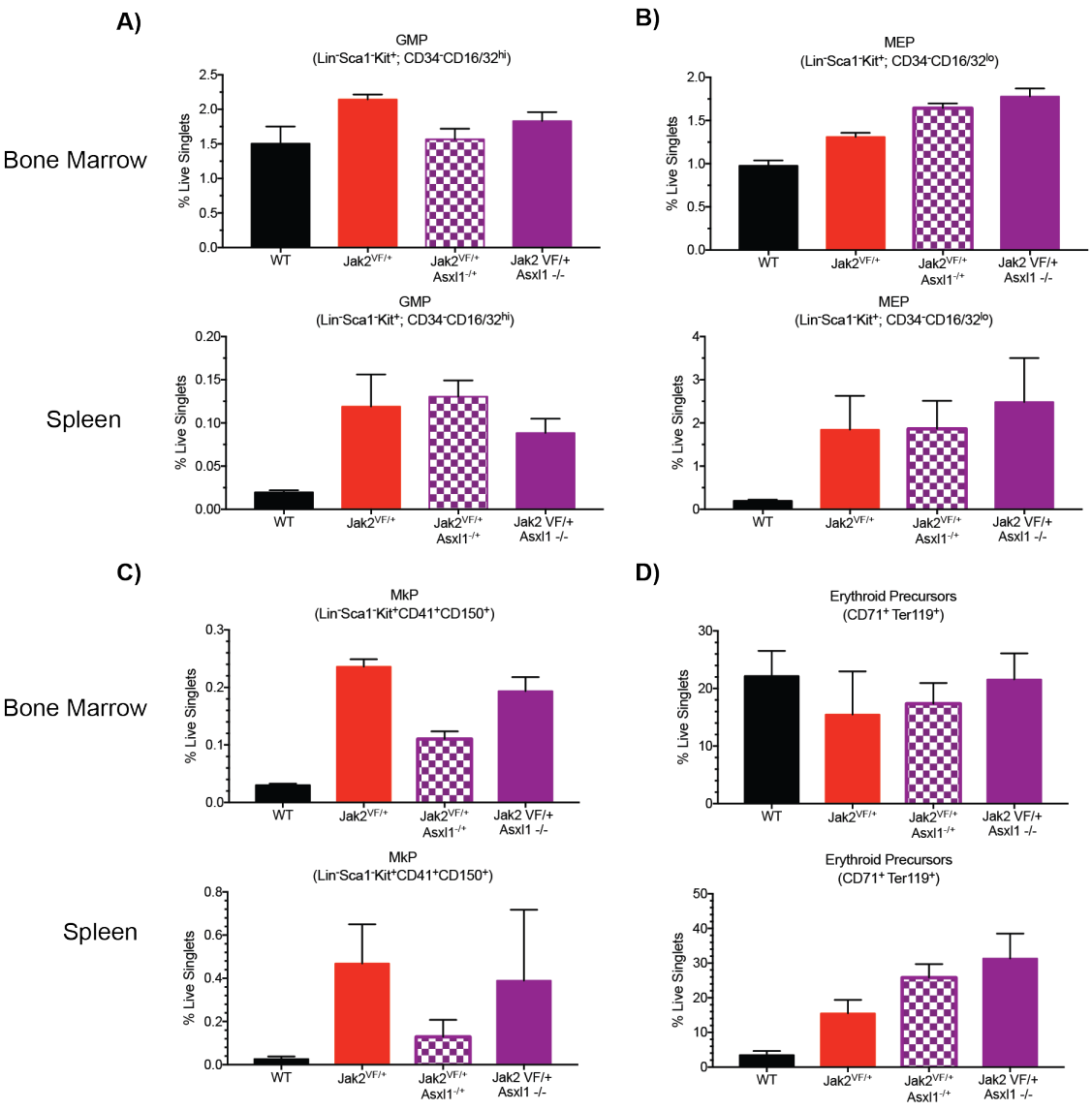

FIGURE 4.6: *ASXL1* LOSS SKEWS *JAK2*^{V617F}-MUTANT MYELOID PROGENITORS.

(A) Frequency of BM and Spleen GMPs. **(B)** Frequency of BM and Spleen MEPs. **(C)** ST-HSCs Frequency of Mk-lineage restricted progenitors (MkPs) in BM and Spleen. **(E)** Frequency of CD71^{+}Ter119^{+} erythroid precursors in BM and Spleen.

Results are representative of 2 independent experiments. n=6 *HSC-Scl-CreERT*$^{+}$ animals per group, 16 weeks post-TAM. Bar graphs and line graphs depict mean ± SEM.

We next sought to determine if this expansion phenotype had functional consequences for MPN stem cells. Given the expansion of the stem cell compartment that we observed upon *Asxl1* loss, and the acceleration of MPN symptom onset, we hypothesized that *Asxl1* loss might potentiate the survival and expansion of MPN stem cells. We performed competitive bone marrow transplantation assays to investigate this question. In vivo, $Jak2^{VF/+}$ HSCs did not display a competitive advantage over WT HSCs after 16 weeks. Loss of one or both copies of *Asxl1*, however, conferred a competitive advantage when combined with $Jak2^{VF/+}$, as assessed by PB chimerism over 16 weeks (**Figure 4.7A**). This competitive advantage was strongest in the LSK compartment, with > 80% of the cells arising from $Jak2^{VF/+}$; $Asxl1^{-/+}$ or $^{-/-}$ donor cells at 16 weeks (**Figure 4.7B**). This observation suggests that *Asxl1* loss promotes MPN evolution by promoting the clonal expansion of MPN stem cells.

Only the LT-HSC compartment is capable of propagating MPN in secondary recipients (Mullally et al. 2012). Given the alterations that we observed in the stem cell compartment of *Jak2/Asxl1* mutant mice, we next assessed the disease-propagating effects of *Jak2/Asxl1* mutant LT-HSCs and ST-HSCs. Sorted LT- or ST-HSCs, along with wild-type support BM cells, were transplanted into wild-type secondary recipients and monitored for disease onset (**Figure 4.8A**). Despite the effect of Asxl1 loss on HSC frequency that we observed in primary mice, *Jak2/Asxl1* mutant ST-HSCs were not able to propagate disease over 16 weeks. No signs of MPN were detectable in the peripheral blood, despite even chimerism over the analysis period (**Figure 4.8B, C**). These observations indicate that *Asxl1* loss does not confer disease-propagating potential to ST-HSCs, despite promoting the expansion of this population.

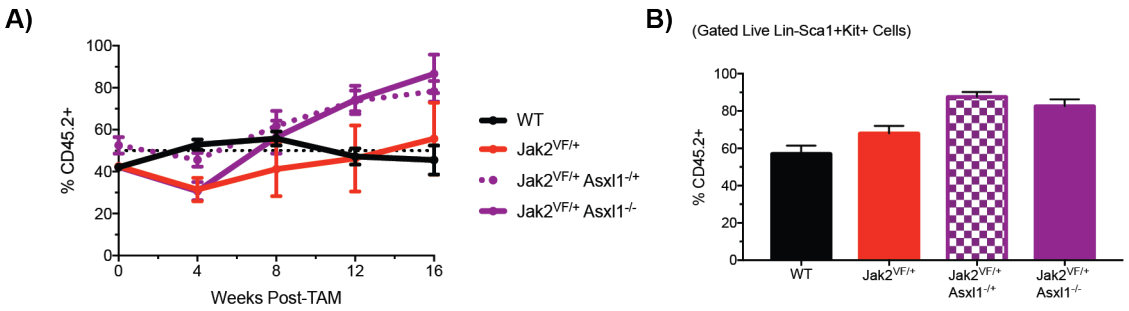

FIGURE 4.7: *ASXL1* LOSS CONFERS A COMPETITIVE ADVANTAGE TO MPN STEM CELLS.

(A) Peripheral blood chimerism over time in competitive transplants. **(B)** CD45.2^{+} chimerism in the BM LSK compartment of competitively transplanted recipient mice at 16 weeks post-TAM.

Results are representative of 2 independent experiments. n=5 animals per transplant arm. Bar graphs and line graphs depict mean ± SEM.

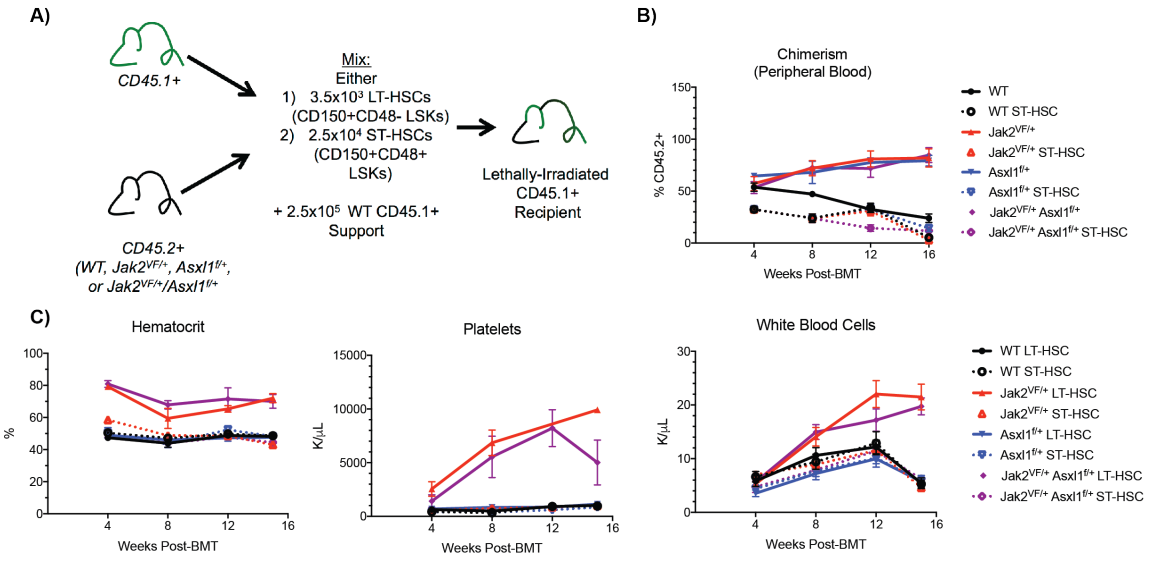

FIGURE 4.8: *ASXL1* LOSS DOES NOT CONFER DISEASE-PROPAGATING CAPACITY TO ST-HSCS.

(A) Schematic of LT-HSC/ST-HSC transplantation experiments. **(B)** LT-HSCs and ST-HSCs engraft, as assessed by monitoring PB chimerism post-transplant. **(C)** PB parameters post-transplantation.

Results are representative of 2 independent experiments. n=5 animals per transplant arm. Bar graphs depict mean ± SEM.

ASXL1 mutations in MPN patients are associated with clonal evolution and relapse during JAK2 inhibitor therapy. We next examined the effect of *Asxl1* loss on MPN stem cell responses to Ruxolitinib, a Type I JAK1/2 inhibitor currently in use for the clinical management of MPN. First, we performed methylcellulose colony formation assays with increasing doses of Ruxolitinib (**Figure 4.9A**). *Jak2*$^{VF/+}$*; Asxl1*$^{-/+}$ cells continued to proliferate and formed more colonies in the presence of Ruxolitinib, compared to *Jak2*$^{VF/+}$ progenitor cells (**Figure 4.9B**). This suggests that *Asxl1* loss promotes MPN stem cell survival in the setting of JAK2 inhibition and can permit the continued persistence of the MPN clone.

We interrogated this possibility in vivo. We transplanted wild-type CD45.1^{+} recipient mice with a mix of 50% *Jak2*$^{VF/+}$ (CD45.2^{+}) and 50% *Jak2*$^{VF/+}$*; Asxl1*$^{-/+}$*; tdTomato*$^{+}$ (CD45.2^{+} tdTomato^{+}) cells. Recipient mice were then treated with either Ruxolitinib or vehicle for 1 month after engraftment and establishment of the MPN phenotype (**Figure 4.9C**). We assessed the frequency of *Jak2*$^{VF/+}$ versus *Jak2*$^{VF/+}$*; Asxl1*$^{-/+}$ after Ruxolitinib treatment by flow cytometry. A slight advantage of *Jak2*$^{VF/+}$*; Asxl1*$^{-/+}$ over *Jak2*$^{VF/+}$ cells in the periphery was detected (**Figure 4.9D**). Furthermore, a slight but significant advantage of *Jak2*$^{VF/+}$*; Asxl1*$^{-/+}$ cells was also observed among cKit^{+} myeloid progenitors in both the bone marrow and spleen (**Figure 4.9E**). Therefore, *Asxl1* loss promotes MPN stem cell survival in response to JAK2 inhibition and potentially promote clonal evolution.

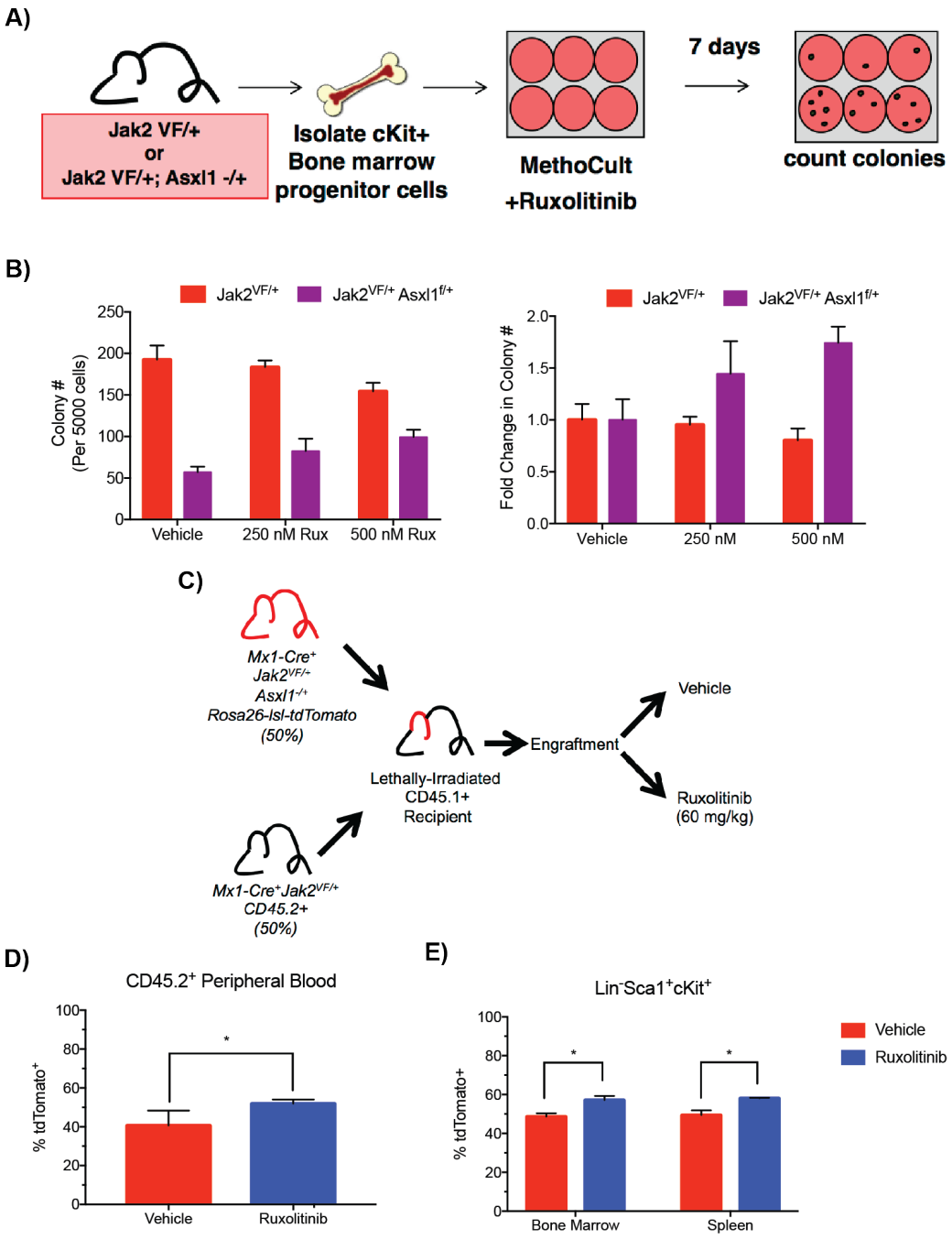

FIGURE 4.9: *ASXL1* LOSS ENHANCES JAK2 INHIBITOR PERSISTENCE IN MPN STEM CELLS.

(A) Schematic for assessing in vitro responsiveness of MPN HSPCs to Ruxolitinib. **(B)** Colony counts, and fold change in colony counts after 7 days of methylcellulose culture. **(C)** Schematic for in vivo competition of *Jak2* and *Jak2/Asxl1* MPN cells. **(D, E)** Frequency of CD45.2$^+$ tdTomato$^+$ *Jak2/Asxl1* mutant cells (PB and gated LSKs) after 4 weeks of Ruxolitinib treatment.

Results are representative of 2 independent experiments. n=5 animals per transplant arm. Bar graphs depict mean ± SEM.

ASXL1 HAPLOINSUFFICIENCY IMPAIRS NORMAL HSC FITNESS

Most *in vivo* studies to date have explored the effects of *Asxl1* deficiency in the context of homozygous deletion. MPN patients, however, present with heterozygous *ASXL1* mutations, and loss of heterozygosity is not reported in the literature to date. Therefore, given our initial observation that monoallelic *Asxl1* deletion is sufficient to cooperate with $Jak2^{VF/+}$, we also sought to investigate if and how heterozygous *Asxl1* deletion affects normal HSC function and hematopoiesis in a $Jak2^{WT}$ setting.

We first characterized the composition of the HSPC compartment in $Asxl1^{-/+}$ mice, compared to $Asxl1^{-/-}$ mice. At 16 weeks post-TAM, $Asxl1^{-/+}$ bone marrow LSKs were not significantly expanded compared to wild type LSKs, whereas $Asxl1^{-/-}$ mice showed significant expansion (**Figure 4.10A**). Interestingly, however, $Asxl1^{-/+}$ splenic LSKs were expanded. Heterozygous *Asxl1* deletion did skew the myeloid progenitor compartment to favor MEPs, as was also observed in $Asxl1^{-/-}$ mice, but to a much lesser extent (**Figure 4.10B**). While *Asxl1* loss is associated with progenitor cell expansion, it also blocks downstream megakaryocyte/erythroid differentiation. Consistent with this, $Asxl1^{-/+}$ mice had fewer BM $CD41^{+}$ Mk cells and erythroid lineage-committed cells than wild type controls (**Figure 4.10C**). Therefore, heterozygous *Asxl1* loss generates an intermediate hematopoietic phenotype compared to full deletion.

Next, we sought to determine if these phenotypic changes influenced the function of normal HSPCs. Functionally, in competitive bone marrow transplants, $Asxl1^{-/+}$ HSCs cells

showed a moderate disadvantage. While peripheral blood chimerism was not significantly impaired in *Asxl1*$^{-/+}$ transplanted recipients (**Figure 4.10D**), LSK compartment chimerism was moderately reduced in *Asxl1*$^{-/+}$recipients from 50% to 30% (**Figure 4.10E**). This largely phenocopies *Asxl1*$^{-/-}$ mice, despite not conferring a peripheral disadvantage. Furthermore, our prior histopathological analysis of *Asxl1*$^{-/+}$ mice at 16 weeks did show slight signs of dysplasia (**Figure 4.4A, C**), consistent with the reported phenotype of *Asxl1*$^{-/-}$ mice. Collectively, these observations suggest that heterozygous *Asxl1* loss is phenotypically similar (albeit less severe) to homozygous deletion with regards to HSC function.

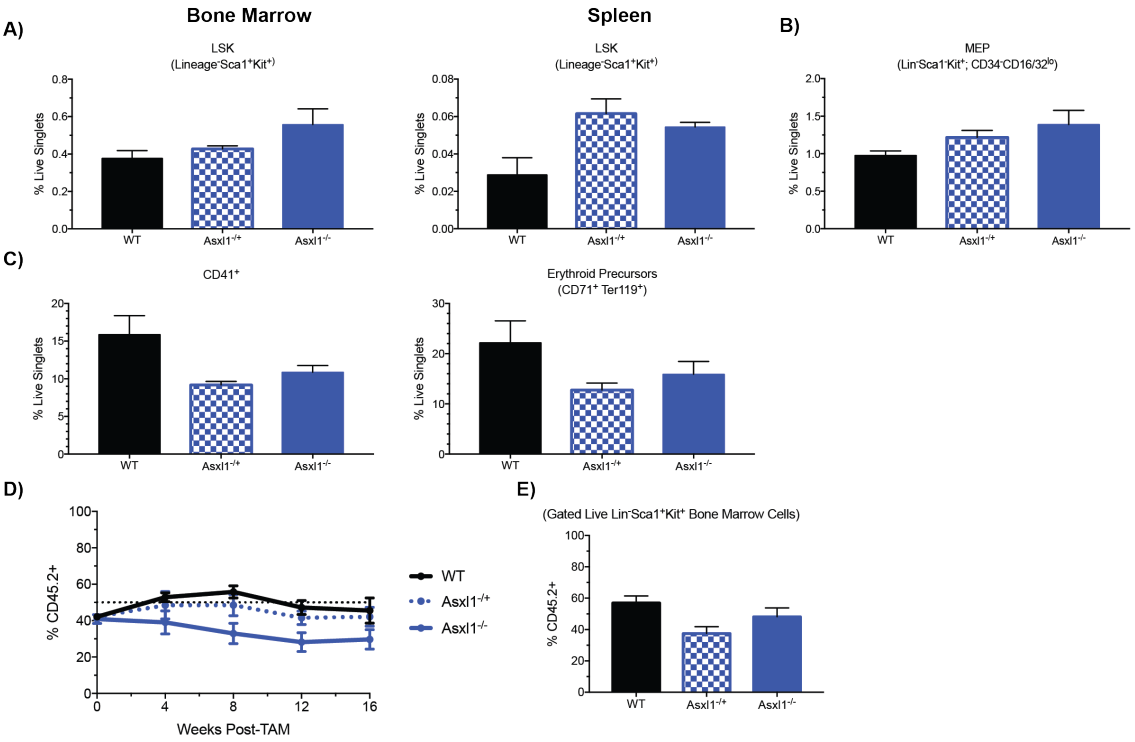

FIGURE 4.10: HETEROZYGOUS *ASXL1* DELETION IMPAIRS NORMAL HSC FUNCTION.

(A) BM and spleen LSKs are expanded in *Asxl1*$^{-/+}$ mice by flow cytometry. **(B)** BM MEPs are also slightly, but not markedly expanded. **(C)** BM Mks (CD41^{+}) and committed erythroid precursors (CD71^{+}Ter119^{+}) cells are decreased in *Asxl1*$^{-/+}$ mice. **(D)** PB chimerism over time after competitive bone marrow transplantation. **(E)** BM LSK chimerism in competitive BMT after 16 weeks.

Results are representative of 2 independent experiments. n=6 primary mice 16 weeks post-TAM in **(A-C),** n=5 animals per transplant arm in **(D, E)**. Bar graphs and line graphs depict mean ± SEM.

ASXL1 LOSS COORDINATELY REGULATES GENE EXPRESSION WITH JAK2^{VF}

ASXL1 has several established roles in chromatin remodeling, as discussed in Chapter 1 of this dissertation. However, *JAK2* can also directly regulate gene expression by phosphorylation of Histone H3 at Tyrosine 41 (H3Y41P) (Dawson et al. 2009). This modification leads to the exclusion of HP1α from chromatin at gene promoters, which leads to subsequent downstream gene activation (Dawson et al. 2009; Dawson et al. 2012). Previous un-published work from our lab reveals that *ASXL1* depletion via RNAi in *JAK2^{V617F}*-mutant cell lines increases levels of H3Y41P. These observations led us to hypothesize that *ASXL1* loss synergizes with *JAK2^{V617F}* to establish aberrant gene expression programs that promote MPN stem cell expansion and survival, potentially by coordinately altering chromatin architecture.

A classical hallmark of *Asxl1* deletion is the global loss of the H3K27me3 mark. We first confirmed that *Asxl1* deletion reduced global levels of H3K27me3 in hematopoietic cells. We performed western blots for H3K27me3 on purified histones from spleen cells; H3K27me3 levels were decreased in bulk splenocytes from *Jak2$^{VF/+}$Asxl1$^{-/+}$* and *Jak2$^{VF/+}$Asxl1$^{-/-}$* mice. (**Figure 4.11A**). We also observed a concomitant increase in *Hox* cluster gene expression, and *Meis1* at the transcriptional level in cKit^{+} cells (**Figure 4.11B**). These observations confirm that *Asxl1* loss potentiates global changes to the chromatin and transcriptional landscape in MPN cells. Importantly, these experiments demonstrate that loss of just one copy of *Asxl1* is sufficient to alter H3K27me3 with functional effects on downstream transcriptional activity.

Beyond canonical regulation of STAT transcriptional activity, *JAK2* is implicated in the transcriptional regulation of *LMO2*, an established leukemia oncogene and pro-survival factor, via removal of HP1α from the *LMO2* promoter (Dawson et al. 2009). We observed that *Asxl1* loss increased *Lmo2* expression significantly in *Jak2*$^{VF/+}$-mutant cells, at both the transcriptional and protein levels (**Figure 4.11c**).

Initial chromatin immunoprecipitation (ChIP) profiling studies of H3K27me3 distribution were not sufficient to demonstrate that this effect occurs due to synergistic promoter remodeling. However, this could be due to several technical and biologic limitations, which are discussed below. In addition to their own discrete effects on HSCs, the observed synergistic effect on *Lmo2* expression suggests that *ASXL1* loss and *JAK2*^{V617F} coordinately regulate a gene expression program in HSCs that promotes the expansion and evolution of the MPN clone.

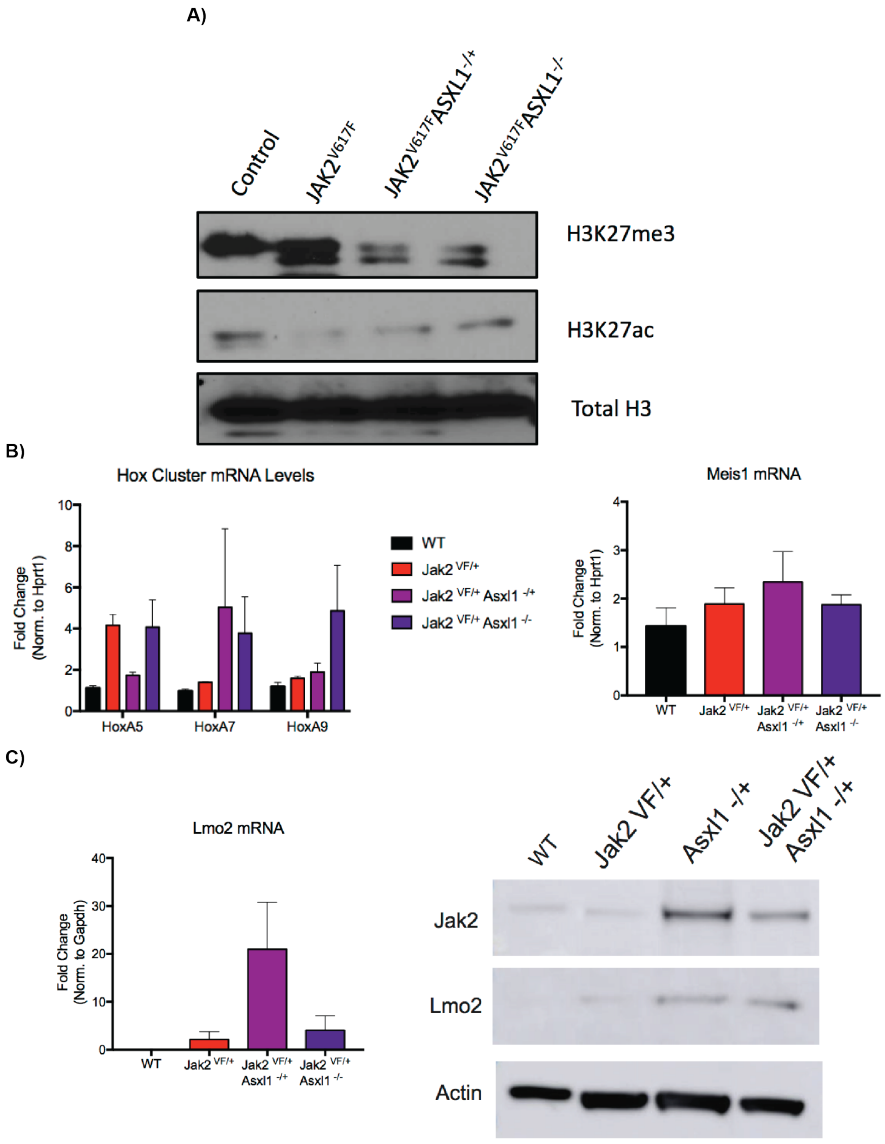

FIGURE 4.11: *ASXL1* COORDINATELY REGULATES GENE EXPRESSION IN *JAK2*-MUTANT CELLS.

(A) Western blotting on purified histones isolated from whole spleens of *HSC-Scl-CreERT*$^{+}$ mice 16 weeks post-TAM. **(B)** qPCR analysis of Asxl1 targets (Hox cluster genes and Meis1) in cKit^{+} BM cells of *HSC-Scl-CreERT*$^{+}$ mice 16 weeks post-TAM. **(C)** Expression of *Lmo2*, as assessed by qPCR (mRNA) and Western blotting (protein) of *HSC-Scl-CreERT*$^{+}$ mice 16 weeks post-TAM. mRNA was assessed on cKit^{+} BM cells, western blotting was performed on whole spleen lysates from *HSC-Scl-CreERT*$^{+}$ mice 16 weeks post-TAM.

Results are representative of 4 independent experiments. n=4 animals per genotype. Bar graphs depict mean ± SEM.

DISCUSSION

In this chapter, we show that *Asxl1* loss cooperates with *Jak2*^{V617F} to promote the expansion and survival of MPN stem cells. *Asxl1* loss accelerated disease onset in an established *JAK2*^{V617F}-driven MPN model. Furthermore, *Asxl1* loss impaired overall survival, accelerated fibrotic progression, and shifted the disease histology to one resembling a more aggressive MPN/MDS overlap syndrome. These observations are concurrent with reports of *JAK2/ASXL1* mutant MPN patient cases. *Asxl1* loss, while deleterious to normal HSCs, cooperates with *Jak2*^{V617F} to improve stem cell fitness and overall survival. The effects of *Asxl1* loss appear to be most dominant in the stem cell compartment, but the effects of *Asxl1* loss on more distal progenitor cell populations or mature cell lineages during disease progression warrant further investigation. We also observed that *Asxl1* loss promoted MPN stem cell proliferation under the stress of JAK2 inhibition. These observations, that *Asxl1* loss increases MPN stem cell fitness at steady-state and under treatment stress, suggests that *ASXL1* loss promotes the clonal expansion and evolution of *JAK2*^{V617F}-mutant HSCs during MPN pathogenesis.

Overall, *Asxl1* loss cooperates with *Jak2*^{V617F} in a manner that largely phenocopies *Ezh2* loss. Prior reports describing compound *Ezh2/Jak2* mutant murine MPN models also report impaired overall survival, accelerated symptom onset, dysplastic histopathologic features, increased stem cell fitness, and increased/worsened fibrosis (Shimizu et al. 2016; Yang et al. 2016; Sashida et al. 2016). Presumably, a good majority of phenotypic redundancy could be attributed to decreased H3K27me3 levels and subsequent impairment of PRC2-mediated gene repression in HSCs.

Asxl1 loss could also have potentially different effects on lineage-committed progenitor populations than *Ezh2* deletion. *Ezh2* deletion overall increases the frequency and fitness of *Jak2*^{V617F}-mutant megakaryocytic and erythroid precursors. *Asxl1* loss, however, seemed to have more discrete effects on these populations. In isolation, *Asxl1* deletion impairs megakaryocytic/erythroid progenitor cell differentiation. The deleterious effects of *Asxl1* loss in promoting progenitor cell differentiation appears to be rescued by *Jak2*^{V617F} in our model. As *Asxl1* has additional chromatin regulating functions beyond PRC2 recruitment, and a growing body of work suggests that there are PRC2-independent H3K27me3 peaks, it is possible that there could be gene expression programs in *Jak2*^{V617F}-mutant HSCs that are regulated by Asxl1 in a PRC2-independent manner. For instance, both ASXL1 and JAK2 are reported to regulate HP1α chromatin occupancy (Dawson et al. 2009; Lee et al. 2010). Thus, ASXL1 and JAK2 could coordinately regulate PRC2-independent gene expression in HSPCs. Further chromatin and transcriptional profiling of this possibility is warranted.

Furthermore, elegant proteomic studies indicate that EZH2 and PRC2 complex formation is differentially regulated during hematopoiesis, and different complexes form in distinct progenitor cell populations. It is possible that Asxl1 could have differential effects on chromatin across the myeloid and hematopoietic ontogeny. Future transcriptional and epigenetic profiling studies, using murine model systems and primary MPN patient samples, will prove invaluable in untangling these questions.

Most studies to date have only investigated *Asxl1* loss in the setting of biallelic homozygous loss, while *ASXL1* mutant patients present with heterozygous mutations. Our results above indicate that *ASXL1* could have a dose-dependent role on HSC function, during normal hematopoiesis and during MPN. Heterozygous *Asxl1* deletion was sufficient to alter Jak^{V617F}-driven MPN in our model, despite only having modest phenotypic consequences as a single genetic event. We only assessed the impact of heterozygous *Asxl1* deletion over a relatively short period in primary mice, and in a BMT setting. Elucidating the full extent of heterozygous deletion on normal HSPC function will require additional work. Transplantation assays also pose a significant functional bottleneck, and only assess limited features of the complex function that is HSC self-renewal. Future studies are warranted to assess ASXL1's roles in HSC aging and larger stress responses. Based on our initial observations, however, further epigenetic and transcriptional profiling studies are warranted to assess the effects of monoallelic *Asxl1* loss on normal and $Jak2^{V617F}$-mutant HSCs compared to homozygous deletion.

Our model employs simultaneous deletion of *Asxl1* and expression of $Jak2^{V617F}$. While informative, this situation does not model the clonal dynamics and sequential process observed in MPN patients. Mutation order during MPN progression remains an outstanding question with tremendous clinical implications. Does *Asxl1*-dependent chromatin remodeling precede the oncogenic stimulus of $Jak2^{V617F}$, or is it more advantageous after MPN initiation? Are compound mutant HSCs still dependent on $Jak2^{V617F}$ for their continued survival? Such questions can only be addressed with more elegant temporally-restricted genetic models, or with single-cell resolution transcriptomic and epigenomic techniques.

This model, and indeed most models in the MPN field, are highly focused on stem cell activity and tend to ignore the contributions of distal myeloid cells. While *Jak2*^{V617F}-mutant megakaryocyte progenitors and mature megakaryocytes are not further expanded upon *Asxl1* loss, we did observe gross morphologic abnormalities upon histological examination. Given the established role of megakaryocytes in promoting myelofibrosis, deeper functional studies on this lineage could prove illuminating. For example, epigenetic profiling of *Asxl1*-associated chromatin marks and Stat5 chromatin occupancy, paired with gene expression profiling, could identify Asxl1-mediated pathways that promote fibrosis, thus and identify candidate biomarkers for progression or alternative avenues for therapeutic intervention.

Collectively, these results demonstrate a role for Asxl1-mediated chromatin regulation in promoting the clonal expansion of *Jak2*^{V617F}-mutant HSCs during MPN pathogenesis. ASXL1 loss, while disadvantageous to wild type HSCs, coordinately regulates disease progression and enhances MPN stem cell fitness at steady-state and in response to JAK2 inhibition. This suggests a synergistic effect of aberrant STAT activation and/or H3Y41P (driven by Jak2^{V617F}) with ASXL1 loss in regulating gene expression programs that mediate HSC self-renewal, differentiation, or survival.

Chapter 5 - DISCUSSION

The majority of patients with classical MPNs (PV, ET and MF) harbor somatic activating mutations in the tyrosine kinase JAK2, thereby making it an attractive therapeutic target in these diseases. However, the relative contributions of aberrant JAK/STAT signaling to disease phenotype, malignant proliferation, and disease progression has not been fully delineated. The dual JAK1/JAK2 inhibitor, Ruxolitinib, was approved by the FDA in 2011 for the treatment of MF, and several other compounds are in late-stage clinical testing. Although these drugs alleviate many of the constitutional symptoms MPN patients and reduce splenomegaly, they have been largely ineffective at reducing mutant allele burden or modifying disease progression(Verstovsek et al. 2012; Cervantes et al. 2013; Pardanani et al. 2013). This highlights a demonstrated need to further understand the molecular and cellular events regulating the expansion, evolution, and survival of the MPN clone.

The hematopoietic system is organized in a hierarchical manner. Multipotent HSCs are a rare population of bone marrow cells that sit at the apex of the hematopoietic ontogeny and follow a carefully orchestrated differentiation cascade that allows the generation of all mature blood cell types. Perturbations in a single HSC that can promote amplification or depletion of a particular lineage lead to a meta-stable state that requires additional alterations to confer a clonal advantage (Nguyen et al. 2012; Pietras et al. 2011). The HSC compartment is an inherently heterogenous population of cells. Differences in self-renewal capacity, proliferation, cell cycle status, and lineage potential have all been uncovered

(Copley et al. 2012). The transformation potential of these various HSC sub-types warrants future investigation, as the genetic tools to perform these studies come in to existence.

Marked intra- and inter-tumoral heterogeneity exists within *Jak2*^{V617F}-driven MPN, and within other hematologic malignancies more generally. Two main theories have been developed to explain these phenomena: the 1) "stochastic model" suggests that all cells in a clonal hierarchy are equally susceptible to malignant transformation (Griffin & Löwenberg 1986), while the 2) "hierarchical (or cancer stem cell) model" suggests that tumorigenic mutations occur either in primitive cells or in cells that can revert to a more primitive state to promote malignancy via aberrant differentiation (Kreso & Dick 2014). The cancer stem cell hypothesis is currently the favored explanation for heterogeneity in myeloid malignancies, given the highly-ordered and hierarchical organization of the hematopoietic compartment (Dick 2008).

Mutant HSCs clonally expand during MPN pathogenesis as the result of developing a hypersensitivity to and/or independence from the physiologic cytokine signals that regulate homeostatic proliferation, survival, and differentiation. Therefore, both cell-autonomous and non-autonomous factors influence the pathogenic trajectory of the MPN clone. The previous two chapters of this thesis discuss: 1) mechanisms by which *Jak2*^{V617F}-mutant Mks promote neoplastic expansion of the wild type hematopoietic milieu, and 2) describe how *Asxl1* loss alters the initiation and progression of *Jak2*^{V617F}-mutant disease, as well as MPN stem cell function in vivo. In this chapter, we discuss some of the biological and clinical implications of these findings.

JAK2^{V617F}-MUTANT MKS PROMOTE CLONAL EXPANSION OF *JAK2*^{WT} HSCS

Based on the discovery of pathogenic driver mutations, myeloid malignancies were previously regarded as primarily driven by mutant cell–autonomous mechanisms. However, cumulative evidence indicates that the mutant clone can exploit physiological niche signals to overcome the control of the bone marrow microenvironment and/or remodel the BM niche into a permissive/self-reinforcing environment that supports disease progression at the expense of normal hematopoiesis.

The first indications of a niche contribution to myeloid malignancies stemmed from reciprocal BM transplant experiments. These experiments elegantly demonstrated that myeloid malignancies can arise from non-mutant hematopoietic cells transplanted into an altered BM microenvironment. Specifically, transplantation of wild-type hematopoietic cells into retinoic acid receptor γ-deleted mice promoted a MPN-like disease (Walkley, Olsen, et al. 2007). Similarly, *Rb* deletion in non-hematopoietic cells promotes a MPN phenotype (Walkley, Shea, et al. 2007). Altogether, these observations were the first indications that alterations in the bone marrow niche exert more than just a “bystander effect” in myeloid transformation. However, the underlying mechanisms are still just beginning to be elucidated. The complexity of HSC niche/clone interactions also poses a challenge, with different vascular, endothelial, stromal and mesenchymal cell types regulating distinct functions in a highly context-dependent manner. In this thesis, however, we demonstrate the *Jak2*-mutant Mks promote expansion and increased erythroid differentiation of the HSC compartment, at least in part, by aberrant production of IL-6.

MK:HSC INTERACTIONS IN THE BONE MARROW

As discussed earlier, previous studies have established Mks as critical components of the bone marrow niche that directly regulate HSC quiescence in a paracrine manner (Bruns et al. 2014; M. Zhao et al. 2014; Nakamura-Ishizu et al. 2015). This suggests that Mks could potentiate the expansion of MPN stem cells to promote disease initiation and/or evolution. Further studies have confirmed a causal role for mutant Mks in MPN pathogenesis, by demonstrating that *JAK2*^{V617F}-mutant Mks can regulate aberrant expansion of the *JAK2*^{WT} HSC pool (Zhan et al. 2016). We extend these studies to show that *JAK2*^{V617F}-mutant Mks promote increased erythroid lineage output by *JAK2*^{WT} HSCs and identify IL-6 as one factor that mediates this effect.

We also demonstrate a larger role for mutant clone-derived Mks in MPN maintenance. Mk depletion in vivo significantly blunted disease burden the aberrant myeloproliferation induced by pan-hematopoietic expression of mutant JAK2/MPL disease alleles. These observations suggest that targeting Mk:HSC interactions could potentially identify additional avenues for therapeutic intervention in MPN. Such strategies, while not sufficient to eliminate the MPN stem cell clone directly, could be used to interrupt the complex feedback loop governing MPN initiation and progression. Progression to myelofibrosis is associated with worsened patient prognosis and increased risk of disease transformation. It can also lead to lethal bone marrow failure. In our model, Mk ablation reduced disease burden in both PV-like and ET/MF murine MPN models. In the latter context, Mk ablation reduced the extent of fibrotic damage. Mk-targeted therapies could

not just suppress clonal expansion, but also ameliorate fibrotic progression. Thus, a further investigation of Mk:HSC interactions is warranted.

SYSTEMIC INFLAMMATION CANNOT BE DISCOUNTED

Our work focused primarily on the role of mutant BM-resident Mks and does not fully explore the role of mutant platelets in MPN pathogenesis. Platelets have established roles in coagulation and hemostasis but are increasingly appreciated as fitting in to a continuum of innate immune activity (Weyrich et al. 2003). Platelets actively participate in leukocyte recruitment in response to vascular injury. Early leukocyte recruitment, especially of neutrophils, is an evolutionarily conserved hallmark of innate immunity critical to the successful control of exogenous infection (Medzhitov & Janeway 1997). Platelets physically interact with different leukocyte subsets during the inflammatory process, and this interaction holds far-reaching implications for leukocyte recruitment and peripheral inflammatory activation (Peters et al. 1999). Platelet-leukocyte interactions are critical for peripheral tissue recruitment, leukocyte activation (Suzuki et al. 2013), as well as the formation and release of neutrophil extracellular traps (Burger & Wagner 2003). These interactions are tightly regulated to limit the extent of vascular inflammation and protect the host from the collateral damage of aberrant inflammation.

We did observe increased platelet-leukocyte aggregate formation in the peripheral blood of *Jak2*$^{VF/+}$*; Pf4-Cre*$^{+}$ mice (data not shown). While we demonstrate that *Jak2*^{V617F}-mutant Mks are important sources of IL-6 in our model, we cannot fully exclude that mutant-

derived platelets promote low-level inflammation by peripheral leukocyte activation. Histological indicators of low-grade inflammation in the spleens (splenic white pulp expansion and follicular activation) provide further evidence for this. Chronic inflammation or defective inflammation resolution, induced by hyper-active platelets, could directly contribute to the neoplastic phenotype observed in this model.

ASXL1 LOSS PROMOTES MPN CLONAL EVOLUTION

In this dissertation, we provide evidence that *Asxl1* loss improves MPN stem cell survival and promotes clonal expansion. Below, we discuss the implications of these observations for MPN pathogenesis and therapy.

MUTATION ORDER MATTERS

While our model demonstrates cooperativity between *Jak2*^{V617F} and *Asxl1* loss/heterozygosity, it relies on simultaneous co-expression of both events in HSCs. Several lines of evidence suggest that genetic events can occur before or after the acquisition of *JAK2*^{V617F}. One of the most compelling observations supporting the existence of a pre-existing clone is the development of *JAK2*^{WT} secondary AML in patients with a preceding *JAK*^{V617F}-mutant MPN (Theocharides et al. 2007). This observation implies the existence of a pre-existing mutant clone that branches into a *JAK2*^{V617F}-mutant MPN clone and a wild-type sub-clone, which then undergoes leukemic transformation (Campbell et al. 2006). The molecular identity and pathogenic alterations governing this

"pre-JAK2" phase is still ambiguous, however. Furthermore, in vivo evidence strongly suggests that *JAK2*^{V617F} is not sufficient to confer a strong self-renewal advantage to HSCs as a single event.

A selective pressure model has been proposed to explain the emergence of the *JAK2*^{V617F}-mutant HSC clone. In this model, a single cell acquires the mutation. The subsequent proliferative advantage creates a clone that rapidly grows but lacks a self-renewal advantage that permits long-term expansion. Thus, each mutant cell is then subjected to the selective pressure of increased replicative stress. The lineage biases observed in the distinct MPN phenotypes could then derive from the intrinsic bias of the *Jak2*^{V617F}-mutant HSC that acquires the self-renewal advantage.

ASXL1 mutations are a common event in patients with myeloid malignancies clonal hematopoiesis. While deletion confers a bulk disadvantage to HSCs in competitive transplants, it does promote expansion of the HSC pool in the absence of the "bottleneck" posed by transplantation studies. The disadvantage is presumed to manifest primarily in downstream progenitor compartments, which lack sufficient differentiation/survival capacity. One of two scenarios could occur in *JAK2/ASXL1*-mutant MPN: 1) *ASXL1* loss occurs second, conferring a selective advantage that permits *JAK2*^{V617F}-mutant HSPCs to avoid exhaustion and continue to clonally expand, or 2) *JAK2*^{V617F} is acquired by a preceding *ASXL1*-deficient clone. Subsequent studies assessing the relative fitness of MPN stem cells compared to WT stem cells without transplantation (e.g. limited recombinase activation) are needed to study the fitness of MPN stem cells in a more faithful context

EPIGENETIC ALTERATIONS AND MPN STEM CELL FITNESS

The epigenetic basis for the coordinate regulation of disease evolution in *JAK2/ASXL1*-mutant MPN is yet to be fully elucidated. Both *JAK2*^{V617F} and *ASXL1* have discrete roles in regulating chromatin architecture and subsequent gene expression. Our initial studies suggest that *JAK2* and *ASXL1* coordinately regulate a gene expression program in HSCs that permits clonal expansion, involving at least *Lmo2* and other pro-survival factors. Future work, including in-depth epigenomic and transcriptional profiling in bulk and in single cells, will be needed to elucidate the genetic loci that are regulated by each allele.

Most studies to date have only investigated the impact of *ASXL1* loss on chromatin architecture and gene expression in HSCs. Given the histologic and dysplastic changes that we observed in *JAK2*^{V617F}-mutant MPN upon *Asxl1* loss, *Asxl1* loss likely has discrete effects on downstream progenitor populations and mature cells. Future work will also be needed to assess how *JAK2* and *ASXL1* coordinately regulate gene expression in response to JAK2 inhibition.

Our work also demonstrates a role of heterozygous *Asxl1* deletion in promoting clonal expansion during MPN pathogenesis. Specifically, we observe that monoallelic Asxl1 deletion is sufficient to cooperate with *Jak2*^{V617F} and to alter the function of normal HSCs. Most in vivo deletion studies to date have only investigated the effects of homozygous deletion on chromatin state and gene expression. Given that most MPN patients present with heterozygous mutations, with no apparent loss of heterozygosity, there is a vital need

to better understand the effects of monoallelic *ASXL1* loss on chromatin state and gene expression. Our work suggests that ASXL1 expression levels nuance its effects on HSC function in both normal and malignant contexts. Collectively, mouse models of *ASXL1* deletion or mutant expression reveal that there is extensive variety to ASXL1's role on chromatin state in HSCs (Abdel-Wahab et al. 2013; Inoue et al. 2018; Nagase et al. 2018). Future insights using the mouse models developed in this thesis will be crucial to better understanding how *ASXL1* loss coordinately regulates the MPN clone.

THERAPEUTIC IMPLICATIONS

Preliminary work in this thesis demonstrates that *Asxl1* loss confers an advantage to MPN stem cells under selective pressure during JAK2 inhibitor treatment. This implies that JAK2 inhibitor treatment could either 1) select for a preceding *ASXL1* mutant MPN subclone or 2) promote the acquisition of an *ASXL1* mutation. Further clinical and preclinical work assessing clonal dynamics will be invaluable in discerning between these possibilities.

STAT5: A SKELETON KEY TO MPN PATHOGENESIS (AND THERAPY)?

STAT5 activation is a long-established molecular hallmark of MPN (DAMESHEK 1951). Expression of the three canonical MPN driver mutations causes constitutive STAT5 activation, leading to the increased expression of STAT5 target genes, such as the pro-survival and proliferative factors *Bcl-xL, Ccnd1,* and *cMyc*. Furthermore, a STAT5

activation signature is detectable across the genetic and clinical MPN spectrum (Rampal, Al-Shahrour, et al. 2014). Several groups have reported that *STAT5* is indispensable for the initiation and maintenance of *JAK2*^{V617F}-driven MPN. Co-deletion of *Stat5a* and *Stat5b* in *Jak2*^{V617F} mouse models normalizes blood counts, spleen size, and myeloid progenitor expansion (Funakoshi-Tago et al. 2010; Walz et al. 2012; Yan et al. 2012). Furthermore, *Stat5* deletion also abrogates Epo-independent colony formation (Yan et al. 2012). Conversely, over-expression of constitutively active STAT5 on its own promotes a lethal myeloproliferative syndrome in vivo (Kato et al. 2005). Additional data from our lab shows that JAK inhibitor persistent cells reactivate downstream STAT5 signaling by the formation of JAK2 heterodimers with JAK1 and TYK2. Collectively, these results highlight the fundamental role of STAT5 activation in MPN initiation and maintenance. They also make a compelling case for STAT5 inhibition in MPN therapy. However, the therapeutic window for this strategy is very small, given the dependence of normal hematopoiesis on STAT5, Direct STAT5 inhibition is thus unfeasible using current approaches. For the subset of MPN patients with *JAK2*^{V617F} mutations, small molecules which either directly inhibit the mutant allele or show increased mutant/wildtype inhibitory specificity would offer the potential for increased therapeutic efficacy and would allow for chemical probe-based studies aimed to delineate the role of mutant JAK2 in different lineages and temporal/spatial contexts.

Beyond its canonical roles in regulating hematopoietic cell proliferation and survival, STAT5 also regulates HSPC differentiation and lineage commitment, as evidenced by mouse models - Stat5 is absolutely dispensable for adult erythropoiesis (Socolovsky et al. 2001). While many of its target genes are conserved across ontogeny, STAT5 binding is also highly cell type-specific and likely changes as stem/progenitors progress through the

hierarchy in response to environmental/niche cues. Recent elegant ChIP-Seq studies indicate that STAT5 transcriptional occupancy shifts during megakaryocytic differentiation in response to TPO. In the absence of TPO, unphosphorylated STAT5 co-localizes with CTCF to repress megakaryocytic differentiation, and shifts away from these sites after TPO-mediated phosphorylation to canonical STAT5 target sites that activate pro-survival and proliferative pathways (H. J. Park et al. 2016). No studies to date have documented how constitutive STAT5 phosphorylation, via *JAK2*^{V617F} or another MPN driver mutation, affects STAT5 chromatin occupancy and transcriptional activity.

Given the highly context-specific nature of STAT5 binding, it is very possible that *Jak2*^{V617F} differentially effects STAT5-driven gene expression in HSCs versus Mks, or other mature cell lineages. Based on the results described in chapter 3, *JAK2*^{V617F} clearly has discrete pathogenic effects on mature cell lineages that are worth further mechanistic investigation.

The advent of single-cell resolution transcriptomic techniques, and the development of low cell input chromatin profiling methodologies will be invaluable in elucidating how oncogenic JAK/STAT pathway activation re-directs STAT5 transcriptional activity. These techniques could be employed in the future to identify novel V617F-specific transcriptional dependencies. These dependencies, while also providing insight into how *JAK2*^{V617F} potentiates multiple disease phenotypes, could potentially serve as novel therapeutic targets.

Chromatin remodeling in HSCs via *ASXL1* loss or other epigenetic regulator mutations will likely influence STAT5 binding and/or transcriptional activity. H3Y41p coincides with STAT5 binding at cis-regulatory elements to promote active gene expression (Dawson et al. 2012). Given the established consequences of *ASXL1* mutations on promoter/enhancer architecture and gene expression, coordinate regulation of STAT5 binding by both mutations is a compelling possibility. Future work characterizing the chromatin landscape in *Jak2*^{V617F} versus *Jak2*^{V617F}*/Asxl1* mutant HSCs will be invaluable in identifying gene expression programs that promote clonal expansion of MPN stem cells, either during disease progression or in response to therapy. The elucidation of mutant clone-specific STAT5 (or other STAT) transcriptional networks could ultimately lead to the future identification of MPN clone-specific dependencies.

FINAL CONCLUSIONS

While *JAK2*^{V617F} is an established oncogenic driver, it is not sufficient to promote clonal expansion as a single event. The results within this thesis describe features intrinsic and extrinsic to the MPN clone that permit disease expansion and progression. We reveal that *Jak2*^{V617F}-mutant Mks promote the expansion and aberrant erythroid differentiation of wild type HSCs. We also characterize the effects of *Asxl1* loss on *JAK2*^{V617F}-mutant HSCs during disease progression and in response to JAK2 inhibitor therapy. Collectively, these studies highlight the broad range of factors that influence the ability of a *JAK2*^{V617F}-mutant HSC clone to potentiate a myeloproliferative state. It is our hope that subsequent studies by the MPN field will shed further light on these important issues and lead to mechanism-based therapies which markedly improve outcome for MPN patients.

1) Mutant Mks promote aberrant HSC expansion during MPN initiation in a cell non-autonomous manner

2) *ASXL1* loss coordinately regulates MPN stem cell expansion

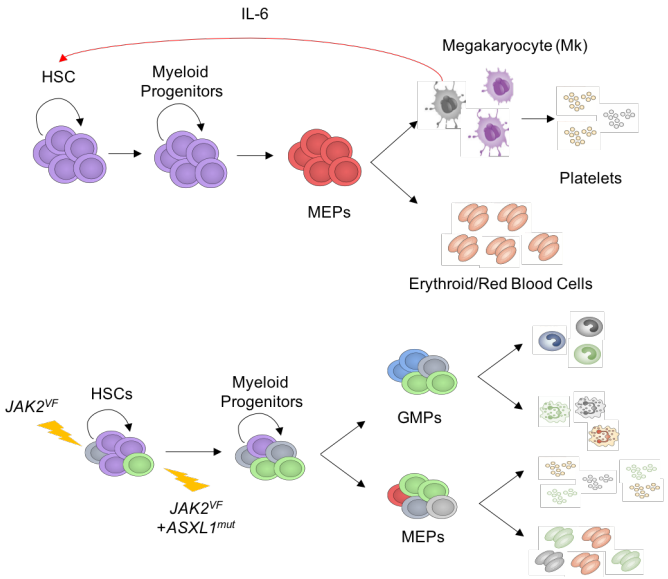

FIGURE 5.1: CONCLUSIONS

CHAPTER 6.- REFERENCES

Abdel-Wahab, O. & Levine, R.L., 2013. Mutations in epigenetic modifiers in the pathogenesis and therapy of acute myeloid leukemia. *Blood*, 121(18), pp.3563–3572.

Abdel-Wahab, O. et al., 2012. ASXL1 mutations promote myeloid transformation through loss of PRC2-mediated gene repression. *Cancer cell*, 22(2), pp.180–193.

Abdel-Wahab, O. et al., 2011. Concomitant analysis of EZH2 and ASXL1 mutations in myelofibrosis, chronic myelomonocytic leukemia and blast-phase myeloproliferative neoplasms. *Leukemia*, 25(7), pp.1200–1202.

Abdel-Wahab, O. et al., 2013. Deletion of Asxl1 results in myelodysplasia and severe developmental defects in vivo. *The Journal of experimental medicine*, 210(12), pp.2641–2659.

Abdel-Wahab, O. et al., 2010. Genetic analysis of transforming events that convert chronic myeloproliferative neoplasms to leukemias. *Cancer research*, 70(2), pp.447–452.

Akada, H. et al., 2010. Conditional expression of heterozygous or homozygous Jak2V617F from its endogenous promoter induces a polycythemia vera-like disease. *Blood*, 115(17), pp.3589–3597.

Aranaz, P. et al., 2012. CBL mutations in myeloproliferative neoplasms are also found in the gene's proline-rich domain and in patients with the V617FJAK2. *Haematologica*, 97(8), pp.1234–1241.

Aravind, L. & Iyer, L.M., 2012. The HARE-HTH and associated domains: novel modules in the coordination of epigenetic DNA and protein modifications. *Cell cycle (Georgetown, Tex.)*, 11(1), pp.119–131.

Arber, D.A. et al., 2016. The 2016 revision to the World Health Organization classification of myeloid neoplasms and acute leukemia. *Blood*, 127(20), pp.2391–2405.

Arranz, L. et al., 2014. Neuropathy of haematopoietic stem cell niche is essential for myeloproliferative neoplasms. *Nature*, 512(7512), pp.78–81.

Balasubramani, A. et al., 2015. Cancer-associated ASXL1 mutations may act as gain-of-function mutations of the ASXL1-BAP1 complex. *Nature communications*, 6(1), p.7307.

Bandaranayake, R.M. et al., 2012. Crystal structures of the JAK2 pseudokinase domain and the pathogenic mutant V617F. *Nature structural & molecular biology*, 19(8), pp.754–759.

Barbui, T. et al., 2014. Masked polycythemia vera (mPV): results of an international study. *American journal of hematology*, 89(1), pp.52–54.

Barbui, T. et al., 2015. The rate of transformation from JAK2-mutated ET to PV is influenced by an accurate WHO-defined clinico-morphological diagnosis. *Leukemia*, 29(4), pp.992–993.

Baxter, E.J. et al., 2005. Acquired mutation of the tyrosine kinase JAK2 in human myeloproliferative disorders. *Lancet (London, England)*, 365(9464), pp.1054–1061.

Beer, P.A. et al., 2011. How I treat essential thrombocythemia. *Blood*, 117(5), pp.1472–1482.

Bejar, R. et al., 2011. Clinical effect of point mutations in myelodysplastic syndromes. *The New England journal of medicine*, 364(26), pp.2496–2506.

Blank, U. & Karlsson, S., 2015. TGF-β signaling in the control of hematopoietic stem cells. *Blood*, 125(23), pp.3542–3550.

Bruns, I. et al., 2014. Megakaryocytes regulate hematopoietic stem cell quiescence through CXCL4 secretion. *Nature medicine*, 20(11), pp.1315–1320.

Buch, T. et al., 2005. A Cre-inducible diphtheria toxin receptor mediates cell lineage ablation after toxin administration. *Nature methods*, 2(6), pp.419–426.

Bumm, T.G.P. et al., 2006. Characterization of murine JAK2V617F-positive myeloproliferative disease. *Cancer research*, 66(23), pp.11156–11165.

Burger, P.C. & Wagner, D.D., 2003. Platelet P-selectin facilitates atherosclerotic lesion development. *Blood*, 101(7), pp.2661–2666.

Calaminus, S.D.J. et al., 2012. Lineage tracing of Pf4-Cre marks hematopoietic stem cells and their progeny. K. Freson, ed. *PloS one*, 7(12), p.e51361.

Calvi, L.M. & Link, D.C., 2015. The hematopoietic stem cell niche in homeostasis and disease. *Blood*, 126(22), pp.2443–2451.

Campbell, P.J. & Green, A.R., 2006. The myeloproliferative disorders. *The New England journal of medicine*, 355(23), pp.2452–2466.

Campbell, P.J. et al., 2006. Mutation of JAK2 in the myeloproliferative disorders: timing, clonality studies, cytogenetic associations, and role in leukemic transformation. *Blood*, 108(10), pp.3548–3555.

Cervantes, F. et al., 2013. Three-year efficacy, safety, and survival findings from COMFORT-II, a phase 3 study comparing ruxolitinib with best available therapy for myelofibrosis. *Blood*, 122(25), p.4047.

Chachoua, I. et al., 2016. Thrombopoietin receptor activation by myeloproliferative neoplasm associated calreticulin mutants. *Blood*, 127(10), pp.1325–1335.

Chaligné, R. et al., 2007. Evidence for MPL W515L/K mutations in hematopoietic stem cells in primitive myelofibrosis. *Blood*, 110(10), pp.3735–3743.

Chasis, J.A. & Mohandas, N., 2008. Erythroblastic islands: niches for erythropoiesis. *Blood*, 112(3), pp.470–478.

Chen, E. et al., 2010. Distinct clinical phenotypes associated with JAK2V617F reflect differential STAT1 signaling. *Cancer cell*, 18(5), pp.524–535.

Chen, H. et al., 2018. A Pan-Cancer Analysis of Enhancer Expression in Nearly 9000 Patient Samples. *Cell*, 173(2), pp.386–399.e12.

Cho, Y.-S. et al., 2006. Additional sex comb-like 1 (ASXL1), in cooperation with SRC-1, acts as a ligand-dependent coactivator for retinoic acid receptor. *The Journal of biological chemistry*, 281(26), pp.17588–17598.

Ciurea, S.O. et al., 2007. Pivotal contributions of megakaryocytes to the biology of idiopathic myelofibrosis. *Blood*, 110(3), pp.986–993.

Cleary, C. & Kralovics, R., 2013. Molecular basis and clonal evolution of myeloproliferative neoplasms. *Clinical chemistry and laboratory medicine*, 51(10), pp.1889–1896.

Copley, M.R., Beer, P.A. & Eaves, C.J., 2012. Hematopoietic stem cell heterogeneity takes center stage. *Cell stem cell*, 10(6), pp.690–697.

DAMESHEK, W., 1951. Some speculations on the myeloproliferative syndromes. *Blood*, 6(4), pp.372–375.

Davies, C. et al., 2013. Silencing of ASXL1 impairs the granulomonocytic lineage potential of human $CD34^+$ progenitor cells. *British journal of haematology*, 160(6), pp.842–850.

Dawson, M.A. et al., 2009. JAK2 phosphorylates histone H3Y41 and excludes HP1alpha from chromatin. *Nature*, 461(7265), pp.819–822.

Dawson, M.A. et al., 2012. Three distinct patterns of histone H3Y41 phosphorylation mark active genes. *Cell reports*, 2(3), pp.470–477.

de Haan, G. & Lazare, S.S., 2018. Aging of hematopoietic stem cells. *Blood*, 131(5), pp.479–487.

Delhommeau, F. et al., 2007. Evidence that the JAK2 G1849T (V617F) mutation occurs in a lymphomyeloid progenitor in polycythemia vera and idiopathic myelofibrosis. *Blood*, 109(1), pp.71–77.

Dey, A. et al., 2012. Loss of the tumor suppressor BAP1 causes myeloid transformation. *Science (New York, N.Y.)*, 337(6101), pp.1541–1546.

Di Buduo, C.A. et al., 2015. Programmable 3D silk bone marrow niche for platelet generation ex vivo and modeling of megakaryopoiesis pathologies. *Blood*, 125(14), pp.2254–2264.

Dick, J.E., 2008. Stem cell concepts renew cancer research. *Blood*, 112(13), pp.4793–4807.

Domingues, M.J. et al., 2017. Niche Extracellular Matrix Components and Their Influence on HSC. *Journal of cellular biochemistry*, 118(8), pp.1984–1993.

Eaves, C.J., 2015. Hematopoietic stem cells: concepts, definitions, and the new reality. *Blood*, 125(17), pp.2605–2613.

Ernst, T. et al., 2010. Inactivating mutations of the histone methyltransferase gene EZH2 in myeloid disorders. *Nature genetics*, 42(8), pp.722–726.

Fisher, C.L. et al., 2003. A human homolog of Additional sex combs, ADDITIONAL SEX COMBS-LIKE 1, maps to chromosome 20q11. *Gene*, 306, pp.115–126.

Fisher, C.L. et al., 2006. Characterization of Asxl1, a murine homolog of Additional sex combs, and analysis of the Asx-like gene family. *Gene*, 369, pp.109–118.

Fisher, C.L., Lee, I., et al., 2010. Additional sex combs-like 1 belongs to the enhancer of trithorax and polycomb group and genetically interacts with Cbx2 in mice. *Developmental biology*, 337(1), pp.9–15.

Fisher, C.L., Pineault, N., et al., 2010. Loss-of-function Additional sex combs like 1 mutations disrupt hematopoiesis but do not cause severe myelodysplasia or leukemia. *Blood*, 115(1), pp.38–46.

Funakoshi-Tago, M. et al., 2010. STAT5 activation is critical for the transformation mediated by myeloproliferative disorder-associated JAK2 V617F mutant. *The Journal of biological chemistry*, 285(8), pp.5296–5307.

Gelsi-Boyer, V. et al., 2009. Mutations of polycomb-associated gene ASXL1 in myelodysplastic syndromes and chronic myelomonocytic leukaemia. *British journal of haematology*, 145(6), pp.788–800.

Genovese, G. et al., 2014. Clonal hematopoiesis and blood-cancer risk inferred from blood DNA sequence. *The New England journal of medicine*, 371(26), pp.2477–2487.

Göthert, J.R. et al., 2005. In vivo fate-tracing studies using the Scl stem cell enhancer: embryonic hematopoietic stem cells significantly contribute to adult hematopoiesis. *Blood*, 105(7), pp.2724–2732.

Grand, F.H. et al., 2009. Frequent CBL mutations associated with 11q acquired uniparental disomy in myeloproliferative neoplasms. *Blood*, 113(24), pp.6182–6192.

Griffin, J.D. & Löwenberg, B., 1986. Clonogenic cells in acute myeloblastic leukemia. *Blood*, 68(6), pp.1185–1195.

Grover, A. et al., 2016. Single-cell RNA sequencing reveals molecular and functional platelet bias of aged haematopoietic stem cells. *Nature communications*, 7(1), p.11075.

Guglielmelli, P. et al., 2011. EZH2 mutational status predicts poor survival in myelofibrosis. *Blood*, 118(19), pp.5227–5234.

Harpur, A.G. et al., 1992. JAK2, a third member of the JAK family of protein tyrosine kinases. *Oncogene*, 7(7), pp.1347–1353.

Harutyunyan, A. et al., 2011. p53 lesions in leukemic transformation. *The New England journal of medicine*, 364(5), pp.488–490.

Hasan, S. et al., 2013. JAK2V617F expression in mice amplifies early hematopoietic cells and gives them a competitive advantage that is hampered by IFNα. *Blood*, 122(8), pp.1464–1477.

Heazlewood, S.Y. et al., 2013. Megakaryocytes co-localise with hemopoietic stem cells and release cytokines that up-regulate stem cell proliferation. *Stem cell research*, 11(2), pp.782–792.

Hoischen, A. et al., 2011. De novo nonsense mutations in ASXL1 cause Bohring-Opitz syndrome. *Nature genetics*, 43(8), pp.729–731.

Inoue, D. et al., 2013. Myelodysplastic syndromes are induced by histone methylation–altering ASXL1 mutations. *The Journal of clinical investigation*, 123(11), pp.4627–4640.

Inoue, D., Fujino, T. & Kitamura, T., 2018. ASXL1 as a critical regulator of epigenetic marks and therapeutic potential of mutated cells. *Oncotarget*, 9(81), pp.35203–35204.

Ishii, T. et al., 2006. Involvement of various hematopoietic-cell lineages by the JAK2V617F mutation in polycythemia vera. *Blood*, 108(9), pp.3128–3134.

Jaiswal, S. et al., 2014. Age-related clonal hematopoiesis associated with adverse outcomes. *The New England journal of medicine*, 371(26), pp.2488–2498.

James, C. et al., 2005. A unique clonal JAK2 mutation leading to constitutive signalling causes polycythaemia vera. *Nature*, 434(7037), pp.1144–1148.

Jamieson, C.H.M. et al., 2006. The JAK2 V617F mutation occurs in hematopoietic stem cells in polycythemia vera and predisposes toward erythroid differentiation. *Proceedings of the National Academy of Sciences of the United States of America*, 103(16), pp.6224–6229.

Karaghiosoff, M. et al., 2000. Partial impairment of cytokine responses in Tyk2-deficient mice. *Immunity*, 13(4), pp.549–560.

Kato, Y. et al., 2005. Selective activation of STAT5 unveils its role in stem cell self-renewal in normal and leukemic hematopoiesis. *The Journal of experimental medicine*, 202(1), pp.169–179.

Katoh, M, 2013. Functional and cancer genomics of ASXL family members. *British journal of cancer*, 109(2), pp.299–306.

Katoh, Masuko & Katoh, Masaru, 2003. Identification and characterization of ASXL2 gene in silico. *International journal of oncology*, 23(3), pp.845–850.

Katoh, Masuko & Katoh, Masaru, 2004. Identification and characterization of ASXL3 gene in silico. *International journal of oncology*, 24(6), pp.1617–1622.

Kawamura, M. et al., 1994. Molecular cloning of L-JAK, a Janus family protein-tyrosine kinase expressed in natural killer cells and activated leukocytes. *Proceedings of the National Academy of Sciences of the United States of America*, 91(14), pp.6374–6378.

Klampfl, T. et al., 2013. Somatic mutations of calreticulin in myeloproliferative neoplasms. *The New England journal of medicine*, 369(25), pp.2379–2390.

Kleppe, M. et al., 2015. JAK-STAT pathway activation in malignant and nonmalignant cells contributes to MPN pathogenesis and therapeutic response. *Cancer discovery*, 5(3), pp.316–331.

Korn, C. et al., 2018. Niche Heterogeneity Impacts Evolution of Myeloproliferative Neoplasms Driven By the Same Oncogenic Pathway. *Blood*, 132(Suppl 1), p.98.

Kralovics, R. et al., 2005. A gain-of-function mutation of JAK2 in myeloproliferative disorders. *The New England journal of medicine*, 352(17), pp.1779–1790.

Kreso, A. & Dick, J.E., 2014. Evolution of the cancer stem cell model. *Cell stem cell*, 14(3), pp.275–291.

Krolewski, J.J. et al., 1990. Identification and chromosomal mapping of new human tyrosine kinase genes. *Oncogene*, 5(3), pp.277–282.

Kubovcakova, L. et al., 2013. Differential effects of hydroxyurea and INC424 on mutant allele burden and myeloproliferative phenotype in a JAK2-V617F polycythemia vera mouse model. *Blood*, 121(7), pp.1188–1199.

Lacout, C. et al., 2006. JAK2V617F expression in murine hematopoietic cells leads to MPD mimicking human PV with secondary myelofibrosis. *Blood*, 108(5), pp.1652–1660.

Lee, S.-W. et al., 2010. ASXL1 represses retinoic acid receptor-mediated transcription through associating with HP1 and LSD1. *The Journal of biological chemistry*, 285(1), pp.18–29.

Leung, C.G. et al., 2007. Requirements for survivin in terminal differentiation of erythroid cells and maintenance of hematopoietic stem and progenitor cells. *The Journal of experimental medicine*, 204(7), pp.1603–1611.

Levine, R.L. et al., 2005. Activating mutation in the tyrosine kinase JAK2 in polycythemia vera, essential thrombocythemia, and myeloid metaplasia with myelofibrosis. *Cancer cell*, 7(4), pp.387–397.

Levine, R.L. et al., 2007. Role of JAK2 in the pathogenesis and therapy of myeloproliferative disorders. *Nature reviews. Cancer*, 7(9), pp.673–683.

Li, J. et al., 2010. JAK2 V617F impairs hematopoietic stem cell function in a conditional knock-in mouse model of JAK2 V617F-positive essential thrombocythemia. *Blood*, 116(9), pp.1528–1538.

Li, J. et al., 2014. JAK2V617F homozygosity drives a phenotypic switch in myeloproliferative neoplasms, but is insufficient to sustain disease. *Blood*, 123(20), pp.3139–3151.

Lu, X., Huang, L.J.-S. & Lodish, H.F., 2008. Dimerization by a cytokine receptor is necessary for constitutive activation of JAK2V617F. *The Journal of biological chemistry*, 283(9), pp.5258–5266.

Lundberg, P., Karow, A., et al., 2014. Clonal evolution and clinical correlates of somatic mutations in myeloproliferative neoplasms. *Blood*, 123(14), pp.2220–2228.

Lundberg, P., Takizawa, H., et al., 2014. Myeloproliferative neoplasms can be initiated from a single hematopoietic stem cell expressing JAK2-V617F. *The Journal of experimental medicine*, 211(11), pp.2213–2230.

Machida, Y.J. et al., 2009. The deubiquitinating enzyme BAP1 regulates cell growth via interaction with HCF-1. *The Journal of biological chemistry*, 284(49), pp.34179–34188.

Marty, C. et al., 2010. Myeloproliferative neoplasm induced by constitutive expression of JAK2V617F in knock-in mice. *Blood*, 116(5), pp.783–787.

Mead, A.J. & Mullally, A., 2017. Myeloproliferative neoplasm stem cells. *Blood*, 129(12), pp.1607–1616.

Medzhitov, R. & Janeway, C.A., 1997. Innate immunity: the virtues of a nonclonal system of recognition. *Cell*, 91(3), pp.295–298.

Meggendorfer, M. et al., 2013. SETBP1 mutations occur in 9% of MDS/MPN and in 4% of MPN cases and are strongly associated with atypical CML, monosomy 7, isochromosome i(17)(q10), ASXL1 and CBL mutations. *Leukemia*, 27(9), pp.1852–1860.

Mehta, J. et al., 2014. Epidemiology of myeloproliferative neoplasms in the United States. *Leukemia & lymphoma*, 55(3), pp.595–600.

Mesa, R.A. et al., 2005. Leukemic transformation in myelofibrosis with myeloid metaplasia: a single-institution experience with 91 cases. *Blood*, 105(3), pp.973–977.

Metzeler, K.H. et al., 2011. ASXL1 mutations identify a high-risk subgroup of older patients with primary cytogenetically normal AML within the ELN Favorable genetic category. *Blood*, 118(26), pp.6920–6929.

Meyer, S.C. et al., 2014. Genetic studies reveal an unexpected negative regulatory role for Jak2 in thrombopoiesis. *Blood*, 124(14), pp.2280–2284.

Moliterno, A.R. et al., 2006. Molecular mimicry in the chronic myeloproliferative disorders: reciprocity between quantitative JAK2 V617F and Mpl expression. *Blood*, 108(12), pp.3913–3915.

Mullally, A. et al., 2012. Distinct roles for long-term hematopoietic stem cells and erythroid precursor cells in a murine model of Jak2V617F-mediated polycythemia vera. *Blood*, 120(1), pp.166–172.

Mullally, A. et al., 2010. Physiological Jak2V617F expression causes a lethal myeloproliferative neoplasm with differential effects on hematopoietic stem and progenitor cells. *Cancer cell*, 17(6), pp.584–596.

Murati, A. et al., 2012. Myeloid malignancies: mutations, models and management. *BMC cancer*, 12(1), p.304.

Muzumdar, M.D. et al., 2007. A global double-fluorescent Cre reporter mouse. *Genesis (New York, N.Y. : 2000)*, 45(9), pp.593–605.

Nagase, R. et al., 2018. Expression of mutant Asxl1 perturbs hematopoiesis and promotes susceptibility to leukemic transformation. *The Journal of experimental medicine*, 215(6), pp.1729–1747.

Nakamura-Ishizu, A. et al., 2015. CLEC-2 in megakaryocytes is critical for maintenance of hematopoietic stem cells in the bone marrow. *The Journal of experimental medicine*, 212(12), pp.2133–2146.

Nangalia, J. et al., 2013. Somatic CALR mutations in myeloproliferative neoplasms with nonmutated JAK2. *The New England journal of medicine*, 369(25), pp.2391–2405.

Neubauer, H. et al., 1998. Jak2 Deficiency Defines an EssentialDevelopmental Checkpoint in DefinitiveHematopoiesis. *Cell*, 93(3), pp.397–409.

Nguyen, L.V. et al., 2012. Cancer stem cells: an evolving concept. *Nature reviews. Cancer*, 12(2), pp.133–143.

Nosaka, T. et al., 1995. Defective lymphoid development in mice lacking Jak3. *Science (New York, N.Y.)*, 270(5237), pp.800–802.

Oh, S.T. et al., 2010. Novel mutations in the inhibitory adaptor protein LNK drive JAK-STAT signaling in patients with myeloproliferative neoplasms. *Blood*, 116(6), pp.988–992.

Olson, T.S. et al., 2013. Megakaryocytes promote murine osteoblastic HSC niche expansion and stem cell engraftment after radioablative conditioning. *Blood*, 121(26), pp.5238–5249.

Pardanani, A. et al., 2013. Safety and efficacy of CYT387, a JAK1 and JAK2 inhibitor, in myelofibrosis. *Leukemia*, 27(6), pp.1322–1327.

Parganas, E. et al., 1998. Jak2 is essential for signaling through a variety of cytokine receptors. *Cell*, 93(3), pp.385–395.

Park, H.J. et al., 2016. Cytokine-induced megakaryocytic differentiation is regulated by genome-wide loss of a uSTAT transcriptional program. *The EMBO journal*, 35(6), pp.580–594.

Park, S.Y. et al., 1995. Developmental defects of lymphoid cells in Jak3 kinase-deficient mice. *Immunity*, 3(6), pp.771–782.

Park, U.-H. et al., 2011. Additional sex comb-like (ASXL) proteins 1 and 2 play opposite roles in adipogenesis via reciprocal regulation of peroxisome proliferator-activated receptor {gamma}. *The Journal of biological chemistry*, 286(2), pp.1354–1363.

Passamonti, F. & Rumi, E., 2009. Clinical relevance of JAK2 (V617F) mutant allele burden. *Haematologica*, 94(1), pp.7–10.

Patel, J.P. et al., 2012. Prognostic relevance of integrated genetic profiling in acute myeloid leukemia. *The New England journal of medicine*, 366(12), pp.1079–1089.

Pecquet, C. et al., 2019. Calreticulin mutants as oncogenic rogue chaperones for TpoR and traffic-defective pathogenic TpoR mutants. *Blood*, pp.blood–2018–09–874578.

Pertuy, F. et al., 2015. Broader expression of the mouse platelet factor 4-cre transgene beyond the megakaryocyte lineage. *Journal of thrombosis and haemostasis : JTH*, 13(1), pp.115–125.

Peters, M.J. et al., 1999. Circulating platelet-neutrophil complexes represent a subpopulation of activated neutrophils primed for adhesion, phagocytosis and intracellular killing. *British journal of haematology*, 106(2), pp.391–399.

Pietras, E.M., Warr, M.R. & Passegué, E., 2011. Cell cycle regulation in hematopoietic stem cells. *The Journal of cell biology*, 195(5), pp.709–720.

Pikman, Y. et al., 2006. MPLW515L is a novel somatic activating mutation in myelofibrosis with myeloid metaplasia. *PLoS medicine*, 3(7), p.e270.

Pourcelot, E. et al., 2014. Cytokine profiles in polycythemia vera and essential thrombocythemia patients: clinical implications. *Experimental hematology*, 42(5), pp.360–368.

Prick, J. et al., 2014. Clonal heterogeneity as a driver of disease variability in the evolution of myeloproliferative neoplasms. *Experimental hematology*, 42(10), pp.841–851.

Pronier, E. et al., 2018. Targeting the CALR interactome in myeloproliferative neoplasms. *JCI insight*, 3(22), p.53.

Pronk, C.J.H. et al., 2007. Elucidation of the phenotypic, functional, and molecular topography of a myeloerythroid progenitor cell hierarchy. *Cell stem cell*, 1(4), pp.428–442.

Pronk, C.J.H. et al., 2011. Tumor necrosis factor restricts hematopoietic stem cell activity in mice: involvement of two distinct receptors. *The Journal of experimental medicine*, 208(8), pp.1563–1570.

Puda, A. et al., 2012. Frequent deletions of JARID2 in leukemic transformation of chronic myeloid malignancies. *American journal of hematology*, 87(3), pp.245–250.

Ramos, T.L. et al., 2017. Mesenchymal stromal cells (MSC) from JAK2+ myeloproliferative neoplasms differ from normal MSC and contribute to the maintenance of neoplastic hematopoiesis. K. D. Bunting, ed. *PloS one*, 12(8), p.e0182470.

Rampal, R., Ahn, J., et al., 2014. Genomic and functional analysis of leukemic transformation of myeloproliferative neoplasms. *Proceedings of the National Academy of Sciences of the United States of America*, 111(50), pp.E5401–10.

Rampal, R., Al-Shahrour, F., et al., 2014. Integrated genomic analysis illustrates the central role of JAK-STAT pathway activation in myeloproliferative neoplasm pathogenesis. *Blood*, 123(22), pp.e123–33.

Rane, S.G. & Reddy, E.P., 2000. Janus kinases: components of multiple signaling pathways. *Oncogene*, 19(49), pp.5662–5679.

Rodig, S.J. et al., 1998. Disruption of the Jak1 gene demonstrates obligatory and nonredundant roles of the Jaks in cytokine-induced biologic responses. *Cell*, 93(3), pp.373–383.

Sanchez-Pulido, L., Kong, L. & Ponting, C.P., 2012. A common ancestry for BAP1 and Uch37 regulators. *Bioinformatics (Oxford, England)*, 28(15), pp.1953–1956.

Sanjuan-Pla, A. et al., 2013. Platelet-biased stem cells reside at the apex of the haematopoietic stem-cell hierarchy. *Nature*, 502(7470), pp.232–236.

Sashida, G. et al., 2016. The loss of Ezh2 drives the pathogenesis of myelofibrosis and sensitizes tumor-initiating cells to bromodomain inhibition. *The Journal of experimental medicine*, 213(8), pp.1459–1477.

Scheuermann, J.C. et al., 2010. Histone H2A deubiquitinase activity of the Polycomb repressive complex PR-DUB. *Nature*, 465(7295), pp.243–247.

Schmitt-Graeff, A.H., Nitschke, R. & Zeiser, R., 2015. The Hematopoietic Niche in Myeloproliferative Neoplasms. *Mediators of inflammation*, 2015(1), pp.347270–11.

Schwaab, J. et al., 2012. Activating CBL mutations are associated with a distinct MDS/MPN phenotype. *Annals of hematology*, 91(11), pp.1713–1720.

Scott, L.M. et al., 2007. JAK2 exon 12 mutations in polycythemia vera and idiopathic erythrocytosis. *The New England journal of medicine*, 356(5), pp.459–468.

Scott, L.M. et al., 2006. Progenitors homozygous for the V617F mutation occur in most patients with polycythemia vera, but not essential thrombocythemia. *Blood*, 108(7), pp.2435–2437.

Shimizu, T. et al., 2016. Loss of Ezh2 synergizes with JAK2-V617F in initiating myeloproliferative neoplasms and promoting myelofibrosis. *The Journal of experimental medicine*, 213(8), pp.1479–1496.

Simon, J., Chiang, A. & Bender, W., 1992. Ten different Polycomb group genes are required for spatial control of the abdA and AbdB homeotic products. *Development (Cambridge, England)*, 114(2), pp.493–505.

Sinclair, D.A. et al., 1992. Genetic analysis of the additional sex combs locus of Drosophila melanogaster. *Genetics*, 130(4), pp.817–825.

Sinclair, D.A. et al., 1998. The Additional sex combs gene of Drosophila encodes a chromatin protein that binds to shared and unique Polycomb group sites on polytene chromosomes. *Development (Cambridge, England)*, 125(7), pp.1207–1216.

Socolovsky, M. et al., 2001. Ineffective erythropoiesis in Stat5a(-/-)5b(-/-) mice due to decreased survival of early erythroblasts. *Blood*, 98(12), pp.3261–3273.

Sowa, M.E. et al., 2009. Defining the human deubiquitinating enzyme interaction landscape. *Cell*, 138(2), pp.389–403.

Stegelmann, F. et al., 2010. High-resolution single-nucleotide polymorphism array-profiling in myeloproliferative neoplasms identifies novel genomic aberrations. *Haematologica*, 95(4), pp.666–669.

Storan, M.J. et al., 2015. Brief Report: Factors Released by Megakaryocytes Thrombin Cleave Osteopontin to Negatively Regulate Hematopoietic Stem Cells. *Stem cells (Dayton, Ohio)*, 33(7), pp.2351–2357.

Suzuki, J. et al., 2013. Cytokine secretion from human monocytes potentiated by P-selectin-mediated cell adhesion. *International archives of allergy and immunology*, 160(2), pp.152–160.

Szpurka, H. et al., 2006. Refractory anemia with ringed sideroblasts associated with marked thrombocytosis (RARS-T), another myeloproliferative condition characterized by JAK2 V617F mutation. *Blood*, 108(7), pp.2173–2181.

Takahashi, T. & Shirasawa, T., 1994. Molecular cloning of rat JAK3, a novel member of the JAK family of protein tyrosine kinases. *FEBS letters*, 342(2), pp.124–128.

Tefferi, A., 2005. Pathogenesis of myelofibrosis with myeloid metaplasia. *Journal of clinical oncology : official journal of the American Society of Clinical Oncology*, 23(33), pp.8520–8530.

Tefferi, A. et al., 2011. Circulating interleukin (IL)-8, IL-2R, IL-12, and IL-15 levels are independently prognostic in primary myelofibrosis: a comprehensive cytokine profiling study. *Journal of clinical oncology : official journal of the American Society of Clinical Oncology*, 29(10), pp.1356–1363.

Tefferi, A. et al., 2008. Low JAK2V617F allele burden in primary myelofibrosis, compared to either a higher allele burden or unmutated status, is associated with inferior overall and leukemia-free survival. *Leukemia*, 22(4), pp.756–761.

Theocharides, A. et al., 2007. Leukemic blasts in transformed JAK2-V617F-positive myeloproliferative disorders are frequently negative for the JAK2-V617F mutation. *Blood*, 110(1), pp.375–379.

Thol, F. et al., 2011. Prognostic significance of ASXL1 mutations in patients with myelodysplastic syndromes. *Journal of clinical oncology : official journal of the American Society of Clinical Oncology*, 29(18), pp.2499–2506.

Thomis, D.C. et al., 1995. Defects in B lymphocyte maturation and T lymphocyte activation in mice lacking Jak3. *Science (New York, N.Y.)*, 270(5237), pp.794–797.

Tiedt, R. et al., 2007. Pf4-Cre transgenic mice allow the generation of lineage-restricted gene knockouts for studying megakaryocyte and platelet function in vivo. *Blood*, 109(4), pp.1503–1506.

Tiedt, R. et al., 2008. Ratio of mutant JAK2-V617F to wild-type Jak2 determines the MPD phenotypes in transgenic mice. *Blood*, 111(8), pp.3931–3940.

Triviai, I. et al., 2019. ASXL1/EZH2 mutations promote clonal expansion of neoplastic HSC and impair erythropoiesis in PMF. *Leukemia*, 33(1), pp.99–109.

Ugo, V. et al., 2004. Multiple signaling pathways are involved in erythropoietin-independent differentiation of erythroid progenitors in polycythemia vera. *Experimental hematology*, 32(2), pp.179–187.

Ulich, T.R. et al., 1991. The erythropoietic effects of interleukin 6 and erythropoietin in vivo. *Experimental hematology*, 19(1), pp.29–34.

Ungureanu, D. et al., 2011. The pseudokinase domain of JAK2 is a dual-specificity protein kinase that negatively regulates cytokine signaling. *Nature structural & molecular biology*, 18(9), pp.971–976.

Vainchenker, W. & Kralovics, R., 2017. Genetic basis and molecular pathophysiology of classical myeloproliferative neoplasms. *Blood*, 129(6), pp.667–679.

Vannucchi, A.M. et al., 2013. Mutations and prognosis in primary myelofibrosis. *Leukemia*, 27(9), pp.1861–1869.

Verstovsek, S. et al., 2012. A double-blind, placebo-controlled trial of ruxolitinib for myelofibrosis. *The New England journal of medicine*, 366(9), pp.799–807.

Walkley, C.R., Olsen, G.H., et al., 2007. A microenvironment-induced myeloproliferative syndrome caused by retinoic acid receptor gamma deficiency. *Cell*, 129(6), pp.1097–1110.

Walkley, C.R., Shea, J.M., et al., 2007. Rb regulates interactions between hematopoietic stem cells and their bone marrow microenvironment. *Cell*, 129(6), pp.1081–1095.

Walz, C. et al., 2012. Essential role for Stat5a/b in myeloproliferative neoplasms induced by BCR-ABL1 and JAK2(V617F) in mice. *Blood*, 119(15), pp.3550–3560.

Wang, J. et al., 2014. Loss of Asxl1 leads to myelodysplastic syndrome-like disease in mice. *Blood*, 123(4), pp.541–553.

Wen, Q.J. et al., 2015. Targeting megakaryocytic-induced fibrosis in myeloproliferative neoplasms by AURKA inhibition. *Nature medicine*, 21(12), pp.1473–1480.

Wernig, G. et al., 2006. Expression of Jak2V617F causes a polycythemia vera-like disease with associated myelofibrosis in a murine bone marrow transplant model. *Blood*, 107(11), pp.4274–4281.

Weyrich, A.S. & Zimmerman, G.A., 2004. Platelets: signaling cells in the immune continuum. *Trends in immunology*, 25(9), pp.489–495.

Weyrich, A.S., Lindemann, S. & Zimmerman, G.A., 2003. The evolving role of platelets in inflammation. *Journal of thrombosis and haemostasis : JTH*, 1(9), pp.1897–1905.

Wickenhauser, C. et al., 1999. Polycythemia vera megakaryocytes but not megakaryocytes from normal controls and patients with smokers polyglobuly spontaneously express IL-6 and IL-6R and secrete IL-6. *Leukemia*, 13(3), pp.327–334.

Wilkins, B.S. et al., 2008. Bone marrow pathology in essential thrombocythemia: interobserver reliability and utility for identifying disease subtypes. *Blood*, 111(1), pp.60–70.

Wilks, A.F., 1991. Cloning members of protein-tyrosine kinase family using polymerase chain reaction. *Methods in enzymology*, 200, pp.533–546.

Wilks, A.F. et al., 1991. Two novel protein-tyrosine kinases, each with a second phosphotransferase-related catalytic domain, define a new class of protein kinase. *Molecular and cellular biology*, 11(4), pp.2057–2065.

Xie, M. et al., 2014. Age-related mutations associated with clonal hematopoietic expansion and malignancies. *Nature medicine*, 20(12), pp.1472–1478.

Yamazaki, S. et al., 2011. Nonmyelinating Schwann cells maintain hematopoietic stem cell hibernation in the bone marrow niche. *Cell*, 147(5), pp.1146–1158.

Yan, D., Hutchison, R.E. & Mohi, G., 2012. Critical requirement for Stat5 in a mouse model of polycythemia vera. *Blood*, 119(15), pp.3539–3549.

Yang, Y. et al., 2016. Loss of Ezh2 cooperates with Jak2V617F in the development of myelofibrosis in a mouse model of myeloproliferative neoplasm. *Blood*, 127(26), pp.3410–3423.

Yonal-Hindilerden, I. et al., 2015. Prognostic significance of ASXL1, JAK2V617F mutations and JAK2V617F allele burden in Philadelphia-negative myeloproliferative neoplasms. *Journal of blood medicine*, 6, pp.157–175.

Yu, H. et al., 2010. The ubiquitin carboxyl hydrolase BAP1 forms a ternary complex with YY1 and HCF-1 and is a critical regulator of gene expression. *Molecular and cellular biology*, 30(21), pp.5071–5085.

Zahr, A.A. et al., 2016. Bone marrow fibrosis in myelofibrosis: pathogenesis, prognosis and targeted strategies. *Haematologica*, 101(6), pp.660–671.

Zaleskas, V.M. et al., 2006. Molecular pathogenesis and therapy of polycythemia induced in mice by JAK2 V617F. C. Sawyers, ed. *PloS one*, 1(1), p.e18.

Zhan, H. et al., 2016. JAK2(V617F)-mutant megakaryocytes contribute to hematopoietic stem/progenitor cell expansion in a model of murine myeloproliferation. *Leukemia*, 30(12), pp.2332–2341.

Zhan, H. et al., 2018. The JAK2V617F-bearing vascular niche promotes clonal expansion in myeloproliferative neoplasms. *Leukemia*, 32(2), pp.462–469.

Zhang, Y. et al., 2018. JAK2V617F Megakaryocytes Promote Hematopoietic Stem/Progenitor Cell Expansion in Mice Through Thrombopoietin/MPL Signaling. *Stem cells (Dayton, Ohio)*, 36(11), pp.1676–1684.

Zhao, J.L. et al., 2013. MicroRNA-146a acts as a guardian of the quality and longevity of hematopoietic stem cells in mice. *eLife*, 2, p.e00537.

Zhao, M. et al., 2014. Megakaryocytes maintain homeostatic quiescence and promote post-injury regeneration of hematopoietic stem cells. *Nature medicine*, 20(11), pp.1321–1326.

Ancora Imparo.